Evaluating Different Methods for Determining Road Grade Best Suited to ITS

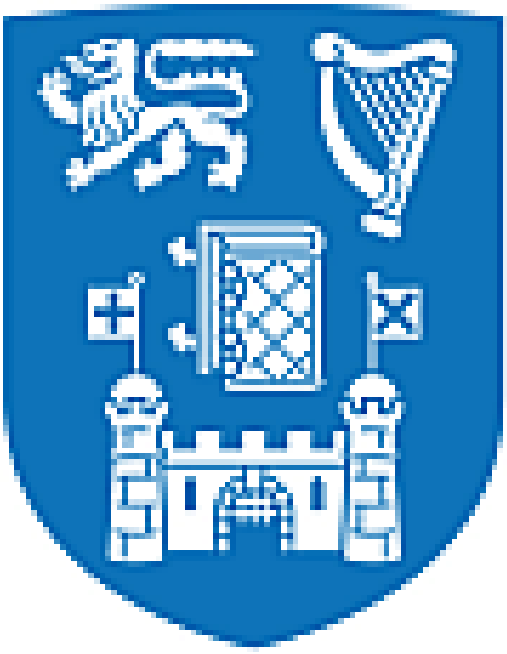

Submitted to the University of Dublin, Trinity College for the degree of M.A.I. in Computer and Electronic Engineering

Jared Magrath

Project Supervisor
Prof. Mike Brady

17th May 2017

Summary

Real–world fuel consumption and emission models are sensitive to road grade estimates. The advances of eco-routing and eco-driving solutions makes the development of large–scale collections of road grade profiles a key instrument in furthering progress. Therefore, there is a need to collect accurate, large scale, road grade profiles. Existing intelligent transport systems (ITS) like modern public bus transportation systems provide an opportunity to collect large amounts of data for post processing development of road grade profiles.

This dissertation explores different techniques for determining road grade estimates suited to ITS. An investigation was performed into why GPS elevation measurements should not be used exclusively to determine road grade. Five studies were replicated and evaluated in real–world experiments against the Google Elevation API. Similarly, a new combined approach of three of the replicated studies was developed.

Road grade has an important role in understanding vehicle performance as real world fuel consumption and emission models are sensitive to road grade estimates (Della Ragione and Giovanni, 2016; Wang et al., 2015). It is estimated that road grade accounts for approximately 1-3% of fuel consumption use in light duty vehicles (Wood et al., 2014a). However, road grade is often not included in fuel consumption models as can be seen in the study by (Zhou et al., 2016). This is mainly due to the difficulties in determining accurate road grade estimates (Wang et al., 2015). However, neglecting road grade in eco-routing leads to over- or under-estimation of fuel consumption.

Eco-routing has emerged as one of the strategies to reduce fuel consumption (Kubička et al., 2016). Eco-routing solutions allow for the prediction of the most fuel-economic routes and have become of interest to the transportation industry as they offer a way to dramatically reduce fuel consumption and emissions. However, there has been little development regarding large scale analysis of road grade effects on eco-routing performance according to the study done by (Levin et al., 2014).

By creating a large dataset of road grade profiles, it may be possible to improve simulations and models of fuel consumption that could be implemented in eco-routing systems. The National Renewable Energy Laboratory (NREL) published a study on measuring large–scale road grade profiles and evaluating the effect of road grade on the energy use of light-duty vehicles (Wood et al., 2014a). The collection of large-scale datasets of road grade profiles and the incorporation of them into energy consumption models could help to improve the eco-routing process in a similar manner to the work done by the NREL.

There are different classifications of intelligent transport systems (ITS). Advanced public transportation systems that utilise estimated arrival and announcement systems are a form of ITS (Figueiredo et al., 2001). There is potential for large-scale post-processing and analysis of data from modern public transportation systems like

buses, as discussed in a paper produced by (Doering and Wolf, 2015). One example of such a bus service is the Tesco Bus Service in Plzen, Czech Republic.

The Tesco Bus Service is used by ZF Openmatics to perform tests and uses information collected from a device called the Bach box (Openmatics, 2016a), an On-Board Unit (OBU) to collect telematic information from the vehicles. The OBU could be used to measure road grade for a large area when used in conjunction with a form of ITS, like that of a public bus service. Advanced public transportation bus systems may also inform this study when considering: their requirements for high position accuracy in real-time fleet management and their repeated traversal of routes, as they normally run on specified routes.

This dissertation evaluates different methods for determining road grade estimations from On-Board Units in advanced public bus transportation systems as a form of ITS. The results highlight the range of approaches to determine road grade which may be applied to ITS when using OBUs. It provides an independent evaluation of existing methods for determining road grade and presents a new combined approach. Lastly, GPS elevation information is explored to improve the understanding of why the measurements by themselves should not be used to determine road grade estimates.

Abstract

Eco-routing offers large fuel saving opportunities for vehicles. However, road grade is often neglected in fuel consumption models as it is difficult to determine accurate estimates. This leads to over-or under-estimation of fuel consumption in energy consumption models.

There has been little development regarding large–scale analysis of road grade effects on eco-routing performance. Since fuel consumption and emission models are sensitive to road grade estimates, providing large–scale road grade profiles would aid in the eco-routing process. Existing Intelligent Transport Systems (ITS) like modern public bus transport could be used to collect large-scale road grade profiles around a city. By creating a large data-set of road grade profiles, it may be possible to improve simulations and models of fuel consumption that could be implemented in eco-routing systems.

The experiments performed in this dissertation utilise On-Board Units (OBU) on a modern public bus service to investigate a number of factors relating to road grade. Different methods for determining road grade are evaluated with the intention to assist in the development of a process for large-scale road grade data-sets using ITS. The results highlight the range of approaches to determine road grade which may be applied to ITS when using OBUs. Ultimately, the study provides an independent evaluation of existing methods for determining road grade and presents a new combined approach to determining road grade.

Declaration

I, Jared Magrath, declare that the following dissertation, except where otherwise stated, is entirely my own work; that it has not previously been submitted as an exercise for a degree, either in Trinity College Dublin, or in any other University; and that the library may lend or copy it or any part thereof on request.

Signature: 

Date: 17/05/2017

Acknowledgements

I want to thank my parents and my family for their support throughout the five years of my degree.

In addition, I would like to acknowledge and thank ZF Openmatics and ZF for the opportunities given to me and for the help provide by them during my internship project. I would specifically like to thank Jan Kosnar, Martin Ponocy, Vaclav Plajt and everyone else in the App team that helped me with my project and made my time in Plzen great.

Lastly, I'd like to thank Mike Brady. Without whom, none of my work would have been possible. His open-minded, approachable and encourage-able nature inspires students to demand more from their education and from themselves. The university is truly luck to have someone like him.

Contents

1 Introduction **1**

2 Motivation **5**
2.1 Development Of Eco-Routing 6
2.2 Effect of Road Grade On Fuel Consumption 6
2.3 Development of Large–Scale Road Grade Profiles 9
2.4 Aim of The Dissertation 10

3 State of the Art **11**
3.1 Conventional Methods for Determining Road Grade 12
3.1.1 Surveying 12
3.1.2 Design Drawing Data 12
3.1.3 LiDAR 13
3.2 Automated Methods for Determining Road Grade 14
3.2.1 Accelerometers and Inclinometers 14
3.2.2 Multiple Runs 15
3.2.3 DEM 17
3.2.4 Sensor Fusion with Barometers and Other Components 18
3.2.5 GPS 19

4 Background **21**
4.1 Bach Box 22
4.2 GPS 23
4.3 Splines and B-Spline Approximations 26
4.4 Digital Elevation Models 27
4.4.1 SRTM 28
4.4.2 ASTER 28
4.4.3 Errors Associated with DEMs 29
4.5 Accelerometers 29
4.5.1 Mathematical Morphology 29
4.6 Digital Signal Processing 30
4.6.1 Digital Filters 30
4.6.2 Effects of filtering on the time series and its spectrum 31
4.6.3 Average Sliding filter 31
4.6.4 Exponential Filter 32
4.6.5 Binomial Filter 32
4.7 Sampling and Interpolation 33
4.7.1 Linear Interpolation 33
4.7.2 Bilinear Interpolation 33

5 Experimental Set-up 34
5.1 Additional Information . . . 35
5.1.1 Getting Data from the Bach Box . . . 35
5.1.2 Code structure . . . 36
5.1.3 Calculating Distance . . . 36
5.1.4 Road Grade Calculations . . . 37
5.1.5 Google API . . . 37
5.2 GPS Investigation . . . 38
5.3 Accelerometer . . . 40
5.4 Digital Elevation Models . . . 41
5.4.1 Bilinear Interpolation of Elevation profile from DEMs . . . 44
5.4.2 Smoothing/filtering of Elevation profile from DEMs . . . 48
5.5 Repeated Runs . . . 50
5.5.1 Multiple Runs . . . 52
5.5.2 Geometric modelling of road way using B-Spline Approximations 54

6 Results 56
6.1 GPS Investigation . . . 57
6.1.1 Initial Investigation Into Possible Reasons For Vertical Positioning Errors . . . 58
6.1.2 Set-Up of A Data Cleansing Approach to Remove Errors . . . 62
6.1.3 Applying Procedure To Data . . . 63
6.1.4 Analysis Of The Results . . . 64
6.2 Accelerometer . . . 66
6.2.1 Measuring Inclination With An Accelerometer . . . 66
6.3 Digital Elevation Models . . . 71
6.3.1 Bilinear Interpolation of Elevation profile from DEMs . . . 73
6.3.2 Smoothing/filtering of Elevation profile from DEMs . . . 76
6.4 Repeated Runs . . . 80
6.4.1 Multiple Runs . . . 80
6.4.2 B-Spline Geometric Representation . . . 83

7 Comparison of The Results 87

8 Combined Approach 89

9 Conclusion 93

10 Future Work 95

List of Figures

4.1 The Bach box, the On-Board Unit used in the experiments, with some of the components associated with the unit shown in the legend on the right of the image (Openmatics, 2016a). 22

5.1 OSM road network (left) and Google satellite view (right) of the test area Plzen, Czech Republic. The total route taken by the Tesco bus, equipped with the Bach box, is shown in green in the left image. Whereas, the red plotted route (in both images) shows the segment used for the experiment [Plotted in R]. 35

5.2 Elevation tile of the coordinates longitude E13-14 and latitude N49-50, the surrounding area of Plzen, Czech Republic taken from the SRTM 1-arc second DEM. 3D representation of the tile on the left compared to the 2D representation on the right. The 2D representation of the tile provides a legend of the elevation in meters [Plotted in R]. 41

5.3 Layout of elevation tiles in SRTM 3-arc second DEM. Elevation values are recorded on 1201x1201, 90x90 m square tiles, for 1x1 degree of longitude and latitude (Nepal, 2016). 42

5.4 Comparison of DEM extracted elevation values of the GPS trace taken from the test area: (A) SRTM 3-arc second; (B) ASTER 1-arc second; and (C) SRTM 1-arc second DEM. 44

5.5 The bilinear interpolation approach to estimating a better approximation of elevation estimates between grids. The image on the left shows a selected point in a series, whereas the image on the left shows the process of determining coefficients for a GPS point which is not at the centre of a grid (Henriques and Bento, 2013). 46

5.6 Route comparison of the experiments seen in Section 5.5. The left image shows the route used in Subsection 5.5.1 and the image on the right shows the route used in Subsection 5.5.2. The green line shows area investigate in the experiments compared to the full route in red. 50

5.7 3D representation of the test vehicle's trip, by comparing the cumulative distance against the longitude and latitude coordinates taken from a trip. The trip shows that the vehicle replicates the same route several times a day, which is shown by the increasing distance over the same longitude and latitude coordinates. 51

5.8 3D representation of the test vehicle's trip being segmented into the test area for Section 5.5.1. By comparing the cumulated distance against the longitude and latitude coordinates and sub-setting the data by the segments coordinates. 52

6.1 Unfiltered elevation profile from the GPS device by itself (left image), and compared to Google elevation API estimates (right image) – with the GPS elevation profile (A) shown in red and the Google elevation profile (B) in black. 57
6.2 OSM road network of the test area (Plzen, Czech Republic) with the route of the test vehicle, equipped with the Bach box, in red. The test vehicle starts from the left hand side and ends on the right hand side. 58
6.3 Comparison of areas where fluctuations in the GPS elevation, longitude and latitude measurements occurred. 59
6.4 Expected error determined from the GPS device: (1.) Expected error position in the horizontal (EPH); & (2.) Expected error position in the vertical (EPV). 60
6.5 The number of satellites visible to the GPS along the trip. 61
6.6 Time-stamp of the GPS receiver for the duration of the trip. The linear profiles indicates that there was no breaks in recording during the trip 61
6.7 Fast Fourier Transform of the raw unfiltered GPS elevation values (black points) compared to the low pass filtered (red points) representation. Highlighting the impact of filtering techniques have on dampening the data-set. 62
6.8 Elevation (left hand-side) and road grade (right hand-side) profiles of the different low pass filters in decreasing order: (1.) Exponential filter; (2.) Average sliding window filter; and (3.) Binomial filter. The resulting profiles from the filtering process is shown in red (A) are compared against the Google elevation API estimates in black (B). 63
6.9 Histograms of road grade estimates: (1.) Google elevation API (top left); (2.) Exponential filtered GPS elevation (top right); (3.) Average sliding window filtered GPS elevation (bottom left); and (4.) Binomial filtered GPS elevation (bottom right) 64
6.10 Raw accelerometer tilt profile by itself on the left and the raw tilt values (A) compared to Google API extracted elevation (B) on the right. 66
6.11 Several step process performed to remove noise from the vibration and acceleration of the vehicle. Using low pass filtering, seen in the top and middle images, to remove vibrational noise and using a mathematical Morphology approach to remove acceleration noise, seen in the bottom image, with the erosion operation (A) and the dilation operation (B) compared to the low pass filtered signal (C). 67
6.12 Comparison of the corrected accelerometer tilt values, using the Mathematical Morphology approach, compared to: the original filtered values (left image); and the Google elevation API road grade estimates (right image). 68

6.13 Comparison of the filtered (low pass filtered and MM approach) accelerometer road grade angle measurements (top image) compared to the acceleration profile of the vehicle (bottom image), taken from the Controller Area Network bus (CAN). 69
6.14 Elevation values extracted from the SRTM 1-arc DEM, with an indication of where elevation values may differ from true elevation (right image). 71
6.15 Areas along the test route where the extracted DEM elevation profile exhibits discrepancies. The first images on the left shows an area of the test route where the road goes over a bridge. Similarly, the middle image shows an point where the road way goes over an overpass. Lastly, the final image on the right shows an incline that occurs near the road way. 72
6.16 Interpolated DEM elevation (1) and road grade (2) profiles. The interpolated values (A), shown in red, are compared to raw DEM elevation estimates (B), seen in black. 73
6.17 Interpolated DEM elevation (1) and road grade (2) profiles. Interpolated SRTM elevation estimates (A) compared to Google elevation API estimates (B). 74
6.18 Several step process of the smoothing/filter process of the SRTM DEM extracted elevation profile. 77
6.19 Filtered smoothed DEM elevation and road grade profiles (A) compared to raw DEM elevation estimates (B). 78
6.20 Filtered/smoothed DEM elevation (1) and road grade profiles (2). The filtered/smoothed profiles (A) are compared to the Google elevation API estimates (B). 79
6.21 Representation of the test routes chosen for the multiple runs experiment (left) and the B-Spline approximation experiment (right). The test areas are a smaller segment, seen in green, of the entire route travelled, seen in red. 80
6.22 3D representation of five repeated runs of the test segment, the different colours representing each run, comparing the elevation to the longitude and latitude coordinate measurements taken from the GPS module. 81
6.23 Comparison of linear regression profile of the combined multiple runs compared against multiple runs on the left and the Google elevation on the right. 82
6.24 Road grade profiles of the multiple runs with 3, 5 and 7 repeated runs, shown in that order (A) compared to Google elevation API road grade estimates (B). 82
6.25 Multiple runs, 10 repeated runs, road grade profile (A) compared to Google API elevation road grade estimates (B). 83
6.26 The several step process in cleansing the erroneous data. The first image on the left shows the elevation change between two points being identified, seen in red. The middle image shows the regression profile, seen in red, of Z and X datasets. The last image on the right, shows the regression profile, seen in red, of Y and X datasets. 84

6.27 Open uniform (A) and uniform (B) knot vector B-Spline approximations compared against the elevation values at easting (left image) and northing coordinates (right image). 85
6.28 Comparison of the B-Spline open uniform knot vector estimates, shown in blue, to the Google elevation API estimates, seen in green, and the GPS elevation values, in red. 85
6.29 Road grade estimates of the B-Spline approximation of the road way (B) compared to the Google elevation API estimated road grade for the segment (A). 86

8.1 Left image – DEM extracted and smoothed/filtered elevation profiles (B) used in combination to determine linear regression of 80 m segments (A). Right image – linear regression, every 80 m, of combined DEM extracted and smoothed elevation profiles (A) compared to Google elevation API estimates (B). 90
8.2 Road grade estimates of the combined approach (A) compared against Google elevation API road grade estimates (B). 91

10.1 Google map of the Dublin, Ireland city boundary, overlaid with GPS data points taken from the Dublin Bus data-set. The data-set is an illustration of a small fraction of the entire data-set available from the Dublin Bus Insight Project. 95
10.2 An illustration of the elevation profile obtain from querying the GPS locational information of the bus route 15 from one of the files provided from the Dublin Bus Insight project. GPS longitude and latitude coordinates are compared against elevation data extracted from a Postgres database containing the SRTM 1-arch tile for the regional area of Dublin. 96

LIST OF ABBREVIATIONS

- A-GPS: Assisted-GPS
- ADAS: Advanced Driver Assisted Systems
- API: Application Programming Interface
- APTS: Advanced Public Transport Systems
- ASTER: Advanced Spaceborne Thermal Emission and Reflection Radiometer
- ATIS: Advanced Traveller Information Systems
- ATMS: Advanced Traffic Management Systems
- Apps: Applications
- BL: Bottom Left
- BR: Bottom Right
- C/A: Course Acquisition
- CAN bus: Controller Area Network bus
- CDMA: Code-Division Multiple Access
- DEM: Digital Elevation Model
- DGPS: Differential-GPS
- DOP: Dilution of Precision
- DR-GPS: Dead Reckoning-GPS
- DSM: Digital Surface Models
- DSP: Digital Signal Processing
- DTM: Digital Terrain Models
- EGNOS: European Geostationary Navigation Overlay Service
- EPH: Expected Error Position in the Horizontal
- EPV: Expected Error Position in the Vertical
- FIR: Finite Impulse Response

- GDEM: Global-DEM
- GPRS: General Packet Radio Service
- GPS/BA: GPS with Barometric Altimeter
- GPS: Global Positioning System
- GSM: Global System for Mobile Communications
- HDOP: Horizontal Dilution of Precision
- HDV: Heavy Duty Vehicle
- IMU: Inertia Measurement Unit
- ITS: Intelligent Transport Systems
- LiDAR: Light Detection and Ranging
- METI: Ministry of Economy, Trade and Industry of Japan
- MM: Mathematical Morphology
- MSL: Mean Sea Level
- NASA: National Aeronautics and Space Administration
- NREL: National Renewable Energy Laboratory
- OBU: On-Board Unts
- OSM: OpenStreetMaps
- P: Precision Code
- PDOP: Position Dilution of Precision
- PRN: Pseudo Random Noise
- SBAS: Satellite Based Augmentation System
- SRTM: Shuttle Radar Topography Mission
- TEDS: Terrain Elevation Data Server
- TL: Top Left
- TOF: Time Of Flight
- TR: Top Right
- UTM: Universal Transverse Mercator
- VDOP: Vertical Dilution of Precision
- VSP: Vehicle Specific Power
- WAAS: Wide Area Augmentation System
- WGS-48: World Geodetic System

Chapter 1

Introduction

Road grade plays an extremely important role in a vehicle's performance (Bae et al., 2001) and fuel consumption (Wood et al., 2014a), making it a vital metric to be considered by the automotive industry. "Road grade is the change in elevation divided by the horizontal distance traveled, usually expressed in percent" (Yazdani Boroujeni and Frey, 2014). As there is an ever growing demand for finding solutions to reduce emissions of greenhouse gases and since the transportation industry generates approximately 14% of global emissions (Agency, 2016), most solutions for reducing greenhouse emissions have aimed to make improvements in the current transportation system (Della Ragione and Giovanni, 2016).

The need for a reduction in greenhouse emissions in the transportation industry has led to the development of eco-driving and eco-routing solutions in recent years (Zhou et al., 2016). Any trip taken by a vehicle is optimized to produce the most economic and environmentally efficient route. Therefore, accurate energy consumption models are a necessity in order to improve the eco-routing process. As Zhou et al. have established (2016), many fuel consumption models neglect the effect of road grade. Road gradient information would allow for better selection of routes to minimise energy consumption and emissions in addition to improving the estimation of fuel consumption in current eco-routing.

In many energy consumption models road grade is ignored and changes in velocity and acceleration are taken as an indication of the effect of road gradient (Levin et al., 2014). This assumption means that most energy consumption models neglect the effect that elevation gradients have on the accuracy of the model (Wood et al., 2014a). The effect of neglecting road gradient information in energy consumption models is the overestimation or underestimation of the overall energy consumption required for certain routes (Levin et al., 2014).

Higher elevation gradients cause higher emissions in CO_2 and other greenhouse gases whereas areas with flatter topography usually have lower emissions (Della Ragione and Giovanni, 2016). However, when comparing the effects of road grade in eco-routing processes, the selection of certain routes with lower/negative road grade estimates can account for an overestimation of fuel consumption, due to the inertia of the downhill gradients (Levin et al., 2014). The opposite can be seen for routes with higher/positive road grade values.

Road gradients have been neglected in the majority of energy consumption models because it is difficult to collect and measure road gradient information (Wang et al., 2015). Accurate road gradient information is generally expensive to acquire as it involves the use of sophisticated GPS devices or expensive measuring equipment (Wood et al., 2014b). Therefore, most modern methods for determining road grade use some sort of automated process combined with a method to determine position. Many approaches use consumer-grade GPS devices to estimate positional information. Although the horizontal accuracy of consumer-grade GPS devices is notable, vertical accuracy in consumer-grade GPS devices is poor in comparison. As such, most automotive methods look to substitute or aid the elevation estimates to determine road grade.

The work of the National Renewable Energy Laboratory (NREL) used elevation information extracted from Digital Elevation Models (DEMs) to determine road grade profiles. Large–scale road grade profiles have been developed by the NREL to assess the impact of the road grade on energy use of modern auto-mobiles (Wood et al., 2014a). Work done by the NREL (Wood et al., 2015) produced road grade profiles of major US highways and assigned Environmental Protection Agency Greenhouse Gas Emissions Model certificates to medium and heavy duty vehicles. The NREL's efforts illustrate the importance of producing large–scale road grade profiles in order to be able to establish the exact effects of road grade.

In order to improve the eco-routing process the development of large scale road grade profiles would aid in the accuracy and ease the estimation of fuel consumption models. One way that this might be achieved is by using Advanced Public Transportation Systems (APTS), which are a form of Intelligent Transport Systems (ITS) (Figueiredo et al., 2001), for example public buses. Modern public bus systems use a combination of Advanced Traveller Information Systems (ATIS) and Advanced Traffic Management Systems (ATMS) to "improve the mass transport service, allowing route information, travel schedules and costs, and real time information about changes in transport systems" (Figueiredo et al., 2001). This means that advanced public bus services usually have highly sophisticated equipment on board the vehicles already to aid fleet management and estimate time of arrival for each bus.

Public buses in China were used to monitor physical environments and road surfaces "using a data exchange interface to feed a data cloud computing system" (Kang et al., 2016). The approach taken by Kang et al., indicates that public buses could be used to determine physical attributes of road-ways. This approach could be extended to measure physical characteristics like road grade in a similar manner. The opportunity of large–scale bus movements were explored by (Doering and Wolf, 2015). The results collected by the researchers indicated that a large range of data for analysis can be determined from the movements of public buses in Seattle and Chicago. Doering and Wolf ascertained that public buses covered a large area of the cities and discovered an interesting phenomena: primarily that buses would travel the same route continuously, however buses occasionally change routes at the end of shifts. The findings of (Kang et al., 2016) and (Doering and Wolf, 2015) are significant in that they reveal that the physical characteristics of road-ways can

be determined, and that large sections of the city may be covered, using advanced public buses. Similarly, the movement of buses, described by (Doering and Wolf, 2015), provides unique opportunities for an approach with ITS that is not available using other approaches in the collection of large scale road grade profiles (such as that done by the NREL) by the repeated movement of buses over the same route and the use of advanced equipment on board the vehicles.

The Bach box, developed by ZF Openmatics (Openmatics, 2016a) can be used to monitor and provide enhanced connectivity to public bus services (AG, 2016). The Bach box is an On Board Unit (OBU) which provides a number of features to fleet management operators including enhanced positional information and real time monitoring. One example of where the Bach box is used as an APTS is the Tesco Bus Service, in Plzen, Czech Republic (Hupák, 2016). This service is a freely available service in Plzen, providing real time announcement information and multimedia connectivity to its passengers using the Bach box.

The Tesco Bus Service is limited in its ability to provide large scale road grade. It can be used for testing purposes and to determine the best method of calculating road grade, suited to ITS. The Bach box has a number of components that can be stored in memory on the device or accessed in real time from the ZF cloud service. Therefore, the Bach box and other On Board Units (OBUs) could be used to determine road grade information from public bus services to provide large scale road profiles. The advantage of using the Bach box, or other equivalent OBU, in public buses would be the homogeneity obtained from the measurements: usually bus companies will operate with a similar vehicle model, due to the economies of scale associated with purchasing a fleet of the same model; and secondly the components in OBUs will need to be the same for all modules. Readings from the Bach box could be used in a post–processing manner to determine the large–scale road grade profiles. The collection of these large scale road grade profiles would then aid the development of the eco-routing process. Finding methods of determining road grade suited to ITS is necessary in order to produce large–scale road grade profiles. There are many different approaches to determining road grade.

This dissertation aims to establish the best method for determining road grade, suited to ITS, with the subsequent aim of developing large–scale road grade profiles. Several road grade approaches are evaluated; five of the approaches are replicated using the Bach box OBU, on the Tesco Bus Service in Plzen. The best method suited to ITS is identified and a new combined approached is presented. The dissertation outlines a theoretical approach to collecting large–scale road grade profiles using ITS, to aid the eco-routing process, and uses real life experiments as validation for the best method of determining road grade suited to ITS and the development of large–scale road grade profiles.

The substance of this dissertation is encapsulated as follows:

- Chapter 2 – establishes the motivations for the dissertation, by exploring the development of eco-routing and how road grade impacts fuel consumption and emissions in vehicles. The need for large–scale road grade profiles is then confirmed and the aims of the dissertation are identified.
- Chapter 3 – explores the current approaches to determining road grade, by comprehensively examining conventional methods compared to newer autonomous approaches, which mostly utilise GPS devices.
- Chapter 4 – contextualizes background information relevant to the dissertation, considering evidence relevant to the studies replicated.
- Chapter 5 – discusses the experiments and methodologies for each of the studies replicated. In addition, additional information about assumptions and equations stated in this dissertation is provided.
- Chapter 6 – explores the results and discussion of the experiments individually. The results and implications for each experiment are discussed.
- Chapter 7 – explores the best method suited to determining road grade from the experiments conducted.
- Chapter 8 – explores a combined approach suggested by the author.
- Chapter 9 – concludes the results and evaluates their significance in the field of road grade.
- Chapter 10 – presents further work to be done with the work presented indiscoveries of this dissertation.

Chapter 2

Motivation

This Chapter provides an outline of the motivations for determining large scale road grade profiles and contextualises the development of eco-routing solutions and the impact of road grade on vehicle fuel consumption. Subsequently, the aims of the dissertation are outlined.

In Section 2.1, recent developments of eco-routing solutions to improve the fuel economy of vehicles is explored. There have been substantial advances towards improving the eco-routing process, however only recently has there been progressions in utilising road grade estimates in fuel consumption models.

Section 2.2 highlights the impact of road grade on fuel consumption and it's influence on the eco-routing process. The effects of road grade on vehicle fuel consumption are well known, however the implications of large–scale inclusion of road grade estimates in eco-routing have only recently been realized.

The development of large–scale road grade profiles have been explored in only a few studies which are examined in Section 2.3. Consequently, the aims of this dissertation are specified in Section 2.4, with particular focus on aiding the development of large–scale road grade profiles.

2.1 Development Of Eco-Routing

Demand for improvements in the transportation industry has increased in recent years. The transportation industry makes up a significant proportion of global emissions and with population increase these emissions are set to escalate. "Transport accounts for 19% of global energy use and 23% of energy-related carbon dioxide (CO_2) emissions, and these percentages are set to rise in the future." (Travesset-Baro et al., 2015). The impact of fuel consumption and emissions are of concern to individuals and to network planners alike (Levin et al., 2014). Many individuals are now conscious of the impact of vehicles on the environment and of the monetary reward for reduced fuel consumption. Similarly, planners wish to reduce tail pipe emissions from vehicles in order to reduce the effect of pollution in urban areas. Meanwhile, manufacturers are also under pressure to make improvements in vehicle technologies (Zhou et al., 2016).

There have been numerous improvements in engine performance as a result of the demand for manufacturers and planners to produce solutions in vehicle technologies. However, these technologies have limited effect, around 5% savings, on the fuel consumption according to the study by (Zhou et al., 2016). Developments into solutions such as eco-routing, show that large fuel saving opportunities are available. Eco-routing is a method where vehicles are navigated on a path that will minimize energy consumption. Usually this results in the adverse effect of longer time for travel as it denotes taking a slower route that will take longer (Kubička et al., 2016).

The effects of eco-routing can vary, the study by (Kubička et al., 2016) reported "...fuel efficiency could be enhanced for 46% of the trips and that fuel saving would be 8.2% on the average.". In comparison, in the study by (Zhou et al., 2016) it can be seen that "...approximately 12-33% of fuel can be saved through improved fuel economy.." when using eco-routing solutions. Again however, the effects of road grade are usually neglected in the fuel consumption models, making it an important factor for future considerations.

Studies have determined the effects of road grade in vehicle prediction models and eco-routing solutions, concluding: that road grade should not be excluded in estimates (Wang et al., 2015; Zhou et al., 2016; Levin et al., 2014). Therefore, developing methods for determining large–scale road grade profiles would aid in improving eco-routing solutions. This is especially true since "...energy consumption is a proxy for mobile emission..", according to the study by (Levin et al., 2014), and so a better determination of fuel consumption models would improve emission models.

2.2 Effect of Road Grade On Fuel Consumption

Vehicle emissions and fuel consumption estimates are affected by a number of factors, according to Zhou et al.: (A) travel related, distance to the destination, etc.; (B) weather related, factors such as colder air – which is denser and can create more aerodynamic drag; (C) driver related, factor like the aggressiveness of the driver in braking and accelerating; (D) traffic related, refers to traffic flows, etc.; and (E) road way related, considers the geometry of the roadway which includes the slope,

curvature and roughness of the road.

The study by (Zhou et al., 2016) concluded that road-way related factors like "driver-related factors and the road slope" cannot be ignored in fuel consumption models due to their impact on fuel consumption. Fuel consumption models give a quantifiable estimate of the energy demands and emission outputs of vehicles by taking a number of inputs from the vehicle. However, "traditional vehicle energy consumption models have neglected an important factor: change in road elevation" (Levin et al., 2014). Road grade or the change in elevation compared to the horizontal distance is an important factor for fuel consumption, accounting for 1-3% of fuel consumption in light-duty vehicles (Wood et al., 2014a).

Positive road grade estimates indicate that the road-way will have an inclination. Similarly, negative road grade estimates indicate declines in the road-way. The reason road grade has such an effect on vehicle energy consumption is because of the "...sinusoidal component of the vehicle weight." (Ribar et al., 2016). This is mainly due to the force required to expel a vehicle up a hill and the resulting opposing force of climbing resistance combined with the weight of the vehicle (Kost, 2014). Therefore, the mass of and the inclination of the road have an influence on the energy consumption of a vehicle (Kidambi et al., 2014).

Currently, there is no standard procedure to quantify road grade in a "second-by-second basis for a moving vehicle", according to the study by (Boroujeni and Frey, 2014), which is what is required for fuel consumption models in eco-routing solutions. Similarly, road grade is usually a combined factor in fuel consumption. Meaning that road grade estimates do not by themselves create higher fuel consumption per se, but rather the combination of the speed, acceleration, etc., of the vehicle combined with road grade will influence the fuel consumption.

Driver behaviours are a factor that heavily influence fuel consumption when combined with road grade. In positive road inclinations, when a vehicle is going up a hill, a driver will usually accelerate in order to maintain a constant speed up the hill, according to the study by (Wang et al., 2015), and this will result in more fuel being consumed. However, the fuel consumption could be minimised if a driver adopted an approach where they sped up before a hill and only accelerated lightly on the hill. Similarly, it was found that when drivers went down a hill they need not apply acceleration but rather use the influence of gravity on the vehicle and so conserve fuel. However, in the study by (Wang et al., 2015), the influence of heavy driver braking behaviour, in the presence of negative road grade or going down a hill, meant that extra fuel was consumed due to the speed fluctuations from the de-acceleration and acceleration of the vehicle.

Light vehicle types, like consumer models, may have variation in "mass of up to 50%" for trips (Kidambi et al., 2014). Whereas, heavy-duty vehicles are more susceptible to road grade estimations due to the apparent variation in loads which "may vary in mass by 400% depending on payload conditions" (Kidambi et al., 2014). The effect of this is that the mass of the vehicle influences the force associated with inclination. Similarly, (Wang et al., 2015) concluded that "differences in the engine

displacement often leads to the different fuel consumption when vehicles run in the same pattern". Therefore, not only does the gradient of the road influence the fuel consumption but so does the vehicle type, displacement and mass of the vehicle.

The influence of traffic in combination with road gradient usually has the effect of increased fuel consumption. This effect is two fold; (A) increased road grade usually resulted in higher traffic – highways are usually built with lower road grade in mind (Boroujeni and Frey, 2014), and so highways with higher road grade estimates usually experience higher traffic conditions (Qinglu Ma, 2016); and (B) higher traffic rates combined with inclinations cause higher fuel consumption and emissions, as seen in the study by (Wang et al., 2015).

The influence of road grade on the eco-routing process can be seen in the selection of routes. Eco-routes which do not account for road elevation will take every road as being flat. Routes with high positive road grade estimates will generally lead to an underestimation in the fuel consumption by the vehicle (Levin et al., 2014). These results are also verified by (Frey et al., 2008), where underestimation of fuel consumption is recorded if road grade is not accounted for. The opposite is apparent for negative road grade values, with overestimation of the fuel consumption if road grade is not accounted for in fuel consumption models (Levin et al., 2014).

When using fuel consumption models, accounting for road grade in two routes that have similar characteristics, like length, driving behaviour, .etc.: (A) a route that has a sharp positive road grade in the beginning of the trip and then a long negative (road grade angle) stretch for the remainder of the trip; and (B) a route which has a long positive (road grade angle) for the majority of the trip and a short negative road grade decline towards the end of the trip. If road grade was not accounted for, the routes would have similar energy consumption estimates. However, according to the studies by (Frey et al., 2008) and (Levin et al., 2014), the first route (A) would lead to a high estimation of energy consumed in the first stretch and then would benefit from the long decline with very little energy consumption. Whereas (B) would have a relatively high level of energy consumption in the first stretch and then would not benefit greatly from the short decline. Therefore, we would see that (B) would have a much larger energy consumption associated with it it and (A) would have a much lower energy consumption associated with it than the estimates without road grade.

There are a number of ways to determine road gradient information from a road, which are discussed in Chapter 3, nonetheless it is still a relatively difficult variable to obtain accurate estimates for (Zhang and Frey, 2006; Wang et al., 2015).

2.3 Development of Large–Scale Road Grade Profiles

The development of large scale road grade profiles has only recently started to come into fruition as is seen in the work the NREL (Wood et al., 2015). The NREL sought to develop large scale road grade profiles to determine the energy and emission certificates for medium and heavy–duty vehicles. The approach taken by the laboratory first attempted to compare their method for determining road grade, seen in the study (Wood et al., 2014b), against the TomTom road grade national database and measurements taken from a specialised vehicle developed by the Southwest Research Institute.

The study (Wood et al., 2015) highlighted the importance of performing large scale road grade profiles to determine how road grade affects different vehicle energy consumptions. The study concluded that the TomTom road grades were accurate. In addition, the study offered interesting discussion of how the road grade estimates were collected. The TomTom road grade estimates were collected using a specialised vehicle equipped with "GPS, differential GPS, inertial measurement unit, gyroscopes, and accelerometers" (Wood et al., 2015). For those routes that the TomTom vehicles had not determined the road grade for, TomTom's customers GPS measurements were used in a multiple runs averaging approach to estimate the road grade.

Conversely,where road grade estimates were estimated, using components found on most Heavy–Duty Vehicles (HDVs) by (Sahlholm and Johansson, 2010), road grade maps of high precision were ascertained. The road grade estimates measured were obtained in order to be used in Advanced Driver Assisted Systems (ADAS) in the HDVs. The study discussed the fact that "commercial efforts to create such maps are under way, but access to them will most certainly be associated with some cost". When examining the TomTom data-set, it is clear that there is a need to determine similar data-sets and make them available to the public to improve the understanding of road grade on a size-able eco-routing process.

According to the study by (Levin et al., 2014) there are few (if any) studies other than their own, on large–scale effects of road grade on the eco-routing process. The study assesses the impact of road grade on the eco-routing process in two cities. The authors Levin et al., concluded that the "empirical results suggest that a greater percentage of trips can be re-routed before an increase occurs when considering gradient". The study used elevation information extracted from the Google elevation API to determine the road grade estimates.

2.4 Aim of The Dissertation

The main aim of the dissertation is to aid in the development of large–scale road grade profiles. The purpose being, the need for accurate road grade information to reduce fuel consumption and emissions in the transportation industry. The road grade information would enable enhanced predictive energy consumption models, like eco-routing, to be able to improve fuel economy in vehicles on a larger scale.

The purpose of the experiments are: (A) to determine why consumer-grade GPS elevation estimates by themselves should not be used to determine road grade; (B) to replicate and validate results of similar studies in the area; (C) to evaluate the most effective method for determining road grade suited to ITS; and (D) to determine how the results fare against a commercially available elevation service like the Google elevation API.

A) There is a lot of information highlighting errors associated with GPS devices. However, there is little information examining why GPS receivers are so poor at measuring road grade. By investigating the GPS elevation profile this should become clearer.

B) By replicating studies it should become more transparent which is best suited for determining road grade. This also verifies the results of the dissertation as they can be compared against the original studies.

C) The results collected in the dissertation will aid in the choice of the best method suited to ITS. Comparison of the results in terms of their accuracy and their limitations inform the selection process.

D) Comparison of the results against a commercial product such as the Google elevation API will help to validate the accuracy of the results in the experiment in addition to opening up comparison of the limitations and benefits.

Chapter 3

State of the Art

This Chapter gives an overview of the current state of art, and background information to aid the understanding of different methods used in the experimental section of this dissertation.

To measure the gradient of a road there are three typical techniques that all relate to each other. The first and most common of these is to use the change in elevation of the horizontal distance covered for a specific segment and to use the associated angle or percentage change. A second technique involves determining the angle measurement using the inclination angle taken from a device that can measure pitch, for example an inclinometer. Alternatively, the use of vertical and horizontal velocities can be used to obtain instantaneous road grade estimates.

Positive road gradients represent areas where the road's elevation is increasing with respect to the horizontal distance and indicates uphill areas. Similarly, areas of negative road gradients represent slopes where the road elevation is decreasing with respect to the horizontal distance, and indicates downhill slopes. Areas of flat road are indicated with road grade equal to zero.

With areas of high inclines causing an increase in fuel consumption in vehicles, the effects of road gradient on fuel consumption is well-known (Frey et al., 2008). A mixture of the above techniques for determining road gradient is employed in the different methods discussed in this Chapter.

Section 3.1 investigates traditional methods of determining road grade. Whereas, Section 3.2 explores the use of modern automated methods for determining road grade.

3.1 Conventional Methods for Determining Road Grade

Road grade has typically been measured using a number of different approaches, from direct surveying of the roadways, seen in Subsection 3.1.1, to reading existing design drawings, observed in Subsection 3.1.2, to more sophisticated methods using Light Detection And Ranging (LiDAR) data, seen in Subsection 3.1.3. Each of the different approaches for determining road gradient has benefits and limitations. In examining the different approaches it is essential to first understand the shortcomings of the current systems for developing large scale road gradient profiles.

3.1.1 Surveying

Surveying entails a direct measurement approach of terrestrial (three dimensional) positions, the distance and angle between these points. Typically, the surveying of road profiles is done using a number of different sophisticated devices, such as total stations, GPS receivers, 3D scanning and inclinometers.

This approach provides accurate estimates of the road network for the specific location. Survey and mapping GPS receivers (Rover receivers) have very high accuracy associated with them. However, are susceptible to interference and also require additional time to acquire accurate estimates for positioning (Wing and Frank, 2011). A levelling process can be performed once two points of elevation have been measured and the angle determined.

A disadvantage of this method is that it requires on-site analysis to acquire accurate estimates of the road's profile. This may require closing of lanes or highway segments to ensure safety during the collection of the measurements. It additionally requires a long period of time to cover a large area of the road network. This inevitability leads to a longer time associated with collecting the results and higher costs associated with employing staff to collect measurements.

3.1.2 Design Drawing Data

Road grade can be calculated from existing design drawings of existing highways. The design drawings of a highway are the drawings originally used to construct the road.

The road gradient can be calculated from the design drawing using approaches discussed in the state of arts of the studies by (Zhang and Frey, 2006) and (Boroujeni et al., 2013). The techniques rely on reading off the blue print drawings to identify the roadway segment and its length. From cumulative distance from the assumed origin, the road gradient can then be read from the corresponding sections.

Design drawings provide a good approach to determining road gradient for areas where design drawings are available. Nonetheless, these drawings are not normally updated and maintained to reflect modifications and changes to the roadways. Many

road-ways that are not highways do not have blue print drawings or they are not readily available. Correspondingly, the design drawings do not provide details regarding vertical curvature, areas where there is a transition between different road gradients. Another limitation of this method it requires manual labour as a result of the absence of digitised drawings and the physical process needed to read the values off the blue prints. The process of reading off the design drawings would lead to a slow set-up and the true representation of the road may not be displayed.

This approach allows for determination of road grade information after the blue prints have already been collected, and requires the physical presence of someone to read the measurements. The approach is intuitive and relatively easy to apply but the limitations make it unsuited for large scale applications that require the determination of large road segments.

3.1.3 LiDAR

Light Detection and Ranging (LiDAR) data is used to create accurate Digital Terrain Models (DTMs) and Digital Elevation Models (DEMs) of the earth. They can offer a high accuracy in terms of estimating road elevation and deriving road gradient (Zhang and Frey, 2006). They are not a conventional method for measuring road grade but their precision, associated cost and the fact that most road grade methods use them for comparisons make them suitable for this Section.

Road gradient is collected by either air-crafts or auto-mobiles with a mounted laser in combination with GPS and other Inertial Measurement Units (IMUs) for precise positional accuracy. When air-crafts are used to collect the LiDAR measurement, positional measurement systems are used to determine the exact location beneath the aircraft. The mounted laser is then used to detect measurements between the relative distance of the ground and the aircraft (Zhang and Frey, 2006).

LiDAR is susceptible to inaccuracies that are comparable to satellites, which are normally used to create DEMs, like geometric coverage from aerial views. LiDAR is also susceptible to positional inaccuracies from IMU and GPS positioning. Nonetheless, LiDAR does have an enhanced resolution due to its relative height to ground level and most navigation systems have very precise positioning systems.

The drawback of LiDAR information is that it is not readily available around the world, as discussed in the state of art of the study by (Boroujeni and Frey, 2014). This can be seen in the test area, where coverage of LiDAR information is not available. In addition it is also generally not available to the public as an open source and so there are higher cost associated with it than with other DEMs. Therefore, LiDAR can be seen as one of the best methods for determining road grade but due to its limited coverage and associated costs it is an ineffective way to measure large–scale road gradient profiles.

3.2 Automated Methods for Determining Road Grade

There are several methods to determine the gradient of a road in an automated manner. Most techniques look to collect road grade information from vehicles, using GPS devices for positional information, and some sort of measuring device to determine the road grade. Consumer-grade GPS devices are not typically used by themselves to determine road grade due to vertical inaccuracies associated with the devices which is discussed in Section 3.2.5.

In order to determine which road grade method was best suited for ITS a set of criteria had to be defined. The criteria which was used in this dissertation is stated below:

- Does not require real time analysis, only post processing approaches are of interest.
- Scalable to any city wide ITS.
- Uses only freely available sources of information to aid the measurements.
- Utilises only the components available on most OBU.

Five studies were investigated in this dissertation. The following Section covers the core constituents most relevant to the five techniques chosen in the study for determining road grade with ITS:

The use of accelerometers and inclinometers to determine road slope are discussed in Subsection 3.2.1. Similarly, methods using multiple runs, with GPS and other sensor measurements to determine road grade, are reviewed in Subsection 3.2.2. The use of elevation values extracted from Digital Elevation Models (DEMs) is examined in Subsection 5.4.

Other methods that were not investigated due to the need for multiple sensors are stated in Subsection 3.2.4 and alternative methods using GPS receivers are discussed in Subsection 3.2.5. These alternative methods using GPS receivers were also not investigated further as they required either multiple GPS receivers in the vehicle or real–time estimation of road grade.

3.2.1 Accelerometers and Inclinometers

Inclinometers are devices that can measure changes in the pitch angle due to changes of gravity. Similarly, an accelerometer is a device which measures linear acceleration applied to a dynamic body, it can be used to measure tilt or pitch during static situations by looking at the change in acceleration due to gravity (Sherborne Sensors Whitepaper, 2014). Issues that plague the use of these sensors in determining accurate estimates of road grade from vehicles are noise and the ability to measure the difference between inclination of the road and the pitch angle of the vehicle.

A method for measuring longitudinal road grade was developed in the paper by (WANG

et al., 2013). The researchers looked at identifying areas in road networks that are prone to accidents, particular areas where there is a curved surface and a slope associated with it. The method looked at producing instantaneous longitudinal road grade, but it is hypothesised that the state based equation developed in the study could be adapted to identify vertical road grade. Similarly, a method to determine parallel mass and road grade longitudinal accelerometer was developed in the study by (Kidambi et al., 2014). The methods in the paper looks at different ways for determining road grade and mass in real time estimations. The researchers developed a new method for determining road grade and estimating mass using a longitudinal accelerometer. However, both these methods look at real–time determination of road grade making them unsuited for the purposes of this dissertation.

One approach that uses an inclinometer combined with different filtration techniques can be seen in the paper by (Mangan et al., 2002). The researchers identified three different filtration techniques that could be used to remove high frequency noise, caused by vibration of the vehicle, and low frequency noise, caused by acceleration and retardation of the vehicle. The researchers, explore the use of a low pass filter to remove high frequency noise cause by vibration of the vehicle and presents three approaches to remove the low frequency noise caused by acceleration/retardation. The analysis of the results can be performed in a post–processing analysis making this method suited for the purposes of the dissertation.

Furthermore, (Massel et al., 2004) investigated different techniques for determining uphill road gradient and the difference in pitch angles of the vehicle. The study looks at real-time determination of inclination angles, differentiating the gradient of the road and the pitch angle of the vehicle. Even though this method uses a real–time analysis, it highlights the importance of the distinction between the pitch angle of the vehicle and the inclination of the road.

Therefore, the use of accelerometers and inclinometers does provide a good determination of road grade. However, the need to differentiate between the vehicle pitch and the road inclination and the noise created by acceleration, retardation, and vehicle vibrations needs to be addressed in order to use this method. Once more, only methods that could be done in a post–processing manner could be examined for this study.

3.2.2 Multiple Runs

One way that vehicles can estimate road grade is by an enhanced approach which uses multiple runs with a GPS and/or other sensors. By continuous runs over a road segment, errors in previous estimates can be mitigated with an averaging process to narrow out the true value of the road gradient . Repeated runs using a GPS receiver in a vehicle can be used to create a Digital Elevation Models (DEM) or a dedicated road grade digital topographic road maps.

Multiple runs of farming equipment equipped with GPS devices were used to create high precision estimates for a DEM in the paper by (Aziz et al., 2006). As will be seen later on in the Chapter, road gradient can be determined from DEMs, shown in

Section 5.4. Although this paper does not explore the use of the DEM in road grade estimates, but rather, considers its use in related work for precision farming, it does highlight the potential of continuous runs over multiple seasons to produce highly accurate DEMs, and enforces the ability to mitigate GPS errors through multiple runs.

One approach that takes a similar approach of using multiple runs to create accurate topographic road maps can be seem in the article (Sahlholm and Johansson, 2010). The paper looks at using vehicle sensor data fused with GPS, using a Kalman filtering technique to produce accurate topographic maps which were then used for look-ahead purposes in Heavy–Duty Vehicles. However, the approach discussed investigates embedded devices in combination with GPS receivers, and requires access to a lot of different signals from a vehicle in real–time. Therefore, an approach that would allow for continuous runs with post processing abilities with less requirement of vehicle parameters is more desirable for the study at hand. However, the authors Sahlholm and Johansson, states that "GPS position estimates are generally bias free when averaged over long time periods and the error is approximately normally distributed.", which indicates the statistical results that can results from utilising multiple GPS measurements.

In the paper by (Boroujeni et al., 2013) such a technique is explored. The researchers look at using multiple runs from a standalone GPS with a Barometric Altimeter (GPS/BA) to increase the accuracy of road grade estimates. This could then be used for second by second basis of fuel consumption models. GPS/BA devices are consumer grade GPS devices that have barometers to aid altitude values in periods of temporary signal loss, as the altimeters are not susceptible to signal loss from satellites. Through multiple runs, using the same direction of travel, the researchers were able to quantify the road grade ability of multiple runs. The runs were divided into segments of specified lengths and linear regression of the points, in the segment, were used to estimate the slope for that segment. From the slope of each segment, the slope coefficient was used to determine the associated road grade for that specific segment. Therefore, as the method suggested in this study used the collection of runs to estimate road grade in a post–processing manner, this manner is suited to this dissertation.

The concept of multiple runs discussed previously was further explored in a later study by (Yazdani Boroujeni and Frey, 2014). The study focused on the difference between mapping grade GPS devices and several consumer GPS/BA devices in being able to estimate road grade. The results were compared against Light Detection and Ranging (LiDAR) estimates of road grade. The results showed that the mapping grade estimates produced highly precise estimates of road grade with multiple runs but were more susceptible to loss of signal periods compared to GPS/BA estimates. It was also shown that with enough multiple runs of the consumer GPS/BA traces could produce as accurate estimates as the mapping grade GPS, and that of LiDAR estimates. The researchers suggested that mapping grade GPS could be used to get a good estimate of the road grade and then in periods of temporary signal loss (like the area indicated in the study – an overpass on the highway) GPS/BA estimates could be used to provide accurate road grade profiles.

Similarly, a geometric model of the Kansas highway was produced using repeated GPS traces taken from a test van (Ben-Arieh et al., 2002). The technique investigates an extensive post–processing and data cleansing approach combined with geometrically defining a 3D representation of a highway using a B-Spline approximation of the different segments. As the procedure for determining road grade from the slope of the geometric representation is roughly the same as the design drawings procedure, this approach may be appropriate for determining road gradient.

Therefore, using multiple runs to create large–scale road grade profiles offers repetitive process that over time would produce highly accurate estimates. A limitation of these approaches is that in areas of complete GPS signal loss, like going through tunnels, as the process depends completely on GPS signals. Similarly, in the case of ITS implementation there would be a large amount of data that needed to be collected and stored which would create an issue with the storage and management of the data.

3.2.3 DEM

Digital Elevation Models (DEMs) are geographic datasets of elevation points for specific terrain coordinates on a digital map. There are many different DEMs available: they differ by resolution; horizontal accuracies; and vertical accuracies. The digital maps are segmented into degrees and then furthered segmented into block grids. The elevation information is taken at the centre point of the block and represents the true elevation at that specific point. The entire block will be represented by that elevation value at the centre point. More description on the specific DEMs used in this dissertation will be given in Chapter 4.

The impact of road grade on fuel consumption for light vehicles was considered in the study by (Wang et al., 2015), carried out in Beijing. The researchers use Google Earth DEM to extract elevation points, using a vector map of Beijing's road network, at a set distance of 5 m, to measure the slope of the road. The method then calculates the road grade for a set segment considering the start and end elevation nodes. Similarly, large–scale road elevations were extracted using the Google elevation Application Program Interface (API) in the paper by (Levin et al., 2014). Both methods use a commercial product that does seem to provide highly accurate estimates. However, since the elevation estimates provided by Google are under specific licensing and there is a querying limit associated with the API an alternative approach would be more desirable for this dissertation. However, these studies do show the associated accuracy in Google's elevation estimates, that they have been used extensively in two larger scale studies to determine the impact of road grade. Hence, it will be seen later in Chapter 6, that the Google elevation API is used in this dissertation as an equivalent to evaluate the results obtained in experiments against.

Another study by (Henriques and Bento, 2013), looked at using the Advanced Spaceborne Thermal Emission and Reflection Radiometer (ASTER) Global-DEM (GDEM) to determine road slope angles for bicycle traffic simulations. The ASTER GDEM provides estimates for elevation for 80% of the land surface on 30x30 m grids/blocks (Asterweb.jpl.nasa.gov, 2016). In the study by (Henriques and Bento,

2013), the GPS system samples every second, and therefore multiple GPS points cover the same grid/block in the DEM, especially when coupled with the relative speed of the cyclist. Since the grids only have a true elevation at the centre point, the researchers used an adapted bilinear interpolation technique to determine a better estimate of the true elevation of the GPS points on each grid, which the GPS points were not located in the centre of the tile. The slope angle was determined from the interpolated data and was used to calculated the road grade.

Similarly, the researchers Boucher and Noyer look at a method of determining road grade instantaneously using a combined process that looks at a fusion process of ASTER GDEM, OpenStreetMaps (OSM) and a vehicle equipped with two GPS devices. The paper is an expansion to the previous paper by (Boucher and Noyer, 2012), with the aim in achieve better estimates of road grade using DEMs, by accounting for all of the errors associated with the vehicle dynamics, map matching and with the DEMs. Although the paper by (Boucher and Noyer, 2014) uses two GPS receivers and an instantaneous process to estimate the road grade, making it not applicable for this dissertation, it does highlight the horizontal inaccuracies in DEMs and the need to account for it.

Lastly, the National Renewable Energy Laboratory (NREL) developed a method for smoothing out erroneous data in the Shuttle Radar Topography Mission (SRTM) elevation, which was appended to GPS speed traces. The smoothing process intended to smooth and remove discrepancies in elevation profile of a vehicle, making it appropriate for determination of road grade (Wood et al., 2014b). The SRTM is a near global DEM and has recently released high resolution, 1-arc second, for coverage areas outside of the United States of America (U.S.Geological.Survey, 2016). The researchers Wood et al., used a smoothing process that filtered out a better approximation of the elevation profile, in order to smooth the profile of high frequency components and remove erroneous discrepancies caused by the collection methods used in satellites. From the elevation profile the road grade could be determined. The researchers compare their approach against the Advanced Driver Assistance Systems (ADAS) Navteq road grade data-set, first using a small scale test case area and then a large–scale data-set, concluding that the approach for the most part provided accurate estimates of road grade.

In summary, determining road grade from DEMs has a significant advantage in comparison with most other approaches seen in this dissertation as many DEMs are freely available and provide a high level of accuracy when combined with GPS locational information which have high positional accuracy.

3.2.4 Sensor Fusion with Barometers and Other Components

Various methods look at using multiple sensors to calculate road grade. One methods uses a combination of GPS and other vehicle parameters that can be accessed from most modern Controller Area Network (CAN bus), although another approach uses a combination of sensors that can be found in specific vehicles like Heavy–Duty Vehicles (HDVs).

In the paper by (Parviainen et al., 2009), the researchers use an Inertial Measurement Unit (IMU) combined with GPS, a barometer and an accelerometer. The method used the GPS device to calculate the positional information and help correct the error accumulation with the IMU. Whereas, the barometer was used to calculate the vertical velocity of the vehicle and this was used to calculate an estimate of the road gradient. This estimate was then used to aid to correcting measurements taken from the accelerometer. The aim of the research was to create estimates of road grade with reduced inertial systems capable of producing accurate estimates of road grade.

Similarly, sensor fusion can be done with torque and velocity measurements to create a correction type estimate of road grade in real–time (Jansson et al., 2006). The approach looked at using the majority of sensors that are available on Heavy Duty Vehicles (HDVs) on the basis that reliable sensors for the sole purpose of estimating road grade are often too expensive.

The approaches state in this Subsection previously produce highly accurate estimates of road grade, but the sensor fusion approach actually uses a combination different measurements: for example an accelerometers, a gyroscope and a high resolution barometer. Therefore, these methods use too many sensors that are typically available in to most On Board Units (OBUs) and take an instantaneous measurement. The methods also rely on real-time estimations. On the other hand, it does signify the importance of the performance gains that are possible from sensor fusion.

3.2.5 GPS

Consumer GPS devices have a high horizontal accuracy (within 3 m) but a high precision of horizontal and vertical accuracy is needed to determine road grade estimations from GPS devices. Once more, consumer GPS devices have vertical inaccuracies which can be almost double that of the position accuracy (Wing et al., 2005). Inferring road grade directly from consumer grade GPS data, using the change of elevation compared to the distance covered method, can result in road grade that is prone to a high level of inaccuracy due to the vertical inaccuracies associated with GPS receivers. Therefore, most approaches at investigating road grade using GPS receivers explore ways to improve the process to be able to produce accurate estimations of road grade.

The paper by (Bae et al., 2001) investigated estimating the longitudinal dynamics of a vehicle to aid adaptive cruise control models in attaining desired levels of safety and closed loop performance. The paper presents two methods to determining road gradient. The approaches use a combination of one and two GPS receivers: to measure the altitude of the vehicle in the pitch plane; and a ratio of the vertical to horizontal velocity at a single antenna to estimate road grade. The resulting road grade is used with the engine torque of the vehicle to estimate the mass of the vehicle.

Similarly, the study by (Boucher and Noyer, 2012) estimates the road gradient in combination with a map fusing process. The study (Boucher and Noyer, 2012), looked at a real time update of map attributes (like road gradient) for personal nav-

igation system or other such systems. The researchers use a Uniform Kalman Filter and mahalanobis fusion technique using two GPS receivers to estimate road gradient information at specific locations on the OpenStreetMap (OSM) road network. The road grade estimation are not the primary concern of the paper but rather the real time update of map attributes. However, the approach taken does seem to prove a high level of accuracy in determining road gradient in real time.

The limitations of these approaches for the study at hand is the need for real time estimations, the use of multiple GPS receivers to obtain a high accuracy of the road grade and the high level of complexity associated with the approaches. However, these approaches highlight the difficulty in measuring accurate road grade using consumer-grade GPS devices alone.

Chapter 4

Background

This Chapter's purpose is to provide the reader with background information about the topics that are most relevant for the replication of studies performed in this dissertation. In addition, supplementary information relevant to subjects investigated in this work will be provided.

The Chapter is organised as follows: Section 4.1 looks at the component that are available on the Bach box On-Board Unit (OBU). Section 4.2 investigates the errors associated with GPS devices. Section 4.3 provides background information into Splines and their applications. Section 4.4 introduces Digital Elevation Models (DEMs) and their associated errors. Section 4.5 investigates the application of accelerometers. Section 4.6 looks at Digital Signal Processing (DSP) techniques. Lastly, Section 4.7 investigates the application of interpolation techniques used in this dissertation.

4.1 Bach Box

The Bach box is an on-board telematics unit, or rather an On-Board Unit (OBU), designed for vehicles. That ZF offers to its customers in order to aid their automotive needs. The Bach box uses a combination of sensors and components to provide real time and post–processing data for vehicle analysis and fleet management purposes. For instance, ZF currently provides Applications (Apps) that afford: real time diagnostics of vehicle performance; area monitoring of fleet information; and other such applications (Openmatics, 2016a).

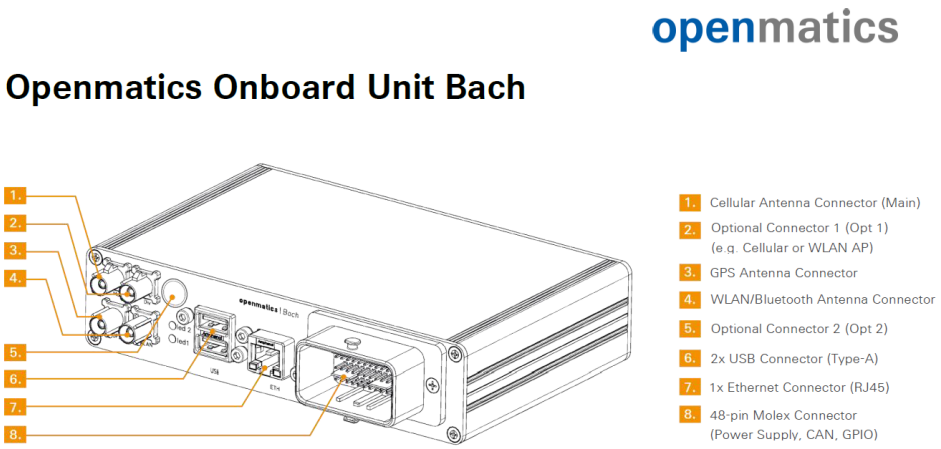

Figure 4.1: The Bach box, the On-Board Unit used in the experiments, with some of the components associated with the unit shown in the legend on the right of the image (Openmatics, 2016a).

The Bach box is the successor to the previous Mozart Box (Openmatics, 2016b), and is currently in use in many transportation fleets. There are a number of extra components on the Bach module that enable it to provide quantitative and qualitative data on vehicles. For instance it is equipped with a GPS receiver, GSM/GPRS modem, 3-Axis Accelerator/Magnetometer, an Altimeter,.etc. Some of these components can be seen in Fig.4.1. All these devices can contribute to an advanced collection of vehicle parameters. The Bach box also has an interface to connect to the vehicles Controller Area Network (CAN bus). This enables the OBU to collect vital information on the diagnostics of each vehicle in a fleet.

The Bach box can collect information from the vehicle and its sensors in order to store or transmit the data, to provide real time or post processing analysis of data. ZF Openmatics Bach box allows for information to be directly uploaded to the ZF Openmatics cloud service using the cellular antenna or to other devices using the WLAN/Bluetooth antenna.

4.2 GPS

Global Positioning System (GPS) devices are a method of obtaining accurate 3-dimension (3D) positional information almost anywhere on earth. GPS signals are transmitted from transmitters (satellites) to receivers by radio waves. Positional information is determined using triangulation, this process takes three know locations to determine 2D positional information by cross referencing the known locations against each other. A similar process is preformed by cell towers to locate users (Kaplan and Hegarty, 2005). Unlike 2D triangulation, 3D triangulation or rather trilateration is a process used by GPS to calculate 3D positioning information of receivers on earth and requires four satellites to estimate 3D positional information.

A GPS receiver can only estimate its exact position if four satellites are in sight of the receiver and the exact positional information of the satellites are known to the receiver. The satellites send their positional information along with an estimated time of sending the message to receivers in the form of an almanac and ephemeris messages. The receiver estimates their exact position from the time-of-flight (TOF) information by using the TOF multiplied by the speed of light to estimate distance from the transmitter. The distance from four satellites at known positions means the position of the receiver can be determined (Kaplan and Hegarty, 2005).

GPS satellites transmit information using Pseudo Random Noise (PRN) codes transmitted over Code division multiple access (CDMA). These PRN codes are divided into two message types: a short (C/A) course acquisition information, which receiver use to initially acquire positional information; and a long (P) precision codes, which receivers use to accurately estimate position. Almanac information is represented by the short course acquisition information, it is a less precise measurement and is used to gauge rough estimates of satellite constellations for GPS receivers to fix onto GPS satellites. However, ephemeris messages are used for exact positional fixes with GPS transmitters and are used to estimate the TOF from a transmitter (Kaplan and Hegarty, 2005).

GPS receivers use the World Geodetic System (WGS-48) where the estimated position are of an ellipsoid representation of the earth. There can be discrepancies between the actual positions on the earth and measurement position recorded from the GPS receiver due to the difference between geoid and ellipsoid height information. The geoid height information represents the Mean Sea Level (MSL) vertical zero reference point at the specific area, and is estimated by the sea's surface ability to conform to gravitational fields. However, due to the MSL ability to conform to gravitational fields there are differences in true zero MSL levels around the world. Similarly, the ellipsoid height information is the estimated zero vertical position of an ellipsoid representation of the earth, at a reference position. Hence, there is a difference between the vertical reference of the geoid and the ellipsoid height information (Kaplan and Hegarty, 2005).

To estimate the positional information determined from satellites, GPS uses Position Dilution of Precision (PDOP) information to estimate the geometrical position of a satellites' influence on GPS receivers ability to estimate accurate positional inform-

ation. PDOP is a representation of both Vertical (VDOP) and Horizontal (HDOP) information of satellite geometry. The DOP information is counter-intuitive, with higher values of DOP inferring lower precision in positional estimates, whereas lower values indicating higher precision in positional estimates (Laboratory, 2016). However, there is a difference between good/low values of PDOP estimates and visibility of satellites. For example, a receiver may have good/low PDOP estimate (meaning that there are enough satellites with an appropriate geometry above the receiver) but if there are obstacles blocking the visibility of the satellites (like buildings in urban areas) then measurements of the receiver will be affected.

There are three classifications of GPS receivers: (A) consumer-grade; (B) mapping-grade; and (C) survey-grade. Mapping and survey-grade GPS receivers offer highly precise locational information, between 1 cm and 2–5 m (Wing et al., 2005). However, consumer-grade GPS devices offer higher horizontal positional accuracy nowadays, and they offer a much more affordable option than mapping and survey-grade GPS devices according to (Boroujeni and Frey, 2014). (Boroujeni and Frey, 2014) used estimates from mapping-grade Differential-GPS (DGPS) devices, valued at fifty times the price of consumer-grade GPS/Barometer aided devices, according to the study. The main differences between consumer-grade and mapping-grade GPS devices are the minimum set PDOP level needed before mapping and survey-grade GPS devices can start acquiring positional information, unlike consumer-grade GPS devices which have no minimum setting. This coupled with an additional averaging of positional information performed by mapping/survey-grade GPS devices makes them more accurate in determining positional information (Wing et al., 2005).

There are many errors that can affect GPS receivers (Laboratory, 2016; Kaplan and Hegarty, 2005):

1. Atmospheric
    - Tropospheric Delay – the troposphere is a layer of the earth's atmosphere which is located around 60 km above the earth's surface. The tropospheric delays a are result of the relative density of the layer due to wet (water vapour) and dry gases and change in density as radio signals travel through to receivers.
    - Ionospheric Delay – the ionosphere is a layer of the earth's atmosphere around 1000 km above the earth's surface. The delay is caused due to the total ionized electron content in the ionosphere creating a propagation delay in the GPS signal.
2. Multipath delay – when a receiver is in an area where the GPS signal can be reflected off obstacles, like an urban area, there will be multiples of the sampled signal delayed at different times due to the reflected time delay.
3. Shadowing – is the loss or attenuation of radio signals due to loss of sight of signals. Radio signals can be blocked by obstacles and the resulting effect can be a reduced intensity of the original signal being received at the receiver.
4. Clock delays

- Satellite clock delay – satellites have a relatively accurate atomic clock, however the clock will drift over a 24 hour period until it is reset by ground base station estimates. These drifts are only in the matter of milliseconds but the variance can make a substantial difference in positional estimates of receivers.
- Receiver clock delay – receivers on the other hand do not use a relatively precise atomic clock but rather use crystal clocks which are less expensive and less reliable. These clocks will create discrepancies over time.

5. Number of satellites and geometry of satellites – receivers need a minimum of four satellites to estimate 3D positional information. However, the placement of the satellites constellation affects the accuracy of the estimates. Especially, the vertical accuracy of the GPS receiver.

6. Ephemeris estimates – satellites transmit ephemeris information which contains an estimate of satellites' positional information. These estimates can be marginally imprecise and slight discrepancies might cause greater inaccuracies in positional information.

7. Receiver measurement noise – receiver's are susceptible to measurement noise created by the electronics used in the receiver devices.

There has been progress to improve GPS measurements by using correctional information. The main improvements to GPS devices have been the integration of Differential and Dead–Reckoning systems with GPS to improve the positional information. Differential-GPS (DGPS) utilises base stations at known locations to correct positional errors, whereas Dead–Reckoning GPS (DR-GPS) use Inertia Measurement Units (IMU) to correct GPS measurements during temporary signal loss.

Dead Reckoning Global Position Satellites (DR-GPS) receivers are generally more costly but they provide higher accuracies within the longitudinal and latitudinal positions. They can also help alleviate some issues that arise with GPS services from urban environments and tunnels. GPS traces by themselves can be very unreliable in vehicle tracking, especially in urban areas where the line of sight of GPS receivers and transmitters are blocked by high rise buildings and effects of multipath cause constructive and destructive interference in the signal. This is why developments in Dead-Reckoning and Inertia Navigation systems have been so important in recent years. These systems combined with GPS provide a better estimate of accurate positioning traces from a vehicle. Dead–Reckoning (DR) devices use a magnetic compass and odometer to determine the vehicles position and when used in conjunction with GPS greatly increase the performance of GPS devices in determining vehicle positions. DR systems allow GPS devices to overcome problems associated with coverage during periods when the devices are going through tunnels or underneath overpasses. GPS devices perform very badly when going through tunnels or under overpasses due to the loss in signal. DR systems greatly improve position accuracy of the vehicle in the longitude and latitude positioning but do not have a great corrective behaviour for altitude accuracy.

DGPS use ground stations to relay and correct GPS error in position of the receiver (Arnold and Zandbergen, 2011). DGPS use time differences between TOF information between a base station and transmitter to estimate errors in the GPS signal. The base station then transmits a corrected signal to the receivers. The corrected signal can accounted for a large number of errors, like the propagation delay of the time between the satellite and the receiver. GPS errors can be corrected by relaying the information to the base/ground stations to make correction and therefore improve the accuracy of the signal. The ground based stations can be used as reference to position, which can relay signals to GPS receivers to help improve accuracies in estimating their own position. These systems are called augmentation control system. Examples include the Wide Area Augmentation System (WAAS), the augmentation system in North America, and European Geostationary Navigation Overlay Service (EGNOS), the augmentation system in Europe. However, there are some errors that can not be accounted for which occur between the receiver and the base station, such as signal loss in urban areas and multipath.

4.3 Splines and B-Spline Approximations

A spline is a long flexible piece of wood that designers and engineers used to assist with constructing frames of auto-mobiles and aircraft. The concept of how splines function is as follows, heavy weights are applied along the spline in order to help conform the spline around certain points; the weights would stabilize the spline at specified points and then, in-between the points; the spline takes its natural formation causing a natural curvature between the points.

The physical solution has many draw backs as designers are restricted by the splines' ability to conform to a curved surface. Another downside of spline approximations in general is that there is no closed form solution for them mathematically; this means that there are an infinite number of operations possible. Splines made advancements in the 1960s when Pierre Bezier developed a computer aided program that allowed the drawing of smooth curves on a computer screen. Splines represented a good way to specify smooth curves on a computer screen (Benjamin T. Bertka, 30th, May 2008).

A Beizer curve allows us to represent a curve with four points and it represents a special case where the Bestein polynomial can be specified to degree (n) of three. The Beizer curve has points that cause maximum pull and points that cause less pull on the curve. This is why on a curve with four control points the maximum pull (must curvature) can be seen with the middle points. The 'B' in B-Spline stands for Basis, specified by the Cox–de Boor formula. B-Splines, like Biezer curves, use control polygons to define the curve. A uniformly open uniform knot vector B-Spline can be derived to actually be a continuous Biezer curve (Starkey, 2016). However, this is a specific case and generally the B-Spline curve is calculated with a closed uniform knot vector and this can be derived from the recursive Cox-de Boor formula.

To show the difference between the uniformly open uniform knot vector and the open knot B-Spline the matrix formation taken from (Starkey, 2016) is shown below, for four control points, in Equation 4.1 and Equation 4.2 respectfully:

$$P(t) = \begin{bmatrix} t^3 & t^2 & t & 1 \end{bmatrix} \frac{1}{6} \begin{bmatrix} -1 & 3 & -3 & 1 \\ 3 & -6 & 3 & 0 \\ -3 & 0 & 3 & 0 \\ 1 & 4 & 1 & 0 \end{bmatrix} \begin{bmatrix} P0 \\ P1 \\ P2 \\ P3 \end{bmatrix} \tag{4.1}$$

$$P(t) = \begin{bmatrix} t^3 & t^2 & t & 1 \end{bmatrix} \begin{bmatrix} -1 & 3 & -3 & 1 \\ 3 & -6 & 3 & 0 \\ -3 & 3 & 0 & 0 \\ 1 & 0 & 0 & 0 \end{bmatrix} \begin{bmatrix} P0 \\ P1 \\ P2 \\ P3 \end{bmatrix} \tag{4.2}$$

The difference is the matrices is due to the knot vectors chosen. The uniform knot B-Spline, seen in the Equation 4.1, will take a knot vector of length 8 and will be uniformly distributed, so the knot vector would be (0, 1, 2, 3, 4, 5, 6, 7, 8). Therefore, when calculating the basis function for each control point the following matrix will be determined. In comparison, the open uniform will have a vector like (0, 0, 0, 0, 1, 1, 1, 1).

The effect of the differences in the B-Splines, seen in Equations 4.1 and 4.2, is such that the Uniform knot vector Equation 4.1 will curve around the control points but will not start at the first control point or end at the last control point. It will start in-between the first and second control point, and end in-between the last and third control point. Therefore, it will be influenced by the control points but will seem to start and end in-between the first and last control point. Whereas, the Open uniform knot vector will start from the first control and end at the last control point.

4.4 Digital Elevation Models

Digital Elevation Models (DEMs) are models of the terrain that include elevation information for specific locations (U.S.G.S., 2016). The DEM samples the terrain at regular intervals. DEMs created by satellites will usually have a resolution associated with them, which corresponds to the angle in which the satellites recorded the elevation information known as arc seconds.

DEMs are bare surface representations of the earth and can be referred to as Digital Terrain Models (DTMs). The bare representation of the earth is taken, meaning that man made constructs and vegetation are left out of the DEM and the bare surface is only present (Geography, 2016). There is a distinction between DEMs and Digital Surface Models (DSMs), where DSMs represent the true elevation recorded at the specific location, therefore vegetation and man made buildings are recorded (Geography, 2016). This is typically seen in LiDAR measurements. This dissertation only deals with DEMs created by satellites due to their prevalence of coverage around the world and the open-sourced availability of these DEMs.

4.4.1 SRTM

The Shuttle Radar Topography Mission (SRTM) was set up to produce high quality data for Digital Elevation Models (DEM) around the world. One of the key aims of SRTM is to make DEM information available to the public free of charge. The SRTM mission was originally carried out by NASA in February 2000 and provides "near-global coverage (up to 60 degrees north and south)" (U.S.Geological.Survey, 2016).

The SRTM recorded information about ground topography and elevation in a collection of recordings carried out with low orbital satellites. The STRM divides up area that it is recording into tiles of 1x1°, each tile is associated to a specific degree in latitude and longitude. The information recorded was categorized into either 1-arc second (approximately spatial resolution of 30 m) or 3-arc second (approximately spatial resolution of 90 m) DEMs depending on the availability of information captured. The majority of North America was categorized as 1-arc second DEM whilst everywhere else is categorized as 3-arc second DEMs until recently when new SRTM 1-arc second DEM became available in some areas outside the U.S.A. (Survey, 2016a).

The main difference between the categories is the size of tiles and therefore the accuracy of information recorded (with smaller tiles providing more detailed elevation information about an area). 1-arc degree SRTM refers to information recorded from the satellite that is at a resolution of 30 m at the equator, meaning that information is recorded on 3601x3601 blocks of 30x30 m within the 1x1°. Similarly, 3-arc degree SRTM data means that the information is recorded on 1201x1201 blocks of 90x90 m within the 1x1°.

4.4.2 ASTER

The Advanced Spaceborne Thermal Emission and Reflection Radiometer (ASTER) Global Digital Elevation Model (GDEM) was a joint operation by the Ministry of Economy, Trade and Industry (METI) of Japan and National Aeronautics and Space Administration (NASA) of United States of America (Asterweb.jpl.nasa.gov, 2016). One of the main goal of the ASTER GDEM was to provide global coverage of elevation information of the earth's surface.

The ASTER GDEM covers 95% of the earth's surface and is currently only available for research purposes (jpl.nasa.gov , 2016). There are different versions of the ASTER GDEM available: the first version used the 3N spectral band and had a vertical accuracy of approximately 20 m (with a 95% confidence interval); the a later version (ASTER V2 GDEM) was released on the 17th of 2011 and has a vertical accuracy of 8.86 m (with a 95% confidence interval) (jpl.nasa.gov , 2016). The ASTER V2 GDEM was recorded with the 3B spectral band.

The ASTER GDEM is provided in 1x1 degree tiles and is available in 1-arc second resolution, meaning that the elevation information is provided in 3601x3601 blocks on 30x30 m grids.

4.4.3 Errors Associated with DEMs

There are vertical and horizontal accuracies associated with DEMs. The horizontal inaccuracies include errors associated with the true horizontal and vertical position measurements.

The paper by (Mukherjee et al., 2013), investigated the vertical accuracy of the SRTM and ASTER DEMs in a mountainous region in India. The main findings of the results are that DEMs, like the SRTM and ASTER DEMs, are subject to different types of errors. Those errors being: gross errors; deficient orientation; and random errors. This means that reading from the DEMs could be subject to any of these errors, where single values may be affected by random errors or a large number of elevation values (gross) are affected. Similarly, the study also concluded that "..other issues related to DEM accuracy are grid spacing and interpolation techniques". When considering the SRTM 3-arc second DEM it can be intuitively seen that the grid size of 90x90 m means that the elevation estimates are not accurate for a large selection of the grid coverage. Furthermore, the interpolation technique that might be used to interpolate estimates that are not on the centre of the tile may not truly reflect that location. On the other hand, the study by (Mukul et al., 2016) performed an accuracy analysis on the 1-arc second SRTM DEM. The results obtained in the study suggested that there are still outlier measurements in the data-set and that these outliers may affect the overall accuracy of the measurements.

The effect of the inaccuracies in the DEMs means that the measurements for all areas may not actually be true estimates of vertical accuracy. As they may be affected by horizontal or vertical positional errors.

4.5 Accelerometers

Accelerometers measure acceleration or force due to gravity and as such can be used to measure the tilt or inclination (Sherbornesenors, 2014). There are different type of accelerometers from a single, dual and triple axis accelerometers.

The accelerometer found in the Bach box is a triple axis accelerometer and so acceleration due to gravity can be measured in three dimensions. The accelerometer measures acceleration in a digital measurement and so acceleration in three dimensions is given a numerical output (x, y, z). These outputs can be used to determine the tilt measurement of the accelerometer.

The angle of tilt, θ, can be measured using arbitrary x and z measurements from an accelerometer using the Equation below (Pedley, 2013):

$$\tan\theta = (\frac{-x}{z}) \tag{4.3}$$

4.5.1 Mathematical Morphology

Mathematical Morphology (MM) is a tool used in image analysis to improve image quality. The principle of MM assumes that images consist of structures which can

be handled by theory of sets, whereby the groups of pixels are classified as sets (Biomathematics and Scotland, 2016).

Application of the theory of sets to MM assumes that groups of pixels can be arranged into particular sets. Taking a black and white image for example, white pixels and black pixels are complementary and performing an operation on one set will have an effect on a complementary set.

The most basic morphology operation is that of erosion. The complementary operation of erosion is dilation. The two widely used operations in MM are opening and closing operations. Opening operations are an erosion operation followed by a dilation operation. Similarly, closing operations are a dilation operation followed by an erosion operation. Both opening and closing operations are idempotent operations meaning that applying the operations more than once produces no further effect.

4.6 Digital Signal Processing

Digital Signal Processing (DSP) looks at applying signal processing techniques to a discrete signal. There are many parts to digital signal processing. This Section seeks to highlight the most significant aspects of digital signal processing to this dissertation.

4.6.1 Digital Filters

Filters are a way to remove unwanted components from a signal. There are two main classifications of filters, analogue and digital filters. Analogue filters deal with continuous time series signals whereas digital filters are the opposite and only deal with finite time series (Kester et al., 2003).

Both have different benefits and detriment in different circumstances but digital filters provide a useful way to estimate to be easily implemented in a software approach to analysing signals as the physical resistor and capacitor components of the continuous analogue filer with digital representations of them.

There are several types of digital filters but they can essentially be divided into two groups of Finite Impulse Response (FIR) filters and infinite response filters. By varying the weight of the coefficients and the numbers of filter taps virtually any frequency response can be realized with an FIR filter (Kester et al., 2003).

Filtering allows us to remove different frequencies that we are interested in a signal. Filters that allow the extraction of only high variations in the time series are called High–Pass filters. Whereas filters that allow the extraction of low variations in the time series are called Low–Pass filters. The last kind of filter is called the Band–Pass filter which combines the Low–Pass filter and the High–Pass filter and only allows the intermediate frequencies to pass through the filter.

Smoothing is a form of filtering that is associated with Low–Pass filters as it tries to remove the high frequencies in the time series and therefore produce a smoother

profile (Meko, 2016). The high frequencies in the time series correspond to high variations in the profile whereas the low frequencies correspond to the small variations in the time series.

Statistical smoothing is a form of Low–Pass filtering which incorporates a series of weights that when cumulatively multiplied by consecutive values of a time series produce a smoother signal. This process can be thought of a sliding window through a time series multiplying the coefficients against the values and getting a cumulative product for each point. Sometimes these weights are called the filtering function and the length of the filter is the total number of weights (Meko, 2016).

Low–Pass filters deal with filtering out parts of the signal that go over an extended frequency. This can be seen as allowing component of the signal to pass through that are below a certain frequency but cutting off or attenuating any parts of the signal over the set frequency.

Typically the weights in a filter will sum up to one, this guarantees that the filtered series mean should approximate to the mean of the original series (Meko, 2016). Another important part of filter weights is that they are symmetrical, in order to avoid phase shifts.

4.6.2 Effects of filtering on the time series and its spectrum

The effect of the Low–Pass filtering on a pure sine wave can be seen as a decrease in the amplitude of the signal (Meko, 2016). Although, most time series are a combination/mixture of different frequencies and so the effect of the Low–Pass filter on the time series is a smoothing effect as high frequency variations are removed from the signal and low frequency variations remain intact. Comparatively, if a time series has little or no high variations in the signal then the Low–Pass filter will have little effect on the overall time series.

4.6.3 Average Sliding filter

The averages moving/ sliding filter performs a running average of the number of taps or weights available. It generally is reasonable to use a simple version where the number of taps is limited to only a few taps to make it easier to implement rather than using the entire length of the data-set as the number of taps (Kester et al., 2003).

$$y[n] = 1/N \sum_{k=1}^{M} x(n-k) \tag{4.4}$$

Taking the above formula and setting N=5 (5 taps) we can then state that the weights along the time series will be wi=0.2,0.2,0.2,0.2,0.2 and therefore to preserve the symmetry along the time series in the filtered output the values of k will typically be k=-2,-1,0,1,2. Therefore any point along the time series will be filtered by

the cumulated sum of the coefficient's multiplied by the x[n-k] values.

$$y[n] = h[n] * x[n] = \sum_{k=1}^{M} h[k]x[n-k] \tag{4.5}$$

The symmetrical approach preserves the phase shifting of the filtered signal but the filtered time series will need to be extended forward and backwards to preserve the total length of the data-set (Meko, 2016). This means that some of the points lost off the back and the front of the series will not be filtered, as the filter value of k will prevent this. Without the use of extensions, the total length will be equal to(N-1)/2. So in this case two points from the front and two points from the back will be removed from the data-set (Meko, 2016).
In order to overcome this, there is typically two approaches, either to: substitute in the long term mean or median or to use reflecting the data across the end points (take the mean across the end points) (Meko, 2016).

The frequency response of a filter describes the effects of a filter or sinusoid inputs at different frequencies. The frequency response has two components the amplitude and the phase. The phase describes the shift in the position of the wave at the frequency along the time axis.

4.6.4 Exponential Filter

Exponential smoothing is typically used on time series where there is no systemic trends and/ or seasonal components. The exponential smoothing is generalized to the "Holt's-Winters" procedure in order to deal with trends that do have a seasonal or trend. This is why Holt's method has been adapted as a forecasting tool for stock prices and other process that have a stochastic nature combined with a seasonal trend (Ord, 2004).

$$s_t = \alpha \cdot x_t + (1 - \alpha) \cdot s_{t-1} \tag{4.6}$$

The Equation 4.6 illustrates the exponential filter. The filter can be seen as a moving average filter which uses a raw input component, x_t, and multiplies that component against a weight, α. This is then added onto, one minus the weight multiplied by the previous input component s_{t-1}. Usually, the weight is decided by the one over the RC component. However, in digital applications the weight can be set.

4.6.5 Binomial Filter

The Binomial filter uses weights that are proportional to the binomial coefficients. The coefficients can be computed by repeatedly convolving the weights [0.5,0.5]. These weights correspond to the probability of true or false.

$$b0 = 0.5, 0.5 \tag{4.7}$$

$$b1 = b0 * b0 = 0.25, 0.5, 0.25 \tag{4.8}$$

As the length of the filter, N, becomes large, the weights for the Binomial filter approximates towards a Gaussian distribution, or normal distribution (Aubury and Luk, 1996). Using a sliding filter the coefficients of the binomial distribution can be applied to a time series.

4.7 Sampling and Interpolation

This Section will continue the background information on Digital Signal Processing (DSP) but will look at two different interpolation techniques that are available. Namely, the linear interpolation, in Subsection 4.7.1, and bilinear interpolation, in Subsection 4.7.2.

4.7.1 Linear Interpolation

Interpolation is a way to fill in or estimate unknown values in a data-set. Usually this is an average of the known samples next to the known sample (Vaseghi, 2008). Interpolation can be used to interpolate missing points in a time series.

Linear interpolation approximates a missing value by using linear regression between two know data points to estimate the missing value (Schafer and Rabiner, 1973). The missing value can be estimated using the formula below:

$$y = y_0 + (x - x_0)\frac{y_1 - y_0}{x_1 - x_0} \tag{4.9}$$

The missing value, y, is interpolated using the known components. The Equation 4.9 shows how a linear estimate of the missing value can be obtained with the known samples in a time series.

4.7.2 Bilinear Interpolation

Bilinear interpolation is typically used in image processing, usually where known points have values associated with them, but in-between the points there are no values associated with them. By taking a particular point with known neighbouring points, it is possible to perform linear interpolation to approximate a better estimate of the missing values.

There are some assumptions taken in using the bilinear interpolation method: the first assumption accepts that the terrain of the surface is continuous and smooth; the second accedes that there is a high correlation between neighbour data points (Nett, 2016).

In image processing, the four nearest pixels to estimate the true value of a point that needs to be interpolated. This is done by using the distance between the known reference pixels are used to determine the coefficients. The coefficients are then used in combination with the neighbour reference pixels to estimate the true value (Nett, 2016). The point nearest to the point that needs to be interpolated will bear the most weight in comparison to the other neighbour points.

Chapter 5

Experimental Set-up

This Chapter sets out the methodologies in all of the experiments. It also aims to highlight additional information into the studies replicated. The experiments undertaken in this dissertation investigate several aspects of determining road grade.

Section 5.1 investigates additional information about the test area and the general set up of the experiments. Section 5.2, looks at the set-up of why GPS altitude values should not be used by themselves to determine road grade. Similarly, Section 5.3 investigates the use of an accelerometer to determine the inclination angle of the test area and the experimental steps performed in the experiment. Sections 5.4.1 and 5.4.2 investigate two methods of replacing GPS altitude values with Digital Elevation Models (DEMs) elevation values, to determine road grade. In comparison Sections 5.5.1 and 5.5.2 look at the set-up of experiments using repeated runs of GPS traces to determine road grade.

5.1 Additional Information

The test area or the route of the test vehicle in this dissertation is subject to one main route-way which the Tesco bus travelled. However, some of the experiments look at smaller segments of the route for replication purposes. The main segment of the test route can be seen below in Fig. 5.1.

Figure 5.1: OSM road network (left) and Google satellite view (right) of the test area Plzen, Czech Republic. The total route taken by the Tesco bus, equipped with the Bach box, is shown in green in the left image. Whereas, the red plotted route (in both images) shows the segment used for the experiment [Plotted in R].

The Tesco Bus Service is a free service provide by the Tesco organisation in Plzen, Czech Republic. It operate a number of different routes between the city boundaries and the main Tesco stores. Only one of the Tesco buses was used. The bus travels the green route shown in Fig. 5.1 (left image). However, only the route in red was considered for the experiment. The red route is indicative of the test vehicle starting from the left hand side (of both images) and ending on the right hand side (seen as the red line). The Tesco bus uses an automatic stop announcement system and telematic information to monitor the vehicle's position and parameters with the Bach box. That information is stored on the Bach box and is transmitted on request to the ZF Openmatics' clouds service, where the information can be extracted.

5.1.1 Getting Data from the Bach Box

Data from the Bach box was uploaded over the cloud based application developed by ZF Openmatics. The data is provided in JSON format and can easily converted into other formats. The data from the test vehicle had to be acquired when the vehicle was running as the On-Board Unit (OBU) needed to be powered before transmission could be activated. The vehicle took several trips during a day at varying times of the day. However, only the red line, shown in Fig. 5.1, was of interest to the experiments. Therefore, data was stored on the Bach box and uploaded at set times when the vehicle was on-line and the OBU was powered up. To differentiate between the entire trip of the vehicle which can be seen in the OSM plotted route, the green line seen in Fig. 5.1, and the segment of interest, the red route, the set test segment

will be referred to as a run. Where the run, only refers to the vehicle's path over the route in red in Fig. 5.1.

5.1.2 Code structure

A class named Signals() was developed to improve the work flow of the experiment. The class was developed in R using the S4 class structure. The class has five variables associated with it: longitude; latitude; cumulative horizontal distance between GPS points; distance accounting for the elevation changes between GPS points; and road grade angle. Taking in the longitude, latitude, and altitude values from the JSON file, the class is set to calculate the cumulative horizontal distances between GPS points, cumulative distances accounting for elevation changes between GPS points, and the road grade angles of the elevation profile. The class also provides easier plotting and access to variables.

5.1.3 Calculating Distance

In order to calculate the distance between GPS points, the Haversine formula was used Eq. 5.1. The Haversine formula represents the distance between two points on a large circular surface (Veness, 2011). Using a reference radius distance of the earth, R, taken as a constant of 6,378 km for this dissertation (the average value of the earth's radius). It takes into account the longitude, λ, and the latitude, φ, coordinates to give a representation of distance long a curved surface. Similarly, $\triangle\varphi$ represents the change in latitude and $\triangle\lambda$ represents the change in longitude.

$$d = R \times 2 \times \arcsin\left(\sqrt{\sin^2(\frac{\triangle\varphi}{2}) + \cos(\varphi_1) \times \cos(\varphi_2) \times \sin^2(\frac{\triangle\lambda}{2})}\right) \tag{5.1}$$

The Haversine formula was used to calculate the horizontal distance between GPS points, similar to the study by (Ribar et al., 2016). The cumulative distance between GPS points was used to represent the horizontal distance travelled by the test vehicle, in meters. Altitude was not accounted for in the distances presented in this dissertation, as it would create varying distances between the different data-sets over the same run when comparing the elevation profiles. However, the class Signals() does have the ability to measure distance with altitude by using Pythagoras' theorem to estimate a better approximation of the true distance travelled by accounting for the elevation difference between GPS points.

Sources of errors in calculating distance of the trip

1. The Haversine formula takes the radius of earth as its average value where the radius of the earth varies as the earth is not symmetrical.

2. Distance between GPS points varies due to the vehicle's velocity and acceleration, and due to the real life driving behaviours (changing of lanes, over-taking of other vehicles etc.).

3. The horizontal distances are only accounted for in the measurement distances of this dissertation and therefore are not a representation of the true distances travelled which needs to account for elevation changes between GPS points.

5.1.4 Road Grade Calculations

For most of the experiments the road grade angle was calculated using the angle between the change in elevation, $\triangle\psi$, compared to the horizontal distance covered, $\triangle d$. Using the elevation at the start and end distance points to calculate the change in elevation. However, experiments which did not use this method will explicitly state how the road grade angle was determined. In the equation below the altitude component above sea level is given by the symbol ψ and cumulative distance by the symbol d. Road grade is represented as the slope angle in the degrees θ (°) for comparison purposes, Eq 5.3. However, as seen in Eq. 5.5 it can easily converted to a percentage value if required.

$$Road\ Grade\ Angle,\ \theta\ (radians) = \arctan(\frac{\triangle\psi}{\triangle d}) \tag{5.2}$$

To calculate the road grade angle θ, the angle between the change in elevation and the horizontal distance is taken. This gives the angle in radians, Eq 5.2.

$$Road\ Grade\ Angle,\ \theta\ (^\circ) = \theta\ (radians) \times \frac{180}{\pi} \tag{5.3}$$

Therefore, the angle needs to be converted to degrees from radians as seen in Eq. 5.3.

$$Road\ Grade\ \% = \frac{\triangle\psi}{\triangle d} \times 100 \tag{5.4}$$

Road grade in Europe is usually expressed in percentages using the change in elevation over horizontal distance, Eq 5.4.

$$Road\ Grade\ \% = \tan(\theta\ ^\circ) \times 100 \tag{5.5}$$

The road grade angle can easily be expressed in percentages by converting it back from the road grade angle as seen in Eq. 5.5. A road grade angle of 45 ° converts to percentage value of 100%.

Road grade estimates in this study were measured at 80 m horizontal distances. The distances in the study were calculated as the cumulative distance between GPS points and the elevation value or pitch angle at the cumulative distance points were used to calculate the road grade angle. As seen in (Ribar et al., 2016), "Relatively high values of sampling interval acts as a smoothing factor, filtering-out higher frequencies and resulting in a smooth dependence between road slope angle and distance travelled". Hence the value of 80 m was selected to determine better estimates. Similarly, if a "..segmented length is too long, real variations in grade within the segment can be averaged out, leading to underestimation of the variability in grade" according to the study by (Boroujeni and Frey, 2014).

5.1.5 Google API

The Google elevation API was used by the researchers in the study by (Levin et al., 2014) to determine large scale fuel consumption analysis for eco-routing purposes. Similarly, the study by (Wang et al., 2015) used the Google Earth DEM, stating that it has a low standard deviation in the error of the DEM elevation values, to

create road profiles in Beijing. The study uses a vector map of the road network to extract elevation information. Therefore, the Google Earth DEM can be thought to be very accurate. When coupled with the fact that the study by (Levin et al., 2014) used the Google Elevation API to derive road grade estimates, the assumption that the DEM Google provides highly accurate elevation estimates was made in this dissertation. Therefore, this dissertation uses the Google elevation API to compare elevation and road grade estimates in the experiments performed.

However, the Google elevation API is limited to a query limit of 2500 points when using the evaluation package. The use of the other commercial packages querying can become expensive as there is a cost associated with large-scale queries.

5.2 GPS Investigation

This section sets out the experimental set-up and the hypothesis of investigating GPS elevation values as a way to determine road grade. The investigation looks into why GPS elevation readings should not be exclusively used to measure road grade. The investigation follows the same procedural steps seen in data cleansing operations developed for data warehouses (Rahm and Do, 2000; Müller and Freytag, 2005):

1. Initial investigation into possible reasons for errors
2. Set up of a data cleansing approach to remove errors
3. Applying procedure to the data
4. Analysis of the results

The main issue with the use of GPS data in determine road grade is that the elevation estimates are prone to errors. More specifically: random errors caused by multipath; free space loss; and atmospheric effects, etc. Modern consumer-grade GPS devices can use correction systems and algorithms to increase their accuracy and reduce the effects of errors. For instance correction systems like Assisted-GPS and Differential-GPS. However, these systems tend to improve the horizontal positioning more than the vertical positioning and are not effective if there is loss of signal between the receiver and the base station/geo-stationary satellites. Another fundamental issue with the elevation in GPS is the positioning of satellites above the receiver. GPS satellites need to be positioned further apart to improve the elevation estimates of receivers.

One way to reduce the errors associated with elevation might be to investigate the effects of smoothing algorithms to be able to cleanse GPS elevation data of erroneous data. Data cleansing is the processing of detecting and correcting or removing erroneous data. Data cleansing provides a step by step process to mitigate errors and discrepancies in large collections of data. One main area of focus for data cleansing is operations in data warehouses, where there is wide variety and high probability of inaccurate or misleading data. Data Warehouses are systems for storing and analysing information for business intelligence (Rahm and Do, 2000).

Data cleansing has been of interest in recent years due to the fact that there are more available sources of data than ever before.

Using data cleansing techniques used in modern data collection warehouse management systems errors in GPS elevation can be identified and hopefully mitigated with a removing procedure. Most data cleansing approaches involve several key phases as seen in the studies by (Müller and Freytag, 2005) and (Rahm and Do, 2000).

The step performed in this experiment were as follows:

1. Initial investigation into possible reasons for errors
    - A data analysis or data auditing phase, where the data is initially reviewed by an expert or someone with knowledge of possible causes of errors in the data. The main aim here was to identify patterns of anomalies and determine where errors may occur.
2. Set-up of a data cleansing approach to remove errors
    - The next step in the process was to set a work flow specification or work flow mapping where the intended work flow for the data cleansing was thought-out and a set of procedures was made. Following this the work flow was executed and a test case was performed on a smaller subset of the entire data-set.
3. Applying procedure to data
    - Execution of the data cleansing procedure to remove any errors and anomalies. This prevents the errors and anomalies from affecting the overall accuracy of the data-sets, in this experiment, statistical smoothing operations were used to smooth out errors in the elevation profiles.
4. Analysis of the results
    - The entire process was analysed to investigate the effects of the data cleansing operation. Then the entire process was re-run in a repetitive operation (this step was not performed in the experiment).
5. The results were then compared against the Google elevation API estimates.

5.3 Accelerometer

The experiment investigates using an accelerometer at measuring road gradient, using the tilt estimates. Inertial Measurement Units (IMU) on the Bach device can be used to calculate the pitch of the vehicle. An accelerometer is a device which measures linear acceleration applied to a dynamic body, it can be used to measure tilt/pitch during static situations by looking at the change in acceleration due to gravity in 3-Dimensions (3D). However, when coupled with dynamic movement and acceleration of a vehicle it can be difficult to determine the tilt of the vehicle because of the noise created. De-noising the accelerometer signal could help to determine the inclination of the road derived from the pitch angle.

The experiment undertaken investigates the effectiveness of measuring road gradient using one of the approach stated in (Mangan et al., 2002). The study by Mangan et al. uses an inclinometer to determine the inclination of the road. The Bach box does not have an inclinometer, however it does have an accelerometer which could be used to calculate the tilt of the vehicle in a similar manner to the inclinometer. Inclinometers measure horizontal and vertical angular inclination, whereas accelerometers measure linear acceleration and de-acceleration of dynamic systems (Sherbornesenors, 2014). Although, accelerometers can be used to measure tilt of a vehicle they are prone to less accuracy than that of an inclinometer as they normally have a lower resolution. It was hypothesised that a rough estimate of the road inclination can be determined using the first approach suggested in (Mangan et al., 2002). There are several approaches suggested in the study by Mangan et al. to remove noise caused by acceleration of the vehicle. However, all of the approaches use a low pass filter to remove vibrational noise created by the vehicle and then differ on their methods for removing noise due to acceleration and retardation on the vehicle.

The first approach suggested in the study uses a low pass filter applied to the initial signal to dampen high frequency variations. Then a process using Mathematical Morphology (MM) was applied to the signal to remove the noise created by acceleration. The low pass filter can remove the high frequency variations in the signal, caused by vibration from the vehicle, but cannot remove the low frequency variations caused by acceleration and de-acceleration. The MM approach provides a means of geographical transformations based on shapes of objects and can be used to removed the low frequency variations caused by the acceleration of the vehicle by comparing the MM approach to a reference shape. In the original study, the researchers Mangan et al., measure the inclination angle of a vehicle in a test lab. The researchers vary the acceleration of the vehicle and create an incline for the test vehicle using a ramp. The use of the ramp means the shape that the MM process has a good ability of removing a large proportion of the noise created by the acceleration as a constant reference shape can be determined.

The steps followed in this dissertation are seen below:

1. The pitch/tilt angle was calculated from the accelerometer data.
    - The x, z values obtained from the accelerator were used to calculate the

pitch angle.

2. A low pass filter was applied to the accelerometer tilt measurements to remove high frequency components.
   - An exponential low pass filter was applied, with $\alpha = 0.1$.
3. The Mathematical Morphology approach was applied to remove the low frequency components of the signal caused by the acceleration of the vehicle.
   - This was done by applying an erosion morphology method to the signal.
   - Followed by a dilation morphology method to the signal.
4. The corrected signal was then compared to the Google elevation API estimates.

5.4 Digital Elevation Models

Digital Elevation Models (DEMs) allow for an alternative way to estimate elevation of road ways by using GPS coordinates to extract elevation values from a DEM. There are a number of different DEMs available, however only a few of them, with a high resolution, are available free to the public.

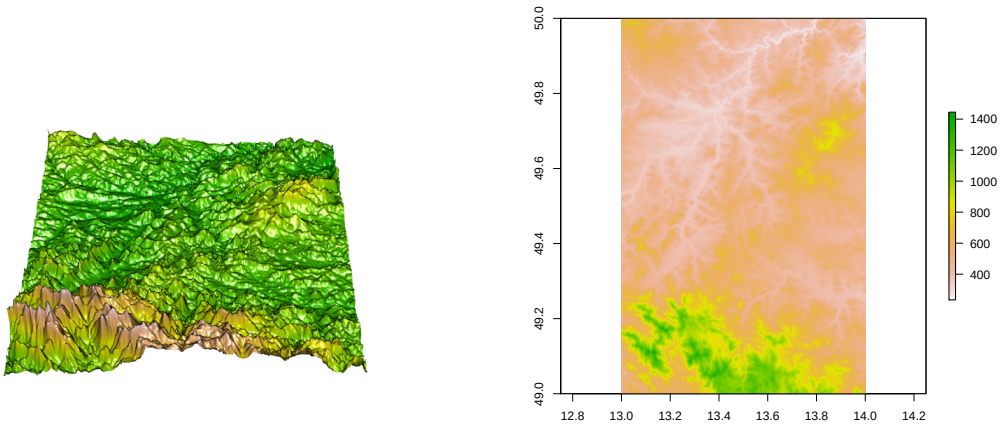

Figure 5.2: Elevation tile of the coordinates longitude E13-14 and latitude N49-50, the surrounding area of Plzen, Czech Republic taken from the SRTM 1-arc second DEM. 3D representation of the tile on the left compared to the 2D representation on the right. The 2D representation of the tile provides a legend of the elevation in meters [Plotted in R].

Two methods for extracting elevation estimates of road ways are presented here. The first method in Subsection 5.4.1 explores the use of bilinear interpolation to determine better estimates of elevation values from the DEM and smooth out the elevation profile from elevation jumps/declines between grids. The need for better estimates of elevation values is due to the elevation estimates corresponding to that of the centre of the grid for the entire area of the grid. If there would be multiple GPS points covering one of the 30x30 m grids then all of the GPS points will have

the same elevation values. Similarly, Subsection 5.4.2 explores smoothing out discrepancies and irregularities in the elevation profiles extracted from DEMs, using a several step smoothing/filtering process. The discrepancies and irregularities arise from the fact that the SRTM DEM is a bare earth representation and as such is void of man made objects and vegetation. In this case instances like bridges and overpasses, are not present. This means the elevation estimates are taken at the lowest point.

The two approaches replicated in this dissertation, highlights significant challenges with DEMs. Firstly, DEM values are constant for the entire grid surface and therefore there is a need to estimate a better approximation of the true elevation value in-between grids. Secondly, the differences in the grid's elevation values causes the slight inconsistencies along the elevation profiles (due to the elevation jumps/declines between grids). Lastly, the Shuttle Radar Topography Mission (SRTM) DEM measures elevation values are taken at their lowest point, as it is a Digital Terrain Model (DTM), and so discrepancies can occur in areas like overpasses and bridges where elevation is measured at a lower value than there true estimate. These challenges will be discussed further in Sections 5.4.1 and 5.4.2.

Extracting elevation from DEMs To understand how the elevation information from DEMs can be extracted the example of the tile N27E086, which is a 3-arc second SRTM tile, is explored below in Fig. 5.3.

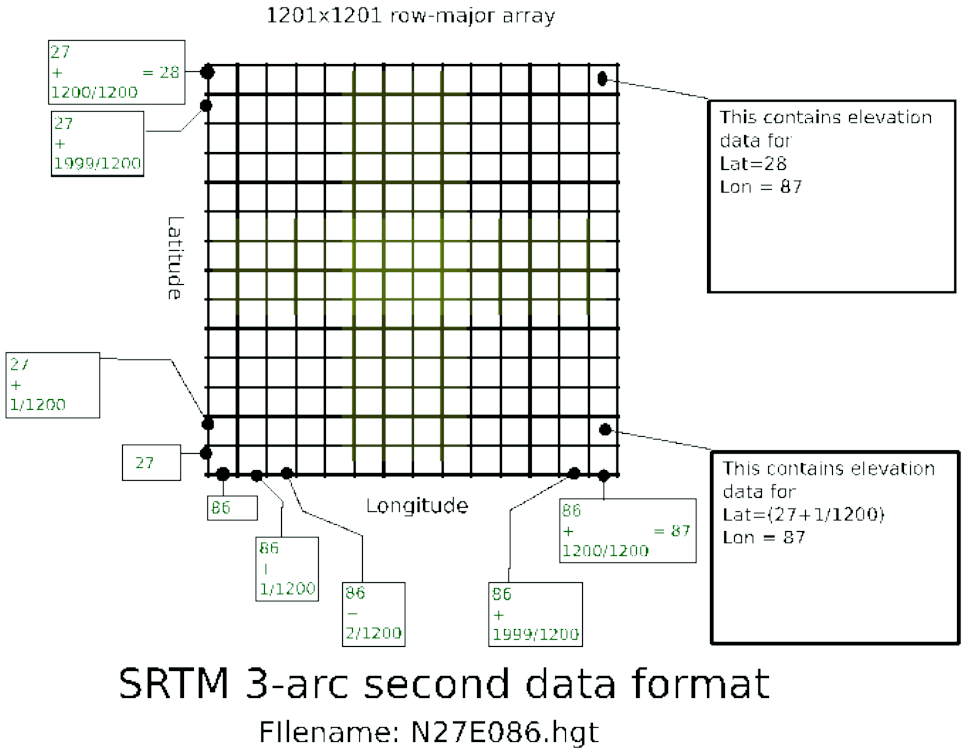

Figure 5.3: Layout of elevation tiles in SRTM 3-arc second DEM. Elevation values are recorded on 1201x1201, 90x90 m square tiles, for 1x1 degree of longitude and latitude (Nepal, 2016).

The tile's name N27E086, means that the tile covers the entire area from +27° until the neighbouring tile +28°, in latitude, and from +86° until +87°, in longitude (measuring from the left-hand side, starting at N27E086 until the top-right N28E087). Therefore, the information inside this tile is captured in 3-arc seconds. 3-arc seconds is an angular measurement and this equates to 3/3600 of a degree. The information about the elevation for each latitude and longitude is then recorded in sections of 1201x1201 grids. So to visualize this, Fig 5.3 shows that the latitude is divided into sections of 1201 and that each grid equates to 27 + (x/1200) degrees. Therefore the first block from the starting point N27 will be 27 + (1/1200) degrees and the last block will be 27 + (1200/1200). The same logic is applied when the SRTM a 1-arc second DEM tile is used, where the tile can be split into sections of one degree per hour or 3601x3601 grids.

To extract elevation information straight from DEM tiles there are several methods, three methods were explored: (1.) The steps shown in (Nepal, 2016) can be used, which uses a Python program to extract elevation information from the .hgt files. The elevation information in the tiles are sets of 16 bit signed integer values and so using the corresponding instance of latitude and longitude, the elevation value can be extracted; (2.) Similarly, in R the library Raster can be used to load the DEM into a raster format and a similar process as seen in (1.) can be used to extract information using the function extract(). Which takes a matrix of longitude and latitude coordinates; and (3.) the tiles can be loaded into a Postgres + PostGIS database and elevation information can be extracted by selecting specific longitude and latitude points. However, only the approaches (2.) and (3.) were used in the dissertation. Where extracting the elevation directly from the raster tile produced the same values as loading it into the database. The code for the two different methods are shown below in Listings 5.1 and 5.2 respectfully.

```
SELECT ST_Value(rast, ST_Transform(ST_SetSRID(ST_Point(long,
    lat),4326), 4326)) FROM public.databaseTable WHERE
    ST_Intersects(rast, ST_Transform(ST_SetSRID(ST_Point(long,
     lat),4326), 4326));
```

Listing 5.1: To extract elevation from DEMs using the Postgres + PostGIS database the following select statement can be used to extract a single GPS point at a time.

```
srtm1 ← raster("n49_e013_1arc_v3.tif")
GPS_data ← data.frame(cbind(longitude,latitude))
elevation ← extract(srtm1,GPS_data)
```

Listing 5.2: To extract elevation from DEM tiles using the R package Raster the following code can be used, where longitude and latitude coordinates are combined into a data-frame.

Listings 5.1 requires that the Raster image, the tile, has already been loaded into the database table. The longitude and latitude coordinates are feed into the statement one at a time in a loop. Whereas the extract function in Listing 5.2 queries a data frame of the coordinates directly from the raster image.

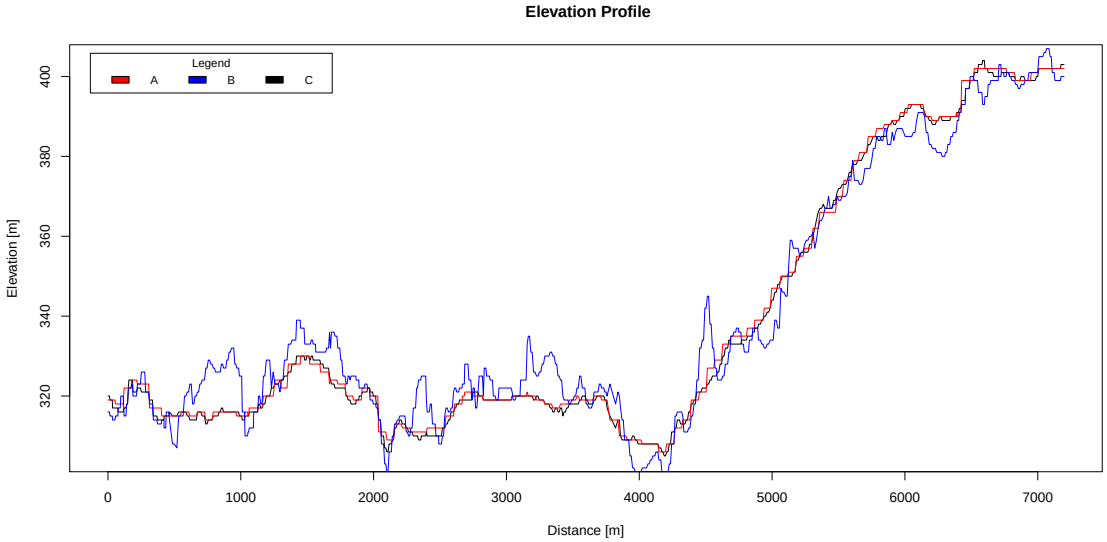

Figure 5.4: Comparison of DEM extracted elevation values of the GPS trace taken from the test area: (A) SRTM 3-arc second; (B) ASTER 1-arc second; and (C) SRTM 1-arc second DEM.

The Shuttle Radar Topography Mission (SRTM) 1-arc second DEM was used for all of the experiments where DEM elevations were used to calculate road grade (Survey, 2016b). Due to the higher resolution of the DEM compared to SRTM 3-arc second DEM (Survey, 2016a), and the lower variability to similar 1-arc second DEMs in the test route, like that of the Advanced Spaceborne Thermal Emission and Reflection Radiometer (ASTER) Global Digital Elevation Model (GDEM) (jpl.nasa.gov , 2016). The Fig. 5.4 illustrates the differences between the DEMs on the test route. The ASTER GDEM (B) has higher variability for elevation values when compared to the SRTM 1 and 3-arc second DEMs, over the same run. The test area of the GPS trace is within the SRTM raster tiles for N49E013. The tiles were downloaded from the Earth Explorer site (Survey, 2016c).

5.4.1 Bilinear Interpolation of Elevation profile from DEMs

The experiment used bilinear interpolation to estimate better estimates of the elevation values extracted from the SRTM DEM. Due to the resolution of the DEM tiles being equivalent to 30x30 m grids, with the centre point being the only point equating to the elevation for the entire grid, there is a need to estimate a better approximation of the true value of elevation for other areas of the grid other than the centre. Especially, if there are multiple GPS points that are not in the exact centre point on a single grid. Multiple GPS points may lay on the same grid when the speed of the vehicle is low, combined with a high sampling rate from a GPS receiver (the GPS device in the experiment samples every second). In order to correct the elevation profile and determine a better estimate of the true elevation values an extension of bilinear interpolation was used.

The ragged, stair like, elevation profiles seen in Fig. 5.4, for all of the DEMs, are due to multiple GPS points on a single elevation grid. Meaning all of the points on a grid will have the same constant value, that combined with the elevation jumps

between grids causes the ragged profile. When the GPS traces move to the next tile there can be an elevation jump or decline which is not a true representation of the location's elevation but rather the centre point of the tile. These two effects cause the elevation profiles to be represented in blocks or stair like formation, which have the adverse effect of creating a sharper road grade angle if not accounted for. By taking into account the elevation values of surrounding tiles a better approximation for the GPS point on the tile can be calculated. The experiment showed that the interpolation produces a smoother elevation profile and reduces the effects of elevation jumps and declines in the profile, however it does not completely smooth the elevation profile.

The experiment looked at evaluating the methods employed in the study by (Henriques and Bento, 2013). Where the researchers do not use filtration techniques to improve the ragged profile. Rather they look at an interpolation technique which utilises coefficients of the distance to neighbouring elevation grid and the distance to the current elevation grid combined with the elevation values of the grids surrounding the GPS point to approximate a new elevation estimate.

The researchers used an adaptation of bilinear interpolation to estimate better approximations of elevation values obtained from the ASTER GDEM, and to deal with the elevation jumps between tiles. One of the aims of the study by (Henriques and Bento, 2013) was to determine how slope angles affected bicycle traffic simulations. As stated in the study, the slope of the road is not always included when designing a simulation in VISSIM (a simulation tool for traffic simulation and analysis). Therefore, the researchers look to use GPS values obtained from cyclists to approximate an estimate for position to pass to a Terrain Elevation Data Server (TEDS), developed by the researchers, which then extracted the elevation values (from the ASTER GDEM) to be interpolated. The slope information and the 2D positional information were then projected to the simulation mapping system in the study. The GPS traces were collected from an on-line social platform which shares GPS traces. Routes of 5 km to 30 km in mountainous regions of Portugal were selected in the study by (Henriques and Bento, 2013).

The main differences between the study by (Henriques and Bento, 2013) and the replication of the study performed in this dissertation were: (1.) the analysis of vehicle GPS trace instead of bicycle GPS traces; (2.) the end goal of the researchers, the goal of the dissertation is to improve eco-routing services by providing an evaluation of different means of determining road grade; (3.) no further analysis on the effects of road slope on traffic performances were performed in this dissertation; and (4.) the use of the SRTM DEM instead of the ASTER GDEM.

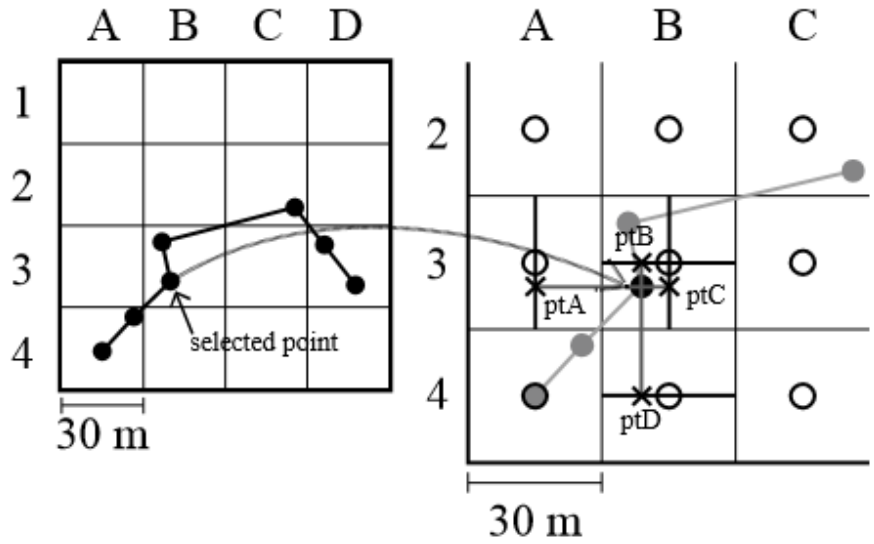

Figure 5.5: The bilinear interpolation approach to estimating a better approximation of elevation estimates between grids. The image on the left shows a selected point in a series, whereas the image on the left shows the process of determining coefficients for a GPS point which is not at the centre of a grid (Henriques and Bento, 2013).

The image above Fig. 5.5 illustrates the process of using bilinear interpolation to approximate a better estimate of the elevation for each GPS point. The steps for interpolating each of the GPS points were as follows:

1. Determine the approximate location of the GPS point on the DEM tile.
    - The 1-arc second SRTM DEMs will have a centre point on each axis every 0.0002777778 (1/3600) degree points. Therefore, a rough estimate of the position of the grid in which the point is located on can be determined by dividing the longitude and latitude decimals of the GPS point by the fraction 1/3600.
2. Determine the grid orientation.
    - Depending on the the approximate location of the GPS point an estimate of where the GPS point is located on the grid can be determined in relation to the centre point.
    - The grids were divided up into quadrants of Bottom Left (BL), Bottom Right (BR), Top Left (TL), and Top Right (TR) to determine a approximation of where the GPS lies in relation to the grid. This was then used to determine which of the three neighbouring grids influence the GPS point's elevation.
    - For example, the BL quadrant will be influenced by the grid it is in, and the three surrounding grid to the left and below it. This is illustrated in Fig. 5.5.
3. Determine the vertical distance of the x-axis to the GPS point in the grid location

- The distance between the GPS point and the vertical line of the centre of the grid is calculated using the Haversine formula.
- The vertical weight can then be assigned by dividing the distance by 30 m, the equivalent distance from one centre point of a grid to the next grid centre point.
- The weighted distance is now equivalent to the vertical distance of the centre line and the vertical distance of the opposite neighbouring grid when taking one minus the weight. Therefore, the weights for the x-axis to the centre and the neighbouring grid can be determined.

4. Determine the horizontal distance of the y-axis to the GPS point in the grid location.

   - The distance between the GPS point and the horizontal line of the centre of the grid is calculated using the Haversine formula.
   - Then the Horizontal weight can be assigned by dividing the distance by 30 m.
   - The weighted distance is now equivalent to the horizontal distance of the centre line and the horizontal distance of the opposite neighbouring grid when taking one minus the weight.

5. Depending on the grid location BL, BR, TL or TR the weights are assigned.

   - Each elevation value for all of the grids that influence the GPS point are extracted from the database.
   - Determining the elevation values of the vertical-axis at the neighbouring grid and the vertical-axis line of the centre where the GPS point is located, is performed using the horizontal distance weight which was calculated and the closest grid elevation values to approximate a new elevation estimate.
   - Similarly, determining the elevation values of the horizontal-axis at the neighbouring tile and the horizontal-axis line of the centre is performed using the vertical distance weight which was calculated and the closest grids elevation values to approximate a new elevation estimate.

6. The elevation values calculated can now be used to determine a better approximate of the elevation value.

   - By applying the vertical and horizontal weights to the relevant elevations and obtaining an average of the vertical and horizontal elevations results in a new estimate for the elevation.

7. The road grade angle was calculated and then compared against the Google elevation API estimates.

   - Distances 80 m were used to calculate the road grade angle.

5.4.2 Smoothing/filtering of Elevation profile from DEMs

The experiment used a GPS trace, taken from the test vehicle to extract elevation values from the SRTM DEM, using the locational coordinates (longitude/latitude) to query the closest elevation value to the GPS point. The elevation profile was then filtered to remove discrepancies in the profile and improve the smoothness of the profile. From the filtered elevation profile the road grade was extracted. The filtering/smoothing technique was performed in a several step process developed by (Wood et al., 2014b).

The researchers Wood et al. developed a smoothing process to remove discrepancies in the elevation profiles extracted from the SRTM DEM, as well as to smooth out the elevation profile. The discrepancies in the elevation profiles were caused by the collection method of the SRTM satellite – the SRTM satellite collected information as a Digital Terrain Model (DTM) and therefore will record the lowest point at the location it is measuring. This has the adverse effect of measuring the lowest points at place like bridges and overpasses. If not corrected this will inevitably lead to inaccuracies in the road grade profile. Subsequently, there is also a need to smooth out the elevation jumps/declines caused by GPS points on different grids and the elevation differences between these grids. The SRTM 1-arc second DEM has a resolution of approximately 30 m meaning elevation information will be presented on 30x30 m girds, with the centre point representing the true estimate of elevation for the entire grid. Therefore, as the elevation values between grids may differ it creates elevation jumps/declines from grid to grid which are irregular to the true elevation and therefore need to be smoothed out to create a better estimate of the road's elevation profile.

The work done by National Renewable Energy Laboratory (NREL) in the study (Wood et al., 2014b) is later expanded to evaluate the effect of road grade on the energy use of modern auto-mobiles (Wood et al., 2014a) and on general impact of road grade on vehicle energy use (National Renewable Energy Laboratory , 2014). One of the main aims of the original study, and the one investigated in this dissertation, is to find a way to collect reliable road grade estimates using GPS traces collected by the NREL. The researchers, investigate a method of appending high resolution elevation from DEMs to estimate accurate road grade estimates, from GPS positional information with the aims of being able to aid vehicle energy modelling and simulations.

The study performed a several step process to filter/smooth the elevation profile. The raw SRTM elevation profile was first: (1.) compared against horizontal distance; (2.) elevation values were down-sampled into uniformly spaced intervals; (3.) the data was filtered, using a Savitzky-Golay and Binomial filter; (4.) elevation values over a certain value were removed and the missing data points interpolated; (5.) the data was passed through the filter again; and (6.) the elevation values are interpolated back to the original sample length.

A few assumptions had to be taken in order to replicate the study by (Wood et al., 2014b). The researchers did not include the number of points their filter or what spacing interval they used to determine the uniform down-sampling. Therefore, a

nine point Savitzky-Golay and Binomial filter was chosen and a uniform distance of 50 m was chosen to down-sample the elevation profile, to replicate this study.

1. Compare the Raw DEM values to the horizontal distance
    - The extracted elevation values from the SRTM 1-arc DEM, using the GPS location, were then compared against the cumulative distance.
    - The horizontal distance was calculated using the Haversine formula for spacing between the GPS points.
2. Down-sampling the elevation data.
    - The data was down-sampled/decimated using a uniform distance to determine which points to obtain. As the original distance values would be varied due to the GPS measurements, sampling at a large enough distance will down-sample the data points. Therefore, elevation values were down-sampled at 50 m intervals.
3. Filtering the down-sampled data.
    - The down-sampled data was then filtered using the nine point Savitzky-Golay and Binomial filter.
4. Elevation values over a certain value were discarded and the missing data points were interpolated.
    - Elevation differences, over 10 m, were removed from the dataset. The missing data points were back-filled via linear interpolation.
5. The filter was applied to sample data again.
    - The nine point Savitzky-Golay and Binomial filter was applied a second time to smooth out the profile of any back-filled data points.
6. The data was then interpolated back to its original data-set length, using the down-sampled/filtered data-set.
    - The original distances values were used to interpolate the data-set back to its original length, using linear interpolation of the elevation values for each of the original distance values.
7. The road grade angle was calculated and the results were then compared against the Google elevation API estimates.
    - The road grade angle was calculated using 80 m distances.

5.5 Repeated Runs

Two studies were replicated using repeated runs using the GPS device in the Bach box. The general principle of using repeated runs to estimate road grade is, GPS measurements can be modelled as normally distributed with enough runs, the errors in the elevation profile can then be mitigated and a good approximation of the road grade can be determined over time (Boroujeni and Frey, 2014). This applies to the first study in Section 5.5.1, where repeated runs were combined and linear regression of segments were used to create a road grade profile. However the second study, in Section 5.5.2, multiple runs are used to apply a geometric profile of the road using a B-Spline approximation of the GPS points.

Figure 5.6: Route comparison of the experiments seen in Section 5.5. The left image shows the route used in Subsection 5.5.1 and the image on the right shows the route used in Subsection 5.5.2. The green line shows area investigate in the experiments compared to the full route in red.

In order to segment the route to only include one way direction runs, a small subset of the entire route travelled by the test vehicle was selected to replicate the study by (Ben-Arieh et al., 2004). Similarly, in replicating the study by (Boroujeni et al., 2013) a smaller segment of the total route was used. The two routes are shown above in Fig.5.6.

To get the minimum required set of repeated runs, 10 one way runs as stated in the study by (Boroujeni et al., 2013), there was a need to only select part of the route that could be analysed without mixing up the direction of the test vehicle. Therefore, the route shown in Fig.5.6 (left image) shows the part of the route that excludes times when the test vehicle the test vehicle crossed an intersection when returning on the opposite side of the road. The segmented test area made it easier to segment the runs for the experiment.

Similarly, the small test segment was chosen for replicating the study by (Ben-Arieh et al., 2004) as it was found that very short straight segments were needed to fully replicate the study. Three test areas were tested for the experiment, however it was found out that only small segments could be used with the need to connect all the segments as stated in the study by (Castro et al., 2006), which looked at a

similar manner of geometrically modelling highways using Splines and evaluated the method taken in the study by (Ben-Arieh et al., 2004). In the experiment, it was found that slight bends could be handled but for purposes of the results only this test segment was used to highlight the approach.

The test vehicle took several trips during a day. In order to segment the runs, the direction and the selected test area had to be segmented from the trips. When collecting the data from the vehicle there were several runs in both directions. To visualise this, the trip was compared against against the cumulative distance in the Fig. 5.7.

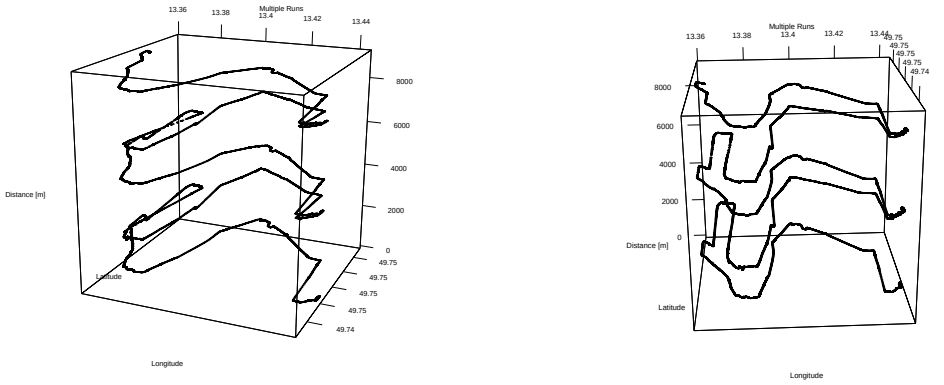

Figure 5.7: 3D representation of the test vehicle's trip, by comparing the cumulative distance against the longitude and latitude coordinates taken from a trip. The trip shows that the vehicle replicates the same route several times a day, which is shown by the increasing distance over the same longitude and latitude coordinates.

To determine which direction the vehicle was travelling for both of the experiments it was necessary to first segment the route and secondly find a way to calculate the trajectory of each of the runs within the segment. To do this the data-sets were subsetted by the segment in terms of longitudinal and latitudinal coordinates. For example, the coordinates for which only data between longitude > 13.44 and latitude < 49.567 were considered. The consequence of this can be examined in the Fig. 5.8, where the distance of one of the trips taken by the test vehicle is plotted against the distances travelled and then segmented in to the coordinates of the segment required for Section 5.5.1. Plotting the trip in such a manner allows for a determination of how the vehicle travels. Sub-setting the data allows for the isolation of the runs from the entire trip and makes it easier to calculate the direction of travel of the vehicle. The 3D route now appears as if it has been cut off in segment, this is because of the segmentation by the location.

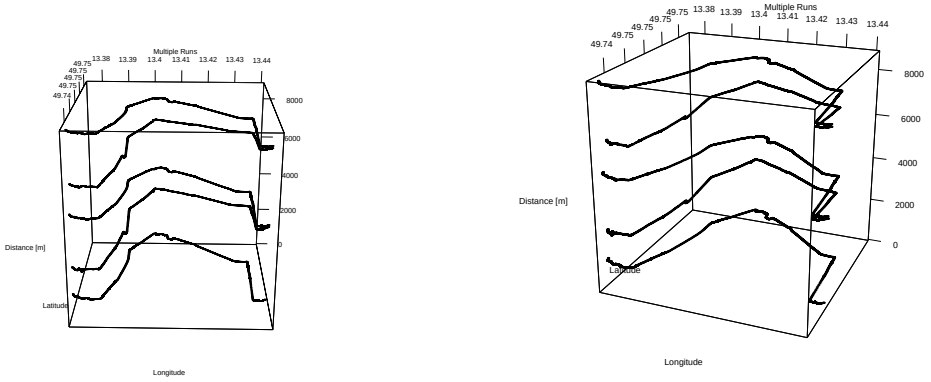

Figure 5.8: 3D representation of the test vehicle's trip being segmented into the test area for Section 5.5.1. By comparing the cumulated distance against the longitude and latitude coordinates and sub-setting the data by the segments coordinates.

Once the data-set has been subsetted, the direction of the run needed to be determined. To do so, the trajectory of each of two GPS points were compared to their vector direction in terms of the vector quadrant it is in. As the vehicle is likely to make several changes in direction over the entire trip, only the sum of the vector directions were considered. This way the direction of each run can be subsetted again into clock-wise or anti-clock wise around the test route.

5.5.1 Multiple Runs

Ten one way runs over the route in Fig. 5.6 were taken and from the runs the average distance was calculated and used to segment the route into 80 m segments. For each of the 80 m segments linear regression was applied and the slope angle was taken to estimate the road grade angle. The test vehicle follows a pre-determined route and when collecting the GPS positional information from the Bach box it was necessary to calculate the direction of travel.

The study by (Boroujeni et al., 2013), investigates standalone GPS devices with a Barometer Altimeter (GPS/BA) to estimate road grade, utilising multiple runs to determine road grade estimates. The GPS/BA was used in the study due to its ability to be less susceptible to interference than that of mapping-grade GPS devices, as seen in their later study by (Boroujeni and Frey, 2014), or other consumer-grade devices that are not equipped with vertical correction systems like barometer altimeters. The repeated runs of the GPS/BA device was combined and used to estimate linear regression estimate of the elevation profile in 80, 160 and 250 m segments. From the linear regression of the segments the slope coefficients were used to calculate the road grade angle.

The researchers took approximately "100 one way" runs of their test route and were able to quantify the number of minimum runs required to determine accurate road grade estimate when compared against LiDAR estimated road grade. Depending on the variation required for of the road grade and the accuracy required, the authors presents a method to calculate the confidence interval of the samples.

One of the main aims of the study by (Boroujeni and Frey, 2014) was to determine road grade profiles for Vehicle Specific Power (VSP) models. The VSP model is a fuel consumption and emission model for vehicles (Zhou et al., 2016). The VSP model requires road grade estimates every second and therefore developing a way to determine road grade profile in a cost affordable manner is of interest to their study. Improving the collection of road grade estimates can then improve vehicle energy consumption and emissions estimates.

The steps taken in replicating this study were:

1. Collection of multiple trips from the test vehicle.
    - As the test vehicle usually travelled the same, almost circular route a few times a day, there was a need to collect a large number of trips.
2. Sub-setting the data.
    - The data (longitude, latitude, altitude, and cumulative distance) was subsetted by the coordinates of the segment.
3. Direction of travel was calculated.
    - To determine the direction of the vehicle, to get only runs in one direction, the runs were subsetted further into clockwise and anti-clockwise directions of travel.
4. Then each individual run was extracted from the clockwise direction data-set.
    - Using the cumulative distance each of the clockwise direction runs were segmented further into an individual run.
5. Recalculate the distances of each of the runs.
    - The class Signals() was used to recalculate the cumulative distances of each of the runs which were subsetted. Only runs that went in the clockwise direction were of interest and selected.
6. The total distance of the segment was determined.
    - The distance of the segmented test area was calculated using the average value of the distances of the each of the runs.
7. The total distance was then used to further segment each run into 80 m corresponding segments.
    - For every 80 m the segment, linear regression of the elevation profile was applied, and the coefficient of the line was used to determine the road gradient angle.
8. The data was then compared against the Google elevation API road grade estimates.

5.5.2 Geometric modelling of road way using B-Spline Approximations

The experiment looked at determining a geometric profile of a segment of the road way, taken by the test vehicle, in order to determine the road grade. The several step process included the collection of the data, segmenting the area, a data cleansing operation and applying a B-Spline approximation to the GPS points to estimate the profile of the road way. From the geometric profile the road grade angle was determined.

The study by (Ben-Arieh et al., 2004) used repeated runs, using a vehicle equipped with a GPS device, of the Kansas highway to determine a geometric representation of the highway. The collection of data was performed under real world drive cycles, that combined variations in elevation values recorded from the GPS device which needed to be corrected for. Therefore the researchers, developed a data cleansing operation and used a B-Spline approximation to represent the geometry of the highway. The results were compared against the design teams drawings of the highway.

The Kansas highway design team collected several runs, using the same collection method, over a period of five years. In order to handle the collection of large amounts of GPS traces the researchers developed a data cleansing operation to combine the data and remove the elevation values that were inconsistent. Geometrically modelling the highway using a B-Spline approximation allows for the estimation of the best fit of the elevation values.

In replicating the study small difference were made due to the location of the test area. There were severeal differences performed in replicating the work, namely the use of the Universal Transverse Mercator (UTM) conformal projection instead of the Lambert conformal projection, the analysis of smaller highway segments in urban areas with bends and then the determination of road grade from the geometric profile. The data needed to be segmented in to small sections and then recombined with the larger data-set. Therefore, only the data of the one segment is shown as the other segments chosen were either too large or had sharp curves which cause the B-Spline approximation to underestimate the position. The study by (Ben-Arieh et al., 2004) did not determine road grade, however it is hypothesised that a geometric representation of a road way would allow for good road grade estimates to be obtained.

The steps taken in replicating this study were:

1. Projection of GPS coordinates.
    - Lambert conformal projections, used in the study, are typically only used in North America and so the UTM conformal projection was used to perform the conversion of spherical to cartesian coordinate.
2. The data was segmented into the test area.
    - The data was segmented into small areas using the longitudinal and latitudinal position of the test area.

3. The direction of travel was determined.
    - The clockwise direction of a two trips were subsetted to be able to extract the runs only in the clockwise direction for that segment.
4. The elevation difference between points were calculated.
    - The elevation values of two consecutive points were used to calculate the elevation differences.
    - Calculating the standard deviation of the elevation difference.
5. Remove outliers from the data using 5 m as the threshold.
    - Identify points greater than 5 m, determining their corresponding location in original data-set and then removing the outliers from the data-set.
6. If the standard deviation of the elevation data is less than 3 m it indicates good variation.
    - Therefore, if the data was standard deviation was less than 3 m, every three points were averaged and step 10 was performed
    - Otherwise, the next step was taken.
7. Calculating the range of longitudinal and latitudinal coordinates.
    - Calculating the maximum and minimum values of the longitude and latitude coordinates, to determine the range of the longitude and latitude coordinates.
8. From the range of longitude and latitude coordinate the least square regression line was applied to the data.
    - If the longitude range was greater than the latitude range, the data was fitted with longitude vs altitude and longitude vs latitude.
    - Else, the data was fitted with latitude vs altitude and latitude vs longitude. The least square approximations was applied to the data-set. Then the residuals of the altitude and the residuals of longitude and latitude were found. Lastly, the regression lines were plotted.
9. The outliers were removed according to the least square regression fit on the data.
    - The standard deviation and mean of the residual values was determined. The outliers were calculated using the formula: Mean + (2*sigma) >= r =< Mean – (2*sigma). The outliers were removed from the original data-set.
10. Every three points were averaged and four control points were selected.
11. The B-Spline uniform model and the B-Spline open uniform model was applied to the data. The road grade was then determined and compared to the Google elevation API estimates.

Chapter 6

Results

The results of the replicated studies are presented in this Chapter. The GPS elevation profile, taken from the Bach box, was investigate as to why the profile should not be exclusively used to determine road grade. Five studies were replicated to determine which of the methods was best suited for determining road grade with advance public bus transportation systems. All the methods look at utilising components that were available on the Bach box and most other On Board Units (OBUs).

Chapter 6 is set out as follows: Section 6.1, investigates why GPS devices should not be used by themselves to determine road grade. In Section 6.2 explores determining road grade from an accelerometer. Section 6.3 considers the use of GPS traces to extract elevation information from DEMs, to then determine road grade. Exploring the use of bilinear interpolation in Subsection 6.3.1 and a several step smoothing/-filtering process of the extracted DEM elevation profile in Subsection 6.3.2. Section 6.4 investigates the use of multiple runs, of GPS traces, to determine road grade. Subsection 6.4.1 uses stand-alone GPS devices with repeated runs to determine road grade. Correspondingly, a B-Spline approximation of a geometric representation of the roadway is used to determine road grade in Subsection 6.4.2.

6.1 GPS Investigation

The results obtained from the GPS device in the Bach box will be presented in this Section. The results investigated why GPS elevation readings should not be used by themselves to measure road grade. The approach adopted follows the same procedural steps seen in data cleansing operations.

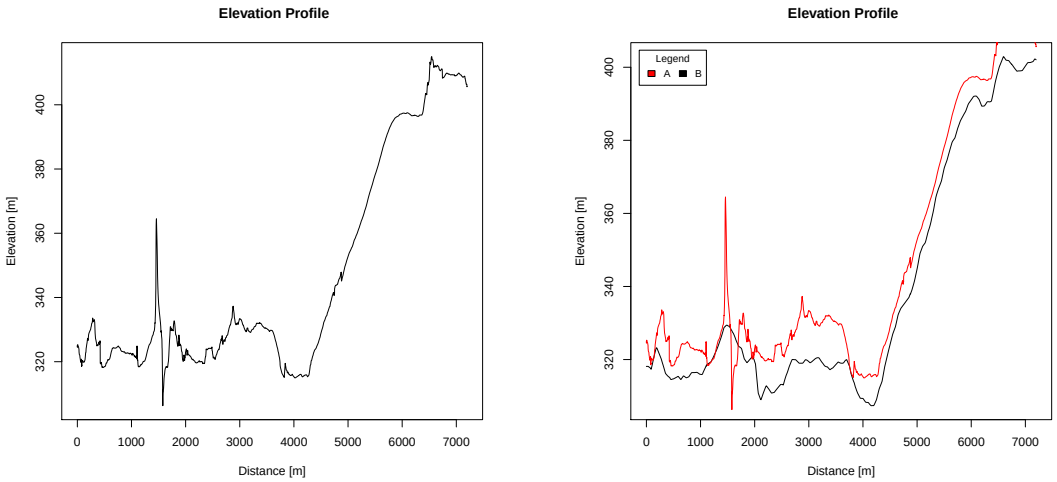

Figure 6.1: Unfiltered elevation profile from the GPS device by itself (left image), and compared to Google elevation API estimates (right image) – with the GPS elevation profile (A) shown in red and the Google elevation profile (B) in black.

The Figures above in Fig. 6.1 compares the elevation profile taken from the GPS device to that of the Google elevation API. The results indicate that the GPS does resemble the Google elevation profile slightly but that the GPS elevation is susceptible to huge spikes in elevation and a general overestimation of the elevation values. The raw GPS elevation profile may seem like a viable solution by itself but when compared to the Google elevation API it becomes apparent that there is a general offset in the data as well as high frequency components which would greatly affect the road grade estimates.

There are three key areas of interest in the elevation profiles seen in Fig. 6.1. When comparing the GPS elevation profile against the Google elevation profile the three key areas are: (A) a minor fluctuation in the elevation profile around 500 m; (B) a major spike around 1500 m; and (C) lastly a minor fluctuation around 3000 m.

The set up of the experiment was as follows:

1. Initial investigation into possible reasons for errors
2. Set up of a data cleansing approach to remove errors
3. Applying procedure to data
4. Analysis of the results

The route of the test vehicle was projected onto Google Maps and OpenStreetMaps (OSM). The elevation profile was compared to the horizontal distance travelled to evaluate problem areas, as seen in Fig. 6.1. The test vehicle travelled the same route several times a day. Similarly, other measurements taken from the GPS module were used to highlight significant errors.

6.1.1 Initial Investigation Into Possible Reasons For Vertical Positioning Errors

This Subsection will investigate the possible sources of errors in GPS elevation profile, in order to investigate whether it is possible to remove errors with a smoothing technique. Possible reasons were hypothesised with the use of background information, in Chapter 4, to the possible causes of errors in GPS receivers. To be able to understand them, the comparison between the Google elevation API estimates and the GPS elevation estimates are investigated. Locations where there are differences between the Google elevation API estimates and the GPS elevation profile should highlight areas where the GPS module was susceptible to errors.

Coarse ellipsoid models of the earth, determined by the GPS manufacturer, would result in elevation information recorded by GPS modules to be slightly offset when compared to the true estimate of height (Arnold and Zandbergen, 2011). This can account for the general offset of the estimated elevation from the GPS device compared to the true height Google elevation API.

The route of the test vehicle goes through the urban area of Plzen, Czech Republic. Fig. 6.2 shows the plotted route on the OSM road network map using the R package OSMAR. The vehicle travels through the main commercial area of Plzen and then through an open area towards the end of its trip. It was found that there was signal loss at one location along the trip, through inspection of the trip on the road network. Which can better be seen in Fig. 6.3 (2). However, when compared to the elevation profile seen in Fig. 6.1, it was found that this location did not correspond with the large spike in elevation the around 1500 m mark and instead reflected an area of a minor spike around 3000 m. Therefore, the smaller spike in the elevation profile (around 3000 m) was thought to be caused by a temporary loss of signal of the GPS module. Significantly, however the horizontal positioning of the vehicle was unaffected by the signal loss, which was probably attributable to the Dead Reckoning (DR) system that the

Figure 6.2: OSM road network of the test area (Plzen, Czech Republic) with the route of the test vehicle, equipped with the Bach box, in red. The test vehicle starts from the left hand side and ends on the right hand side.

GPS module uses.

Most modern consumer-grade GPS devices will incorporate some sort of Satellite-Based Augmentation System (SBAS) to help correct the positional information of GPS receivers (Arnold and Zandbergen, 2011). However, Differential-GPS (DGPS) cannot account for effects of multipath and loss of signal between the receiver and the base stations/the low orbital satellites. Due to the fact that the test vehicle operates in an urban area under real life conditions it is predicted that the biggest factor in error of the GPS receiver's ability to record accurate elevation information will be down to the effects of multipath and loss of signal caused by urban canyons.

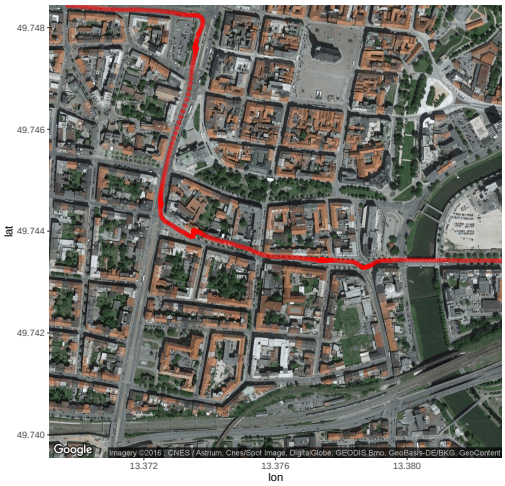

(1) Area corresponding to where the large spike in the GPS elevation profile was located, in the centre of the image, around 1500 m along the route, with a visible horizontal positional fluctuation as well. The horizontal fluctuation caused the vehicle's trajectory to jump to the other side of the road.

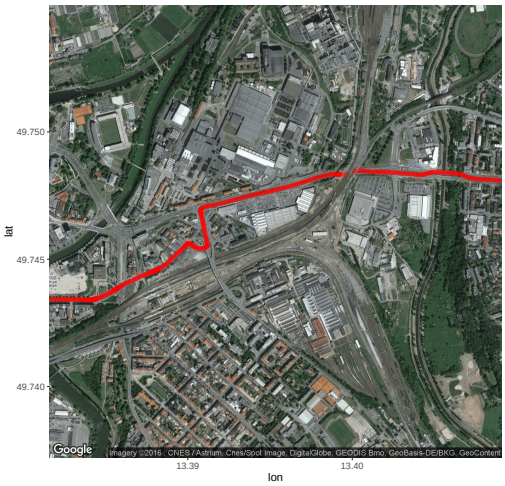

(2) Area corresponding to where the minor spike in GPS elevation profile was located, around 3000 m, with a temporary loss of signal due to the vehicle going under an overpass. Only the elevation measurements are affected and there is no differences in the horizontal positioning.

Figure 6.3: Comparison of areas where fluctuations in the GPS elevation, longitude and latitude measurements occurred.

Some consumer-grade GPS devices will merge GPS positional information with Dead-Reckoning (DR) systems to increase positional information, as seen in the Bach box. The positional corrections are usually only performed for horizontal positioning and still require GPS signals for initial predictions to be able to estimate bias in the Inertia Measurement Units (IMU) . Therefore, the DR-GPS signal will improve the horizontal inaccuracies but could still be susceptible to extreme fluctuations of GPS positional information. For instance, these systems will most likely rely on a fusion process, like a Kalman filter, to correct the GPS positional information with the use of other sensors and these results can be thrown by extreme random measurement values before being corrected by the fusion process. However, the DR-GPS is capable of providing estimates in periods of temporary signal loss of the GPS. It is assumed that the DR-GPS will not have an effect on the vertical

accuracies of the GPS measurements and the horizontal measurements will still be susceptible to extreme random noise.

The knowledge about DR-GPS and D-GPS limitations may explain for the fluctuations seen in Fig. 6.3 (1) and (2). Fig. 6.3 (1). The Figure 6.3 (1) represents the location where the major spike occurred in the GPS elevation profile, there is subsequently a fluctuation in the horizontal position. The GPS trace at this specific point, in horizontal position, fluctuates to the other side of the road, and is eventually corrected by the DR system. The location is represented by large buildings and heavy traffic area. In comparison, Fig. 6.3 (2) shows the area where the minor elevation spike occurred. This area corresponds to an overpass that the vehicle passes under, and the temporary signal loss does not seem to affect the horizontal positional information whereas there is a change in elevation information. Therefore, it is suspected that the GPS might have a correction system for temporary signal loss for horizontal positioning. The large spike in elevation at the location seen in Fig. 6.31 (1) would suggest that this area is prone to multi-path and hence we see a constructive combination of a reflected signal creating the large fluctuation in elevation.

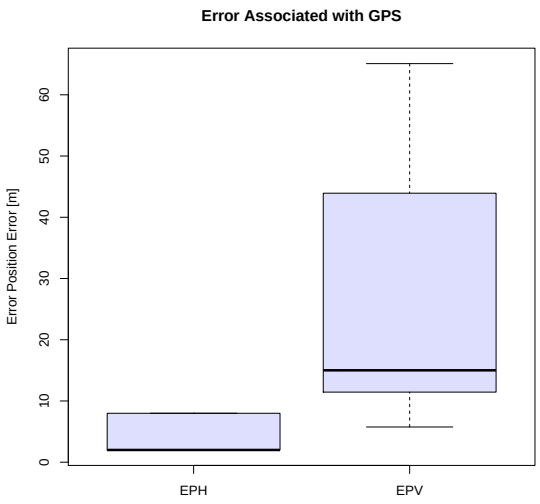

Figure 6.4: Expected error determined from the GPS device: (1.) Expected error position in the horizontal (EPH); & (2.) Expected error position in the vertical (EPV).

Consumer-GPS receivers have a known limitation in vertical positioning mainly due to the positions of satellites and lack of a positional reference from below the receiver. Fig. 6.4 represents the difference between expected error in horizontal (EPH) and vertical position (EPV), in that order taken, taken from the GPS receiver for each point along the trip. The readings show that the distribution of expected errors, indicating that the average horizontal positional error was around 2-3 m, with maximum values around 10 m. In comparison, the average vertical positional error was around 15 m, with outlier values over 60 m. These readings correspond to the manufacturers recommendations for the errors associate with the consumer grade GPS modules (Wing et al., 2005). The vertical position of consumer-GPS receivers are heavily influenced by the angle of the satellites overhead, this is expressed in Fig. 6.4. with the predicted vertical error associated with the readings.

Similarly, there is a need to have a minimum of four satellites at all times to be able to measure 3D position when using GPS receivers. The satellite count never goes below four during the trip, as seen in Fig. 6.5 and although the number of satellites over four does not correlate directly with the estimate of errors in vertical positioning (as the angle of the satellites is of greater consequence) it does give an indication of where errors may occur. From the figure it can be seen that the number of satellites reduces to four around the initial minor peak around 500 m. This could account for the increased elevation peak in this region.

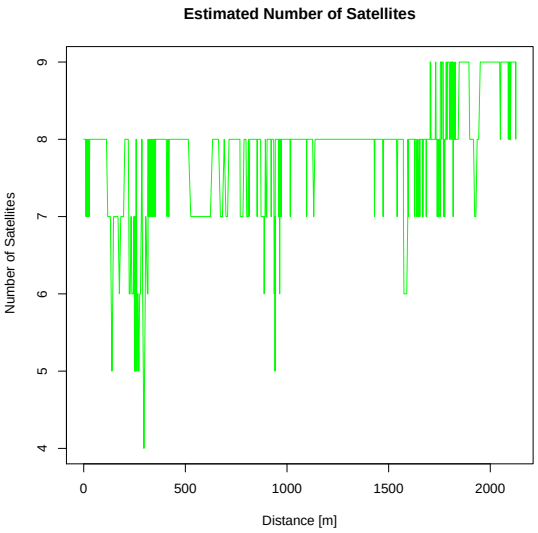

Figure 6.5: The number of satellites visible to the GPS along the trip.

In order to check if there were any duplicate results or periods of no signal, where the GPS receiver (DR included) did not record values, the time-stamp was investigated. As seen in Fig. 6.6 where the time-stamp is linear, which indicates for every GPS point there is a linear relationship with time. If there had not been, then a step profile would have been observed. The linear profile indicates that each GPS point was recorded with approximately a second delay and that there are no complete loss of signal periods.

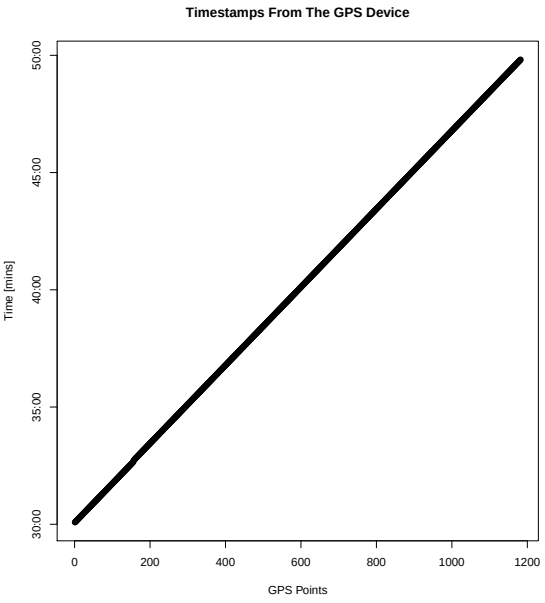

Figure 6.6: Time-stamp of the GPS receiver for the duration of the trip. The linear profiles indicates that there was no breaks in recording during the trip

Therefore, the hypothesised causes of errors that may resulted in the GPS elevation profile in the test vehicle are:

- Areas of temporary signal loss caused by buildings and other obstacles
- Effects of multi-path from buildings and other obstacles
- Low satellite numbers and satellite positioning
- Coarse ellipsoid model of consumer-grade GPS chips

6.1.2 Set-Up of A Data Cleansing Approach to Remove Errors

In order to set up a way to cleanse the data of the anomalies and irregularities a similar approach was taken as seen in (Rahm and Do, 2000) and (Müller and Freytag, 2005). Statistical smoothing processes were chosen to be able to investigate the effects on mitigating the errors in the elevation profiles. Similar to (Duran and Earleywine, 2012), an attempt to try and remove extreme outliers was performed. However, these results were ineffective and so only the smoothing process was applied. Three low pass filters were chosen to investigate the statical smoothing process in being able to reduce the high fluctuations in the signal.

- Binomial filter
- Exponential filter
- Average sliding window filter

A statistical smoothing method was chosen due to its ability to reduce high frequency components in signals. High frequency components are seen as fast changes in the profile, like sharp peaks and trough, which disrupt the continuity of the signal. Fig 6.7 shows the fast Fourier transform of a non-filtered signal (black) and a low pass filtered signal (red) representation in the frequency domain. The image shows the dampening effect that the low pass filter on the elevation points in the frequency domain, where high frequency components are dampened.

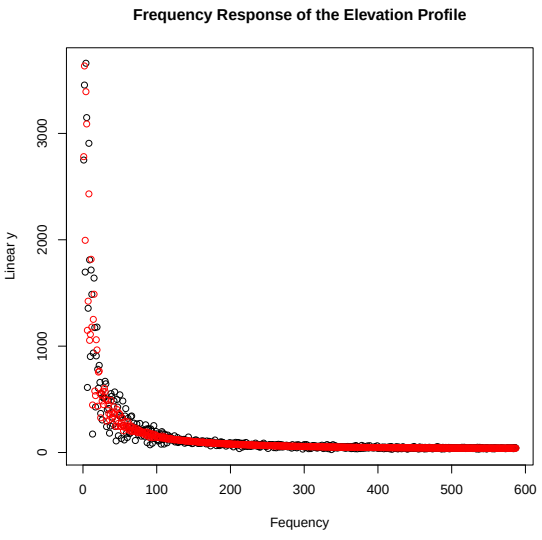

Figure 6.7: Fast Fourier Transform of the raw unfiltered GPS elevation values (black points) compared to the low pass filtered (red points) representation. Highlighting the impact of filtering techniques have on dampening the data-set.

Only the elevation profile was filtered as the distance only corresponded to horizontal distance and did not account for changes in elevation. The value of

$\alpha = 0.1$ for the exponential filter was found by varying the values of α. In comparison, the length of the filters for the average sliding window filter and the exponential filter was set at five points.

6.1.3 Applying Procedure To Data

The three different statistical smoothing approaches were applied to the GPS elevation profile. Fig. 6.8 shows the approach of applying the three different low pass filters on the GPS elevation profile and road grade profiles.

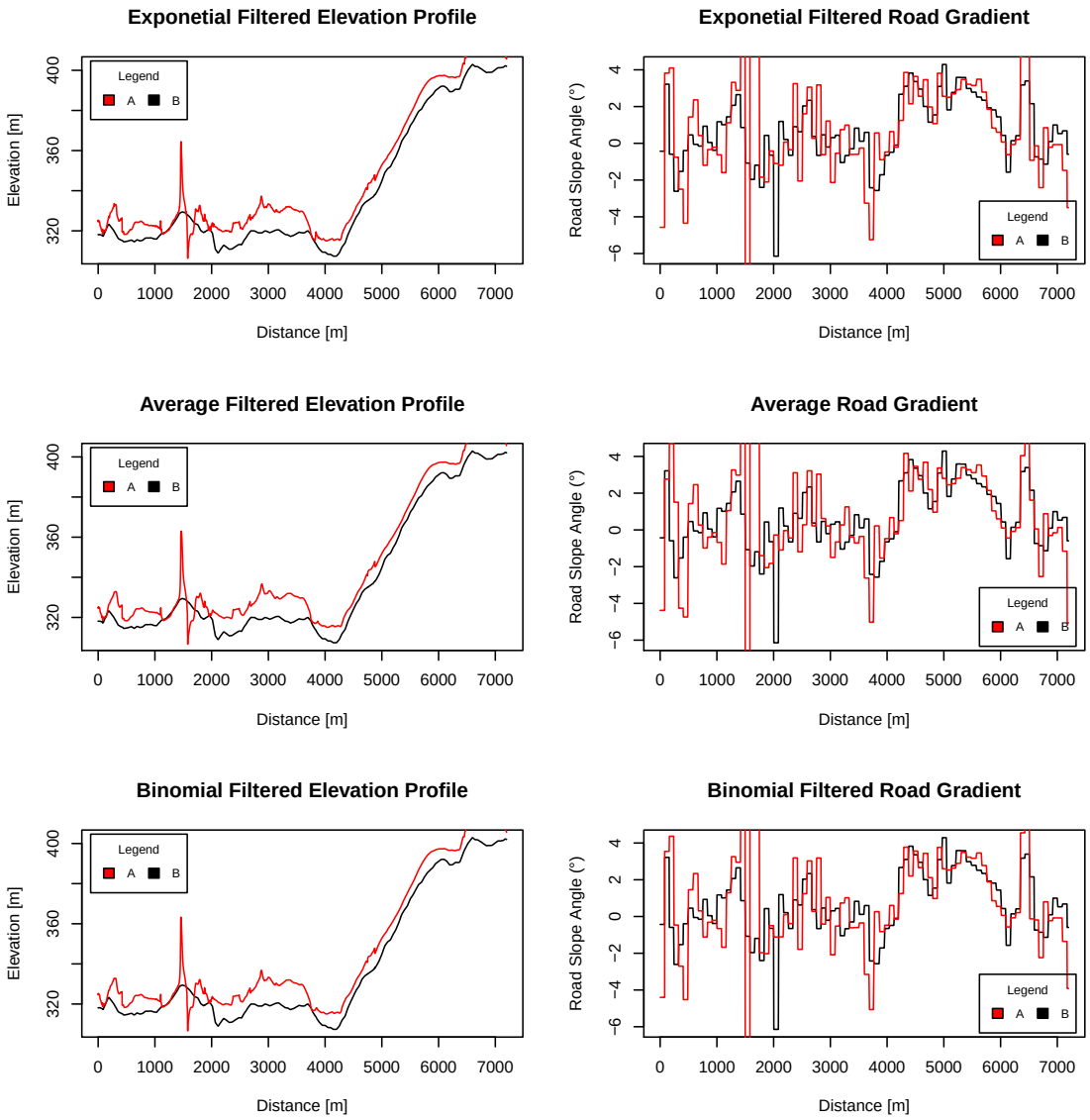

Figure 6.8: Elevation (left hand-side) and road grade (right hand-side) profiles of the different low pass filters in decreasing order: (1.) Exponential filter; (2.) Average sliding window filter; and (3.) Binomial filter. The resulting profiles from the filtering process is shown in red (A) are compared against the Google elevation API estimates in black (B).

6.1.4 Analysis Of The Results

The results from the statistical smoothing procedure can be seen to have very little effect on being able to remove the huge spikes in from the elevation profile. The end result of the experiment, on the road grade profiles can be seen in Fig. 6.8. The road grade estimates show high variation when compared to the Google elevation API estimates. The elevation profiles do seem to have been smoothed out a bit more than their original form, however the large spikes in elevation are not removed.

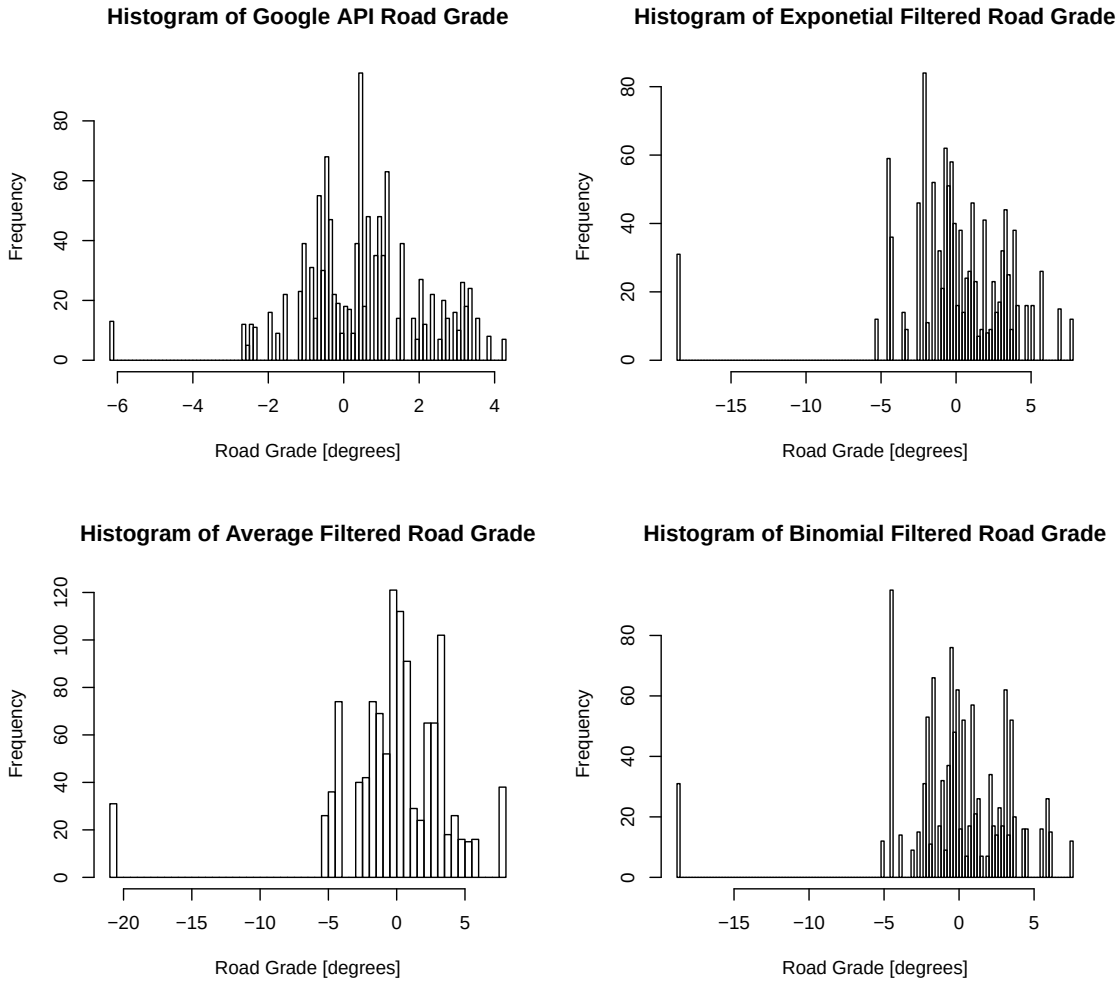

Figure 6.9: Histograms of road grade estimates: (1.) Google elevation API (top left); (2.) Exponential filtered GPS elevation (top right); (3.) Average sliding window filtered GPS elevation (bottom left); and (4.) Binomial filtered GPS elevation (bottom right)

Figure 6.9 illustrates the differences between the road grade estimates of the filtered GPS elevation values compared to the Google elevation API. When looking at the Google elevation API road grade histogram profile the results are almost normally distribute between -4 and 4 degrees, with outliers occurring around -6 degrees. However, the results in the GPS filtered elevation road grade estimates seem to be less of a normal distribution and cover the ranges -5 to 5 degrees, with outliers around -20 degrees. Therefore, on the general trend of the filtered GPS road grade estimates it can be seen that the estimates do not follow the same distribution as the Google elevation API estimates. Similarly, the ranges of the GPS filtered road grade

values differ to the Google elevation API estimates. The results would indicate that there is higher variation in the GPS filtered results, with more extreme ranges, than the Google elevation API estimates.

To calculate road grade, only the rate of change of elevation compared to horizontal distance is of interest. Therefore, an elevation offset will not affect the road grade readings when comparing against the Google elevation API. However, if the rate of change of elevation is sporadic and great (as seen in the GPS elevation) then the resulting elevation profile should not be used. The results indicate that the filtering techniques improved the GPS elevation profiles' smoothness but were unable to remove the elevation spikes found in the elevation profiles.

6.2 Accelerometer

6.2.1 Measuring Inclination With An Accelerometer

The raw accelerometer values taken as acceleration in the x, y, z directions were used to determine the pitch angle of the accelerometer. The raw pitch estimates are shown in Fig. 6.10. The images show the estimates are plagued by noise and that it is hard to determine the true angle of the road inclination from the noise. When compared against the Google elevation API road grade estimates, seen in the image on the right, it becomes clear that the noise from the accelerometer readings need to be corrected. The values taken from the accelerometer do seem to exhibit similar features of the road grade profile of the Google elevation API estimates, however the noise of the accelerometer hinders the measurements.

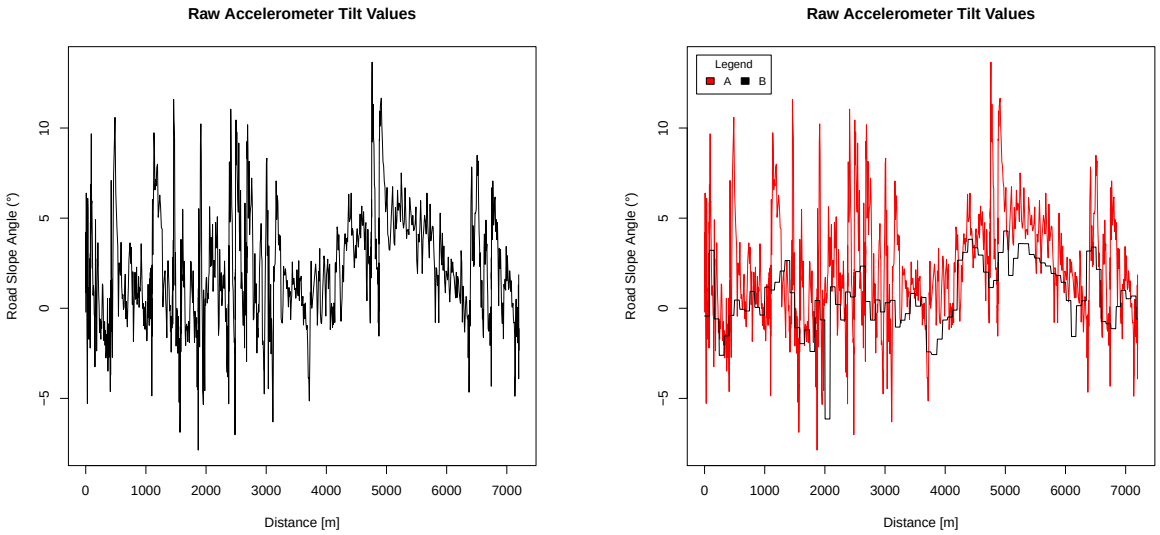

Figure 6.10: Raw accelerometer tilt profile by itself on the left and the raw tilt values (A) compared to Google API extracted elevation (B) on the right.

However, the images in Fig. 6.11 show the different steps under-taken in the experiment. The initial raw values are dramatically improved with the use of the low pass filter (exponential filter with $\alpha = 0.1$), this can be seen in the top two images. The low pass filter has a significant impact in removing noise from the accelerometer created by vibration of the vehicle. The low pass filter statistically smooths the profile according to the previous estimate and the weight, α, applied to it. The result is a smoother profile, however the low frequency components created by the acceleration are still apparent in the profile, seen as areas of spikes that are not consistent with the Google elevation API estimates.

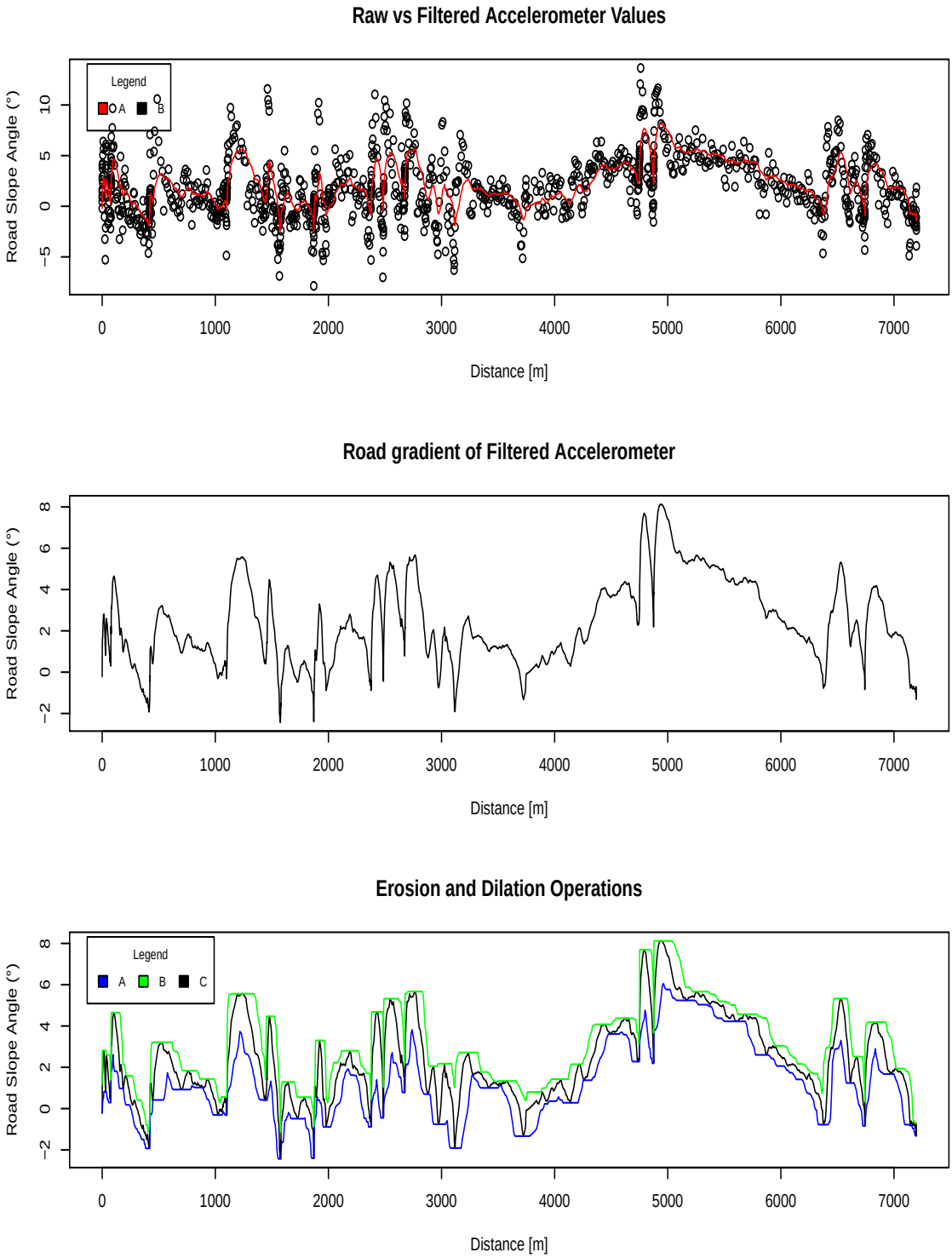

Figure 6.11: Several step process performed to remove noise from the vibration and acceleration of the vehicle. Using low pass filtering, seen in the top and middle images, to remove vibrational noise and using a mathematical Morphology approach to remove acceleration noise, seen in the bottom image, with the erosion operation (A) and the dilation operation (B) compared to the low pass filtered signal (C).

In comparison, the bottom image, in Fig. 6.11, shows the erosion and dilation operations after the low pass filter had been applied. The erosion and dilation follow

a kernel approximation of the pitch/tilt profile. Fig. 6.11, the bottom image, shows the effect of applying the erosion (A) and dilation (B) process individually on the original inclination profile (C), performed with the use of the R package mmand. The erosion process, seen in blue (A) of the bottom image of Fig. 6.11, has the effect of thinning out the points of high fluctuation which creates a lower profile which is more flat than the original. However, the dilation process, seen in green (B) of the bottom image of Fig. 6.11, expands the regions of neighbouring points creating a higher profile. However, this image is just to illustrate the differences between the erosion and dilation process on the inclination profile. The two are combined by applying the erosion followed by the dilation process.

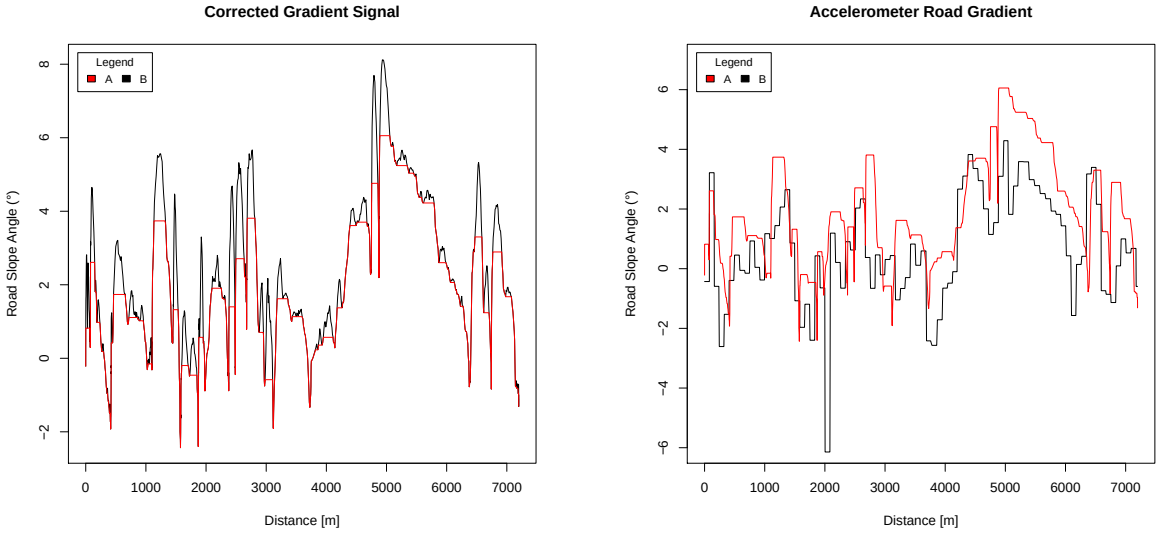

(1) Corrected accelerometer tilt values (A) compared to filtered accelerometer tilt values (B).

(2) Corrected accelerometer tilt values (A) compared to Google elevation road grade estimates (B).

Figure 6.12: Comparison of the corrected accelerometer tilt values, using the Mathematical Morphology approach, compared to: the original filtered values (left image); and the Google elevation API road grade estimates (right image).

The image on the left hand side of Fig. 6.12 highlights the impact of the MM process on the filtered measurements. The results indicate that the MM process was able to remove sharp spikes in the inclination caused by the acceleration of the vehicle. The tilt measurements taken from the accelerometer show a strong likeness to the road grade profile produced by the Google elevation API in Fig. 6.12. However, from the figure it can be seen that the inclination angles are over-estimated in general by the accelerometer. Similarly, there are discrepancies between the measurements in Fig. 6.12, with the accelerometer readings being less subject to variation shown with longer period (flatter periods) of the same road grade estimates.

The results of the erosion and dilation process is such that it does have a significant impact on the estimated pitch angle in Fig. 6.12. The process has the effect of removing some of the spikes in the inclination profile caused by the vehicle's acceleration. However, the acceleration of the vehicle still has an impact on the profile and the MM approach is not fully able to remove all of it noise created by it. Similarly,

the accelerometer measurements are subject to bias, the measurements will tend to drift if they are not correct, as seen in the image on the right hand side of Fig. 6.12. This may be the cause of the over-estimation of the inclination angles recorded by the accelerometer.

It is thought that due to the limitation of: (1) using the accelerometer instead of an inclinometer, the accelerometer is limited by the drift in the readings; and (2) the constantly changing inclination profile of the vehicle compared to the original study, due to the real life test movement of the vehicle, where a relatively stable profile can be seen (Mangan et al., 2002). This would impact the MM process on being able to fully remove noise caused by the acceleration of the vehicle. The use of the ramp in the original study means that the shape of the profile which the MM process has to compare the noise against is rather straight forward. In comparison, in real driving environment where the change in slope of the road is not known and does not resemble a simple shape there is some difficulty in removing the noise caused by acceleration using the MM process.

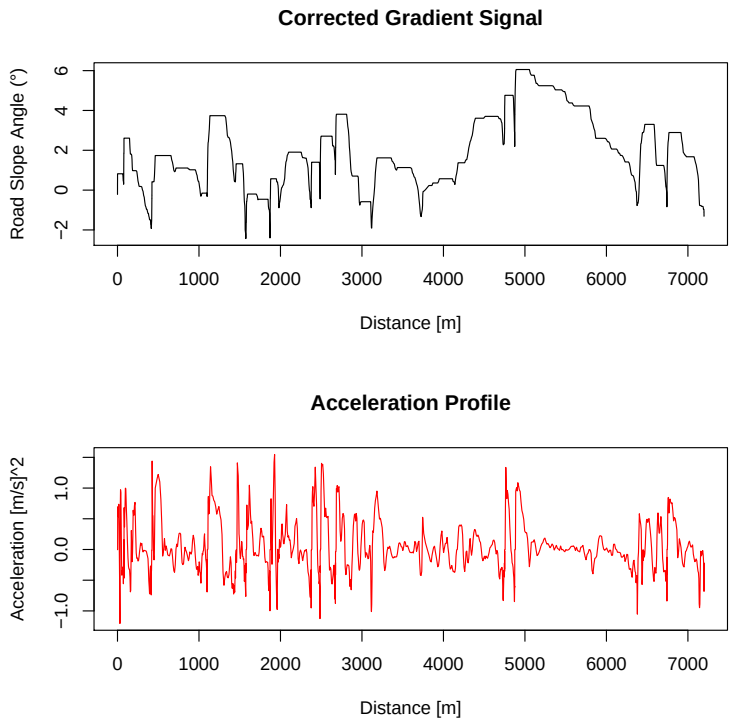

Figure 6.13: Comparison of the filtered (low pass filtered and MM approach) accelerometer road grade angle measurements (top image) compared to the acceleration profile of the vehicle (bottom image), taken from the Controller Area Network bus (CAN).

The true effect of the acceleration of the vehicle on the tilt/pitch angle created by the accelerometer can be seen in the Fig. 6.13. Periods of high acceleration, seen as spikes in the profile of the second image, correspond highly with periods where there were fluctuations in the pitch angle vehicle. From the figure it can be seen that, in periods of low acceleration, the accelerometer is able to measure the inclination values more effectively, specifically seen around the period 4000–6000 m. However, as seen in other areas where there are high periods of acceleration there

are corresponding high inclination angles measured by the accelerometer.

Similarly, the positioning of the Bach box has a significant impact on the readings. The Bach box is positioned in the front of the vehicle next to the driver and because of the bus' chassis the true inclination of the road might not be recorded. It was confirmed by other ZF Openmatics investigations that the placement of the Bach box under the driver inhibited the use of accurate readings from the bus, with the hydraulics in the bus causing the bus to stay level even when on an incline like a hill.

Therefore, in conclusion the approach suggested in the study by (Mangan et al., 2002), is able to reduce the effect of the noise created by the vibration and acceleration of the vehicle to some degree. However, the acceleration noise still plays a significant impact on the inclination profile to be effective and the bias of the accelerometer measurements cause the measurements to be overestimated. The process could be improved by combining the values of the accelerometer with a gyroscope using a fusion process, similar to that seen in study by (Pasaye et al., 2013). However, due to the time constraint of this dissertation a fusion approach was not investigated further.

6.3 Digital Elevation Models

Digital Elevation Models (DEMs) provide elevation information that can be extracted using the GPS location values. The World Global System 1984 (WGS48), the format used for the GPS devices, longitude and latitude coordinates were used to directly query elevation information from the SRTM 1-arc second DEM.

However, DEMs have several associated problems with direct querying of information when used in combination with a GPS trace that need to be corrected. Extracting the elevation direction from the grid where GPS points are not directly on the centre of the grid means that they are not accurately represented, as the estimate for elevation is at the centre of the 30x30 m grid. Similarly, GPS points moving from one grid to another are subject to elevation jumps/declines which can create a stair like elevation profile. Lastly, irregularities can occur in the elevation profile due to the collection method used by the SRTM satellite which measures elevation at its lowest point. This affects man made structures at points like bridges and overpasses were elevation is measured at a lower value than that it truly is.

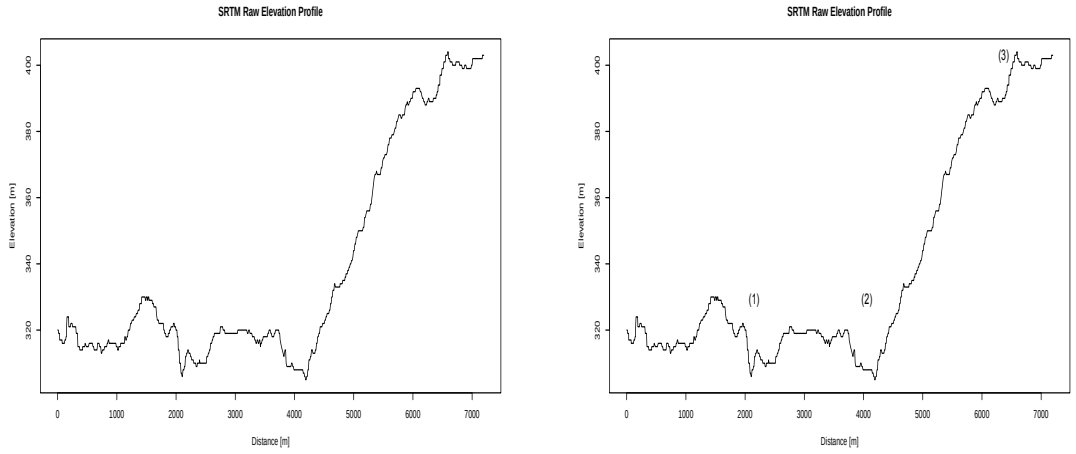

Figure 6.14: Elevation values extracted from the SRTM 1-arc DEM, with an indication of where elevation values may differ from true elevation (right image).

The Fig. 6.14 illustrates the extraction of elevation information from the DEM using the GPS trace of the test vehicle. The figure highlights the different problems associated with the elevation extracted from the DEM. The step like profile can be exhibited, caused by the elevation difference between grids, and similarly sharp declines in elevation are apparent where bridges and overpasses occur on the terrain. Examining the elevation profile in Fig. 6.14 there are several key areas that could cause discrepancies in the road grade profile if not corrected: (1) around 2000 m there is a sharp decline in the elevation; (2) similarly around 4000 m there is another decline; and (3) lastly around 6500 m there is a sharp peak.

The slight variations apparent, the sharp declines (1) and (2) in the elevation profile are apparent around 2000 m and 4000 m. These points are directly attributed to locations where the vehicle travels over a bridge, seen in Fig 6.15 on the left hand side image, and a location where the vehicle travels over an overpass, which can be seen on the image in the middle.

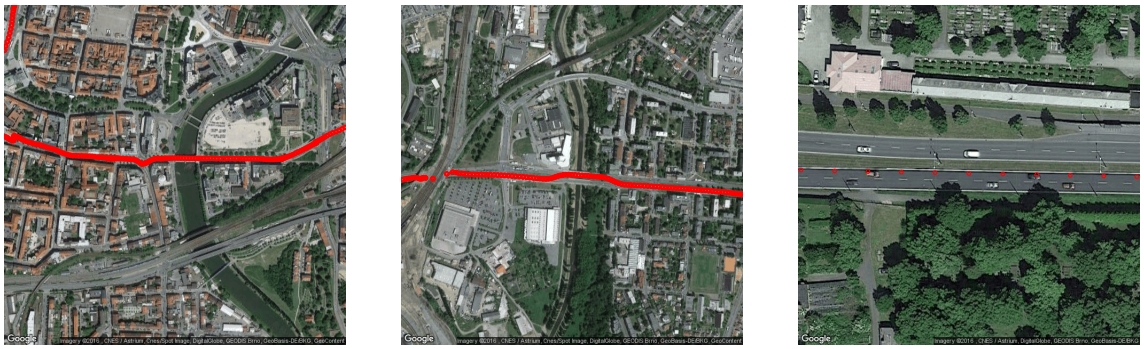

Figure 6.15: Areas along the test route where the extracted DEM elevation profile exhibits discrepancies. The first images on the left shows an area of the test route where the road goes over a bridge. Similarly, the middle image shows an point where the road way goes over an overpass. Lastly, the final image on the right shows an incline that occurs near the road way.

Similarly, the elevation peak (3) that occurs around 6500 m was explored further in the Fig. 6.15 the image on the right. From the image it can be deduced that perhaps the spike was caused by the slope of an embankment that is apparent next to the road–way, attributing to the higher changes in elevation values than should be on the road–way.

In order to address the issues with the elevation profile and to remove the components from influencing the elevation profile in being able to determine accurate road grade estimates the two methods are explored in Sections 6.3.1 and 6.3.2. Road grade values were calculated at 80 m intervals.

6.3.1 Bilinear Interpolation of Elevation profile from DEMs

The study by (Henriques and Bento, 2013) investigates interpolating values of GPS locations, that would not correspond with the centre point of DEM grid, to produce accurate road grade estimates. The approach used a form of bilinear interpolation to approximate a better value of the GPS points, and in doing so, smoothed the elevation profile of the elevation differences between grids.

The elevation profile seen in Fig. 6.16 highlights the interpolated values of GPS points extracted from the SRTM DEM. The Fig. 6.16 (1) illustrates the interpolated elevation (A) profile is somewhat smoother when compared to the raw SRTM elevation profile (B). Therefore, the results indicate that the interpolation method allows for a better approximation of values to produce a more continuous profile. However, some of the discrepancies in the elevation profile are not completely removed or addressed, like the low elevation troughs where a bridge and overpass cause the elevation values to be measure at lower values than their true elevation. This is apparent by the large negative road grade angle measured around 2000 m, which corresponds directly with the location of the bridge.

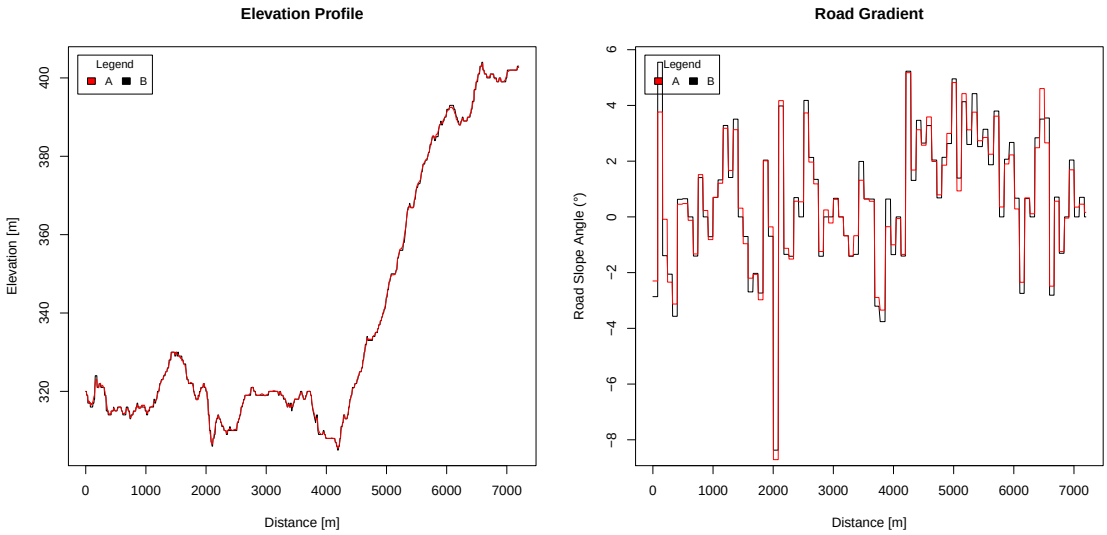

(1) Elevation profile. **(2)** Road grade profile, at 80 m intervals.

Figure 6.16: Interpolated DEM elevation (1) and road grade (2) profiles. The interpolated values (A), shown in red, are compared to raw DEM elevation estimates (B), seen in black.

Figures 6.16 (2) show the road grade estimates of the interpolated data compared to the raw SRTM road grade estimates with 80 m segments. Fig. 6.16 (2) highlights the change in road grade values due to the interpolated elevation (A), compared to the raw SRTM estimated road grade profile (B). The slight changes, seen in Fig. 6.16 (2) suggests that the interpolated data only corrected the road grade profile slightly. In Fig. 6.16 (2) does show the significant influence that the interpolated elevation profile has on determining road grade at and producing a slightly smoother road grade profile (A) than the raw SRTM elevation values (B). When looking at the road grade profile difference in the road grade values are apparently altered with a sort of dampening effect, which indicates the interpolation process had a smoothing

effect on the profile.

In contrast comparing the interpolated elevation and road grade estimates, against the Google elevation API estimates another perspective can be drawn. The elevation profile seen in Fig. 6.17 (1) assert the differences between the interpolated SRTM elevation profile (A) and the Google elevation API profile (B). In Fig. 6.17 (1) the interpolated data, shows a strong likeness to the Google elevation estimates. However, there seems to be slight over and underestimations in the profile, either due to the SRTM DEM or the interpolation method used by Google.

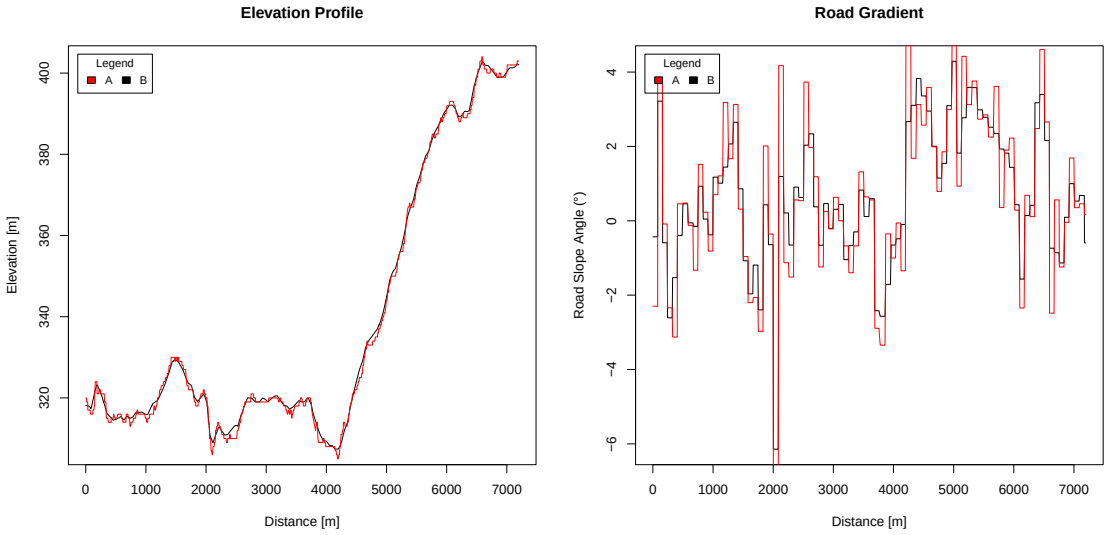

(1) Elevation profile. **(2)** Road grade profile, at 80 m intervals.

Figure 6.17: Interpolated DEM elevation (1) and road grade (2) profiles. Interpolated SRTM elevation estimates (A) compared to Google elevation API estimates (B).

Again comparing the road grade profiles, seen in figures 6.17 (1) and 6.17 (2) of the interpolated elevation data (A) and the Google elevation API data (B), a strong likeness can be determined. However, the slight differences in elevation values of the interpolated data compared to the Google elevation API data cause differences in road grade estimates. Fig. 6.17 (2) exhibits slight differences in road grade estimates, of the interpolated data when compared to the Google elevation API, caused by the overall differences in elevation values at specific distance values. However, the differences in road grade estimates of the two profiles, the interpolated road grade profile (A) and the Google elevation API road grade profile (B), can be better determined when viewing Fig. 6.17 (1). In Fig. 6.17 (2) the road grade profile of the interpolated data (A) exhibits higher road grade values than the Google elevation API estimates (B). The reason for the higher values of road grade could be due to the fact that even though the interpolated elevation profile is better approximate than the raw SRTM value, it still has not undergone an extensive smoothing process and so will have light variations that need to be corrected.

The interpolated elevation estimates do seem to exhibit a good likeness to the Google elevation estimates, and when compared against the raw SRTM elevation estimates an improvement in the smoothness of the profile can be seen. Therefore, the elev-

ation profile of the interpolated data can be seen as a good estimate of elevation. However, there are still in-discrepancies in the elevation profile which are not addressed in the interpolation method. This can be seen with the elevation depression of the bridge and overpass areas of the test area. Similarly, the interpolation process does not fully smooth out the elevation profile of the SRTM extracted elevation and hence for the major difference between the Google elevation API estimates.

From the different comparisons shown above it can be determined that the interpolated elevation data is a better estimate of the true elevation along the road–way than the raw estimates. The effect of better elevation data is that the road grade estimates will be of a higher precision, which is illustrated when comparing the interpolated road grade estimates against the raw elevation estimates. However, the elevation profile of the interpolated data is never fully smoothed out and this creates inconsistencies seen in the road grade profile than that of the Google elevation API estimates. Therefore, the interpolation method provides better estimates of elevation but there is a need to smooth/filter the elevation profile further: to smooth the profile to provide better consistency with the elevation profile; and to remove in-discrepancies caused by the collection method of the SRTM satellite.

6.3.2 Smoothing/filtering of Elevation profile from DEMs

The several step smoothing/filtering technique developed in the study by (Wood et al., 2014b) is explored in this Subsection. The approach looks to: (1.) Compare the elevation profile against the distance travelled; (2.) down sample the elevation profile against the distance travel into equispaced distances; (3.) apply a combined binomial and Savitsky-Golay filter; (4.) remove outliers greater than a certain elevation difference and interpolate the removed points; (5.) re-filter the data-set to smooth the elevation profile; (6.) use the original distance values to interpolate elevation values from the filtered data-set as a reference, to obtain a data-set with a length equivalent to the original data-set.

The several steps performed can be seen in the Fig. 6.18. The first step seen as Fig. 6.18 (1) was to compare the elevation value extracted from the SRTM DEM against the cumulative distance travelled. The discrepancies in the elevation profile have already been described earlier, in Section 6.3, and can be seen in Fig. 6.14.

The next step, seen in Fig. 6.18 (2), highlights the down-sampling process. Where the elevation profile is down-sampled at equispaced distances of fifty meters (every 50 m the resulting elevation values are used to determine a decimated version of the original signal). In the case of down-sampling the data the length, N, of the dataset went from N=1182 to the down-sampled value N=334. The effect of this is highlighted in the figure 6.18 (2), with elevation values down-sampled (A) in red, where the data-points appear at regular intervals with a reduced number points than that of the original data-set.

Fig. 6.18 (3) illustrates the filtering process — applying the nine point Binomial and Savitzky-Golay filter to the down-sampled data-set. The resulting filtered profile can be observed, (A) in red, showing the smoothed profile that seems to be removed of the discrepancies in the original profile.

The process of determining elevation changes that would be considered as outliers did not result in any data-points being removed as an outlier value of 10 m was set. Hence, there were not any elevation values with differences greater than 10 m after the filtration process. Any data-points that would have been removed, would have had to been back-filled using linear interpolation.

The last section in the filtering/smoothing process is shown in Fig. 6.18 (4), where the filtered/down-sampled data-set is used to interpolate the missing values of elevation from the original distance values. Interpolating the elevation values with the original distance values changes the down-sampled length from N=334 back to N=1182 again.

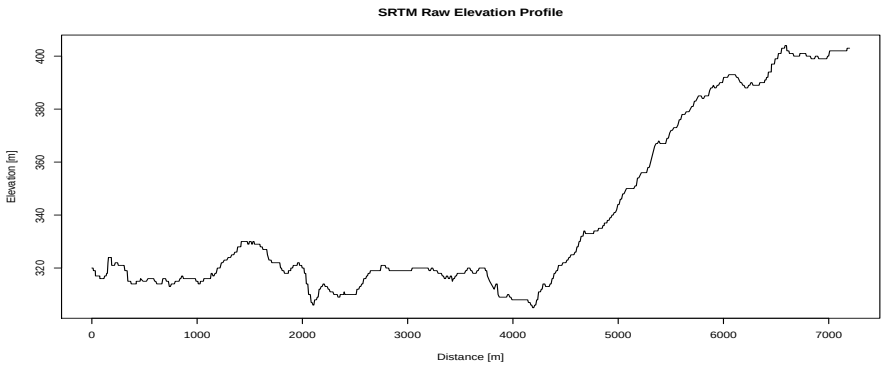

(1) Raw SRTM elevation values vs cumulative distance travelled.

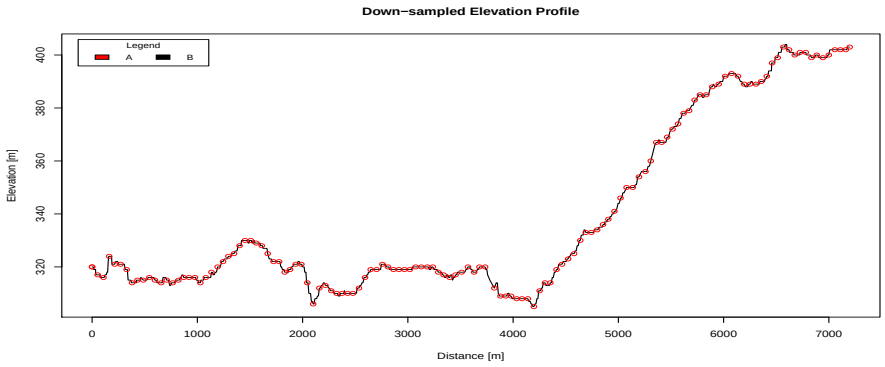

(2) Down-sampling the elevation profile into equispaced intervals.

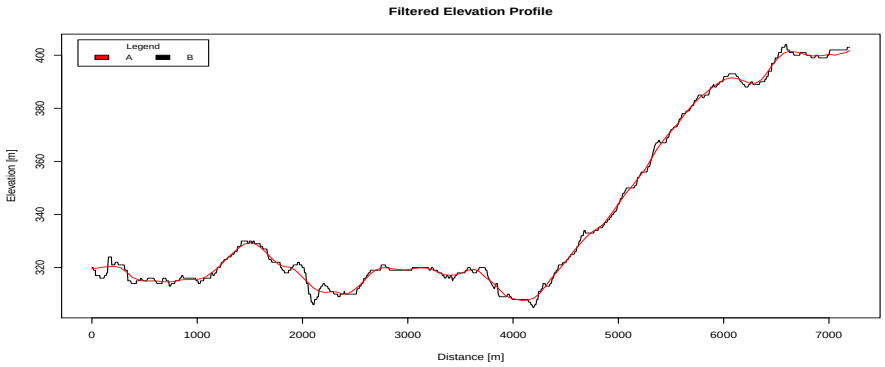

(3) Filtering the down-sampled profile using the combined filter.

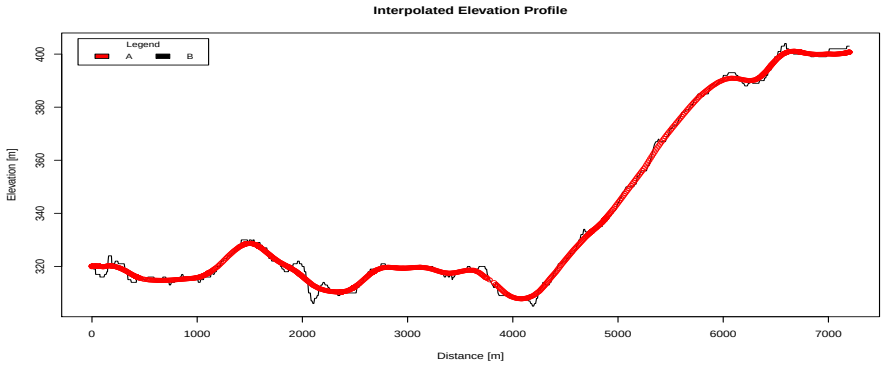

(4) Interpolating elevation values using the original distance values.

Figure 6.18: Several step process of the smoothing/filter process of the SRTM DEM extracted elevation profile.

The result of the replicated filtering/smoothing process discussed in (Wood et al., 2014b) are shown in Fig. 6.19. The elevation profile Fig. 6.19 (1) compares the smoothed/filtered elevation values (A) against the original elevation profile (B). The filtered elevation profile exhibits a smoother profile that seems to have removed the discrepancies as discussed before in Section 6.3. Period of sharp elevation changes were removed from the profile and smoothed out.

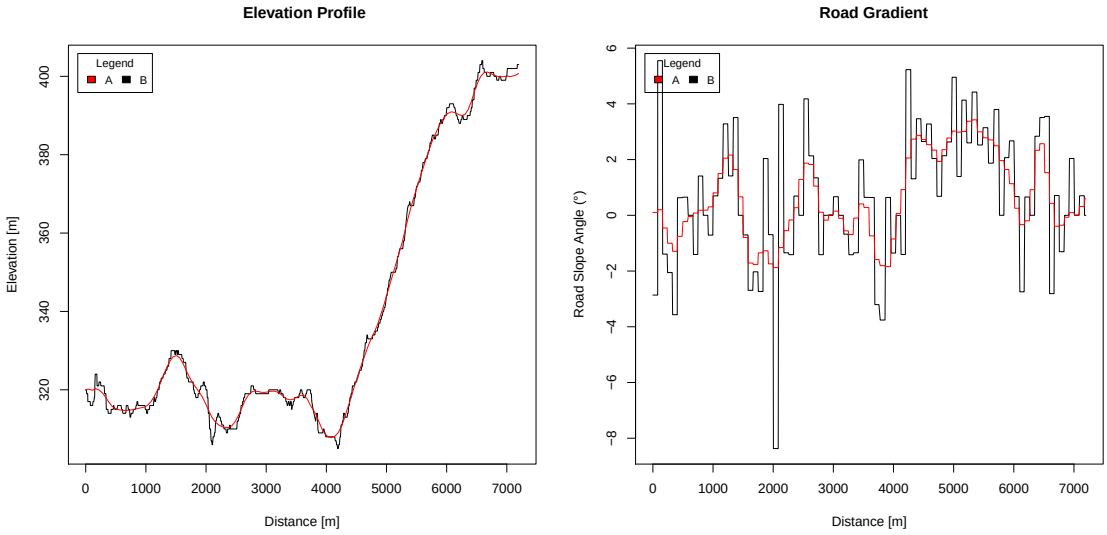

(1) Elevation Profile. **(2)** Road Grade Profile, 80 m intervals.

Figure 6.19: Filtered smoothed DEM elevation and road grade profiles (A) compared to raw DEM elevation estimates (B).

To highlight the effects of the smoother profile, comparing the original road grade estimates (B) against the filtered road grade estimates (B) can be seen in Fig. 6.19 (1) and (2). Fig. 6.19 (2) highlights differences in the road grade profile, at 80 m intervals, that are due to the difference in elevation values that were filtered. The changes in elevation values from the filtering process creates the differences in road grade estimates and the smoothing process ensures that elevation values do not alter as much between each GPS point, reducing the variation between road grade readings.

In comparison, when looking at the differences between the Google elevation API estimates and the filtered SRTM elevation estimates in Fig. 6.20, a degree of accuracy can be assessed. The elevation profiles of the filtered SRTM elevation (A) and the Google elevation API values (B) show a strong likeness and for the most part there is a high correlation between the two. There are slight variations in the two profiles, with the filtered elevation slightly over or underestimating values when compared to the Google elevation estimates. However, when comparing the discrepancies that occur in the SRTM DEM, it becomes clear that the Google elevation API estimates do not account for all of these points where discrepancies are apparent. This is apparent in the high peaks and low troughs of the Google elevation API (B), which corresponds to the locations where the bridge, overpass etc. are located.

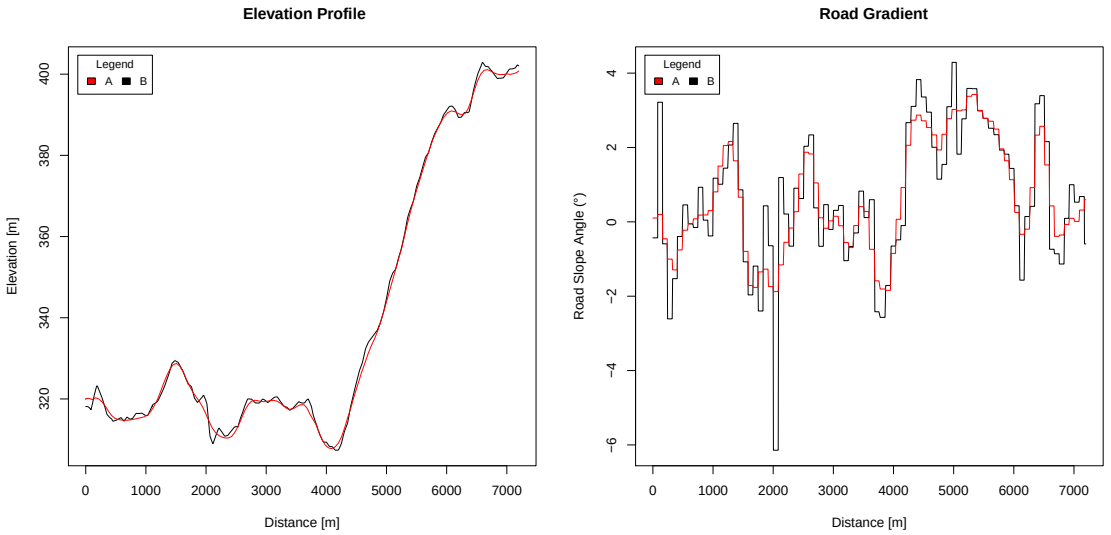

(1) Elevation Profiles. **(2)** Road Grade Profile, 80 m intervals.

Figure 6.20: Filtered/smoothed DEM elevation (1) and road grade profiles (2). The filtered/smoothed profiles (A) are compared to the Google elevation API estimates (B).

When comparing the Figures 6.20 (1) and (2) it becomes apparent that the estimates of the filtered SRTM elevation (A) have a high likeness to the Google elevation API estimates (B), indicating the method has high accuracy. Fig. 6.19 (2) indicates the differences in road grade estimates at 80 m intervals. The road grade profiles at 80 m intervals have variations between the two which is caused by the difference in elevation profiles. Selecting specific elevation values at 80 m intervals causes a constant road grade estimate and when there are slight difference in the elevation values at these distances the road grade values will differ. However, due to the likeness of the profile it can be said that the road grade estimates have a high correlation with the Google elevation API estimates with the differences in the sharp declines and high peaks where the discrepancies occurred in the elevation profile. This highlights the fact further that the smoothing process does seem to remove the right components where discrepancies occur, as the filtered profile is not hampered by higher values of road grade as senn by the Google elevation API estimates.

In conclusion, the elevation and road grade values of the filtered SRTM values are compared against: the original SRTM values; and the Google elevation API estimates. Comparing the change from the original values determines what the effect of the filtering process was in determining more accurate road grade profiles. Similarly, comparing the estimates against a reference value like the Google elevation API estimates allows for a determination of the accuracy of the process. From the results it can be seen that the filtering process was successful in removing discrepancies, like the bridge and overpass, and smoothing the elevation profile to improve the road grade estimates. Similarly, the strong likeness to the Google elevation API estimates advocates a high level of accuracy associate with this method.

6.4 Repeated Runs

Using repeated runs of GPS measurements it is possible to determine an averaging of the road grade estimates or by using a geometric representation of the road–way a road grade profile can be determined.

Figure 6.21: Representation of the test routes chosen for the multiple runs experiment (left) and the B-Spline approximation experiment (right). The test areas are a smaller segment, seen in green, of the entire route travelled, seen in red.

The test routes of the two experiments, performed in Subsections 6.4.1 and 6.4.2, had be segmented into smaller sections of the entire test route. This was mainly due to the route of the test vehicle, the test vehicle takes a route that causes the vehicle to repeat most parts of the road–way, in the alternate direction, and deviate slightly on the returning journey. The trips taken by the test vehicle needs to be segmented to only have runs in one direction and have sections that do not deviate to the other runs. Similarly, for Subsection 6.4.2 it was found that a small straight segment was needed to perform an accurate geometric representation of the road–way.

Fig. 6.21 illustrates the different test segment chosen for the experiment. The image on the left hand side shows the route taken in the experiment in Section 6.4.1. The segment was chosen due to the fact that the test vehicle's route is constant for both directions and there are no deviations onto other roads when the vehicle changes direction. This allows the different trips to be segmented easier into the given directions. Similarly, the image on the right hand side shows the route taken in the experiment in Section 6.4.2. The route chosen was selected due to the short straight segment that was available.

6.4.1 Multiple Runs

In order to replicate the study by (Boroujeni et al., 2013) a segment of road was selected where multiple runs could be collected with consistency. The trips were then segmented into the direction of travel and ten one way (clockwise) direction runs were selected for the experiment.

Figure 6.22: 3D representation of five repeated runs of the test segment, the different colours representing each run, comparing the elevation to the longitude and latitude coordinate measurements taken from the GPS module.

Fig.6.22 shows the segment of the route taken by the vehicle, with five different one directional runs. The image sheds light on the route taken, providing a better visual representation of the trip. Already it can be seen that each run has different elevation readings and slightly different longitude and latitude coordinates. The elevation differences are caused by errors associated with GPS readings whereas the differences in longitude and latitude coordinates are more likely caused by real life driving behaviours, for example changing lanes. However, it can be seen in the images that the elevation values vary more that the longitude and latitude coordinates.

The study by (Boroujeni et al., 2013) utilises linear regression at set distances to segment the trip. In order to calculate the distance of the test area, the average value of the total distances for every run was selected. The combined runs were then further segmented into 80 m segments, where linear regression was applied to the dataset. The slope of each regression line was used to calculate the road grade angle for those segments.

The Figure 6.23 shows the effect of using linear regression of multiple GPS elevation profiles at 80 m segments. When looking at Fig. 6.23 (1) the process of linear regression has in determining a better approximation for the elevation profile becomes clear. The different multiple runs have varying elevation and the linear regression lines (A) appear to average out the results. In comparison looking at Fig. 6.23 (2) the raggedness of the profile becomes clear when compared to the Google elevation API estimates (B). What else becomes apparent is the general elevation difference caused by the GPS device compared to the Google elevation estimates. The elevation profile of the linear regression lines appears higher than the Google elevation API estimates, however as the change in elevation estimates are only of interest, the overall elevation difference between the GPS readings and the Google elevation API readings should not play a factor in determining accurate road grade estimates.

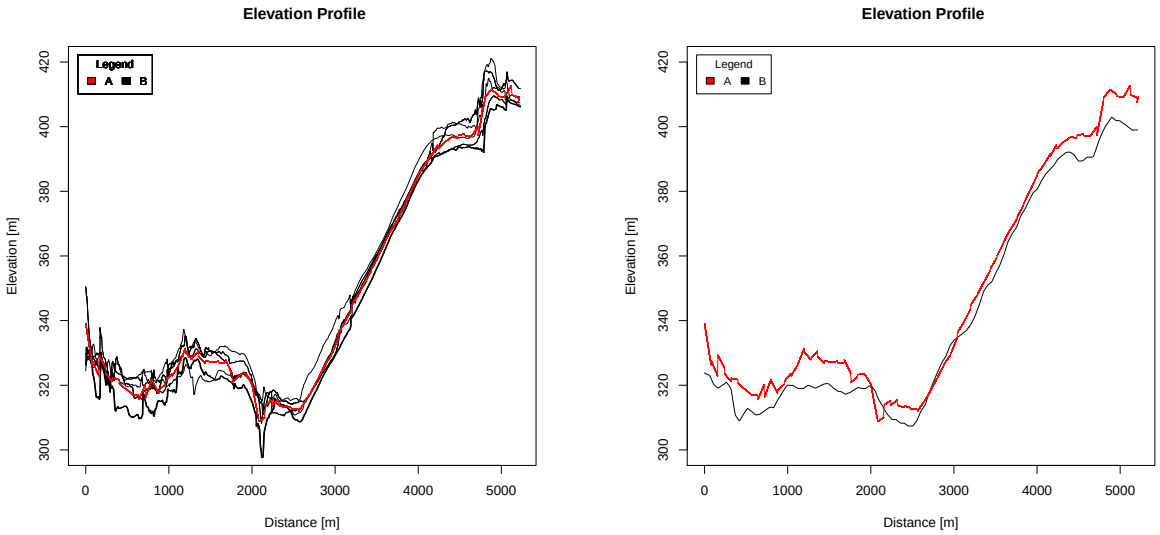

(1) Linear regression of the combined multiple runs, at 80 m intervals, (A) compared to the multiple GPS runs (B).

(2) Linear regression of the combined multiple runs, at 80 m intervals, (A) compared to the Google elevation profile (B)

Figure 6.23: Comparison of linear regression profile of the combined multiple runs compared against multiple runs on the left and the Google elevation on the right.

From the linear regression profile of the multiple GPS elevation profiles, taken every 80 m, the road grade estimates can be determined by taking the slope of the linear regression lines. This can be seen in Fig.6.24, where the slope of the regression lines of the combined multiple runs (three runs in the first image on the left, five runs in the middle image, and seven runs in the last image on the right) (A) and are compared aginst the Google elevation API road grade estimates (B).

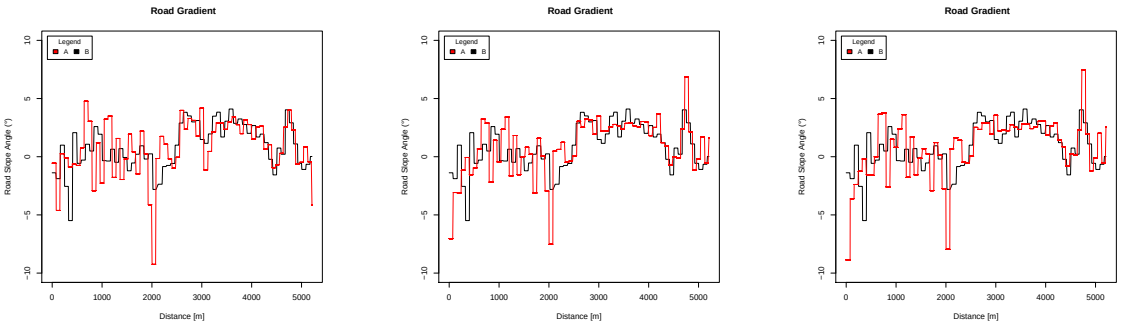

Figure 6.24: Road grade profiles of the multiple runs with 3, 5 and 7 repeated runs, shown in that order (A) compared to Google elevation API road grade estimates (B).

Observing Fig.6.24 it becomes apparent that with more runs the variation exhibited in the road grade profile of the multiple runs (A) decreases and the results seem to converge toward similar values of the Google elevation API estimates (B). However, it is clear that there are quite a few differences between the Google elevation API estimates and the multiple regression estimates. It does highlight the added advantage of the multiple runs approach would be the convergence towards

the best estimate with more runs. Another advantage would be the use of linear regression, meaning that a single elevation value does not determine the road grade value, like that of the Google elevation estimates where elevation values at specific distances determine the road grade angle.

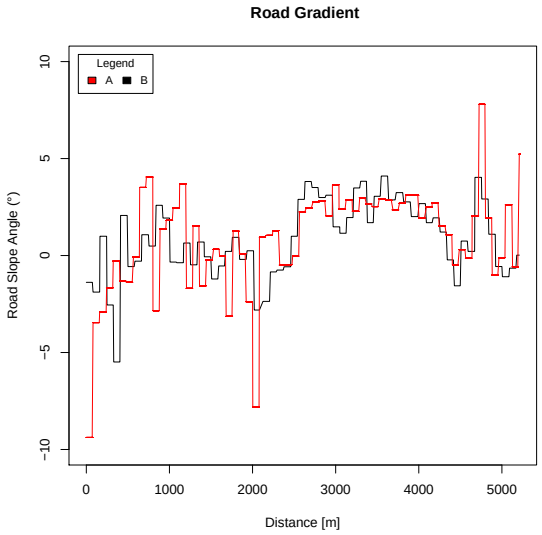

Figure 6.25: Multiple runs, 10 repeated runs, road grade profile (A) compared to Google API elevation road grade estimates (B).

Fig. 6.25 shows the end result of ten repeated runs combined to determine the road grade angle, using linear regression every 80 m, compared to the Google elevation API estimated road grade. The road grade estimates of the multiple runs does differ slightly from the Google elevation API estimates but on the whole there is a strong likeness. The multiple runs estimated road grade angles seem to slightly overestimate and underestimate some areas when compared to the Google elevation API estimates.

In conclusion, the elevation profile of the GPS device seems to over estimate the true elevation values, however this is not of consequence as only the change in elevation is of interest for determining road grade. The multiple runs experiment indicates that with enough repeated runs, of GPS elevation profiles, a good estimate of the road grade can be determined. Furthermore, the estimation of the angle of road grade is not dependant on a single elevation value, which when an outlier occurs may throw the road grade value off, but rather is on the general trend of the elevation data.

6.4.2 B-Spline Geometric Representation

In order to geometrically model the road segment chosen for the experiment, using the B-Spline approximation, the several step data cleansing process, as discussed in Section 5.5.2 and seen in the study by (Ben-Arieh et al., 2004), had to be performed to the data-set.

Several trips were segmented into the test area and sorted on the direction of travel.

The UTM projection was applied to the GPS coordinates, changing longitude and latitude coordinates to easting and northing coordinates. Then the runs were combined and sorted according to increasing distance.

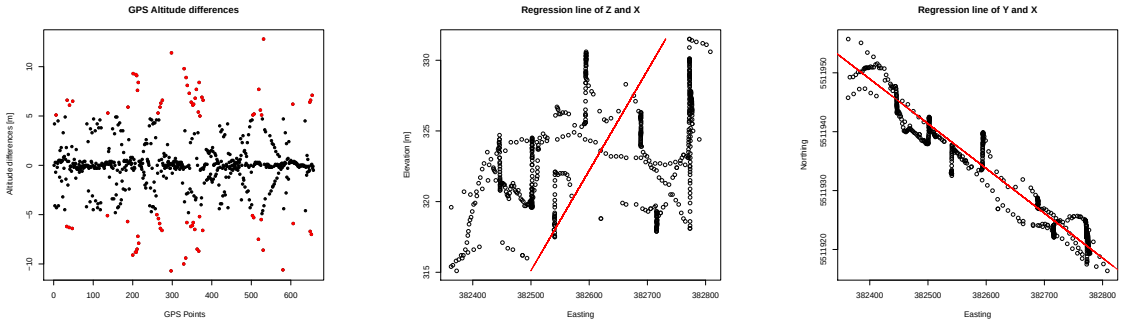

Figure 6.26: The several step process in cleansing the erroneous data. The first image on the left shows the elevation change between two points being identified, seen in red. The middle image shows the regression profile, seen in red, of Z and X datasets. The last image on the right, shows the regression profile, seen in red, of Y and X datasets.

Figure 6.26 illustrates the several step process that occurred after the repeated runs had been sorted for the specific segments. After sorting the data-sets by "increasing mileage", as seen in the study by (Ben-Arieh et al., 2004), the elevation differences between GPS points are determined. Then, to remove outliers from the data-set the elevation differences greater than 5 m were removed. The outlier elevation differences can be seen in the first image in Fig. 6.26 in red.

As the standard deviation of all the differences in elevation points were greater than 3 m the least square step was performed. The elevation values, Z, the easting, X, and northing, Y, values were used to determine the least square analysis. As the X range was greater than the Y values the least square regression of Z and X, and of Y and X were performed. To illustrate this the two last images (middle and left) of Fig. 6.26 are used. The least square regression analysis allows for the determination of residuals of the predicted trend line and the true values. Using the outlier detection of where any point outside of two sigma points greater or less than the mean were removed.

The outlier detection removed several more points from the dataset. The next step was to determine four points to use as control points. Comparing the elevation values to the easting and northing values, as seen in Fig. 6.27, allows for the comparison between the uniform and open uniform knot vector B-Spline approximations.

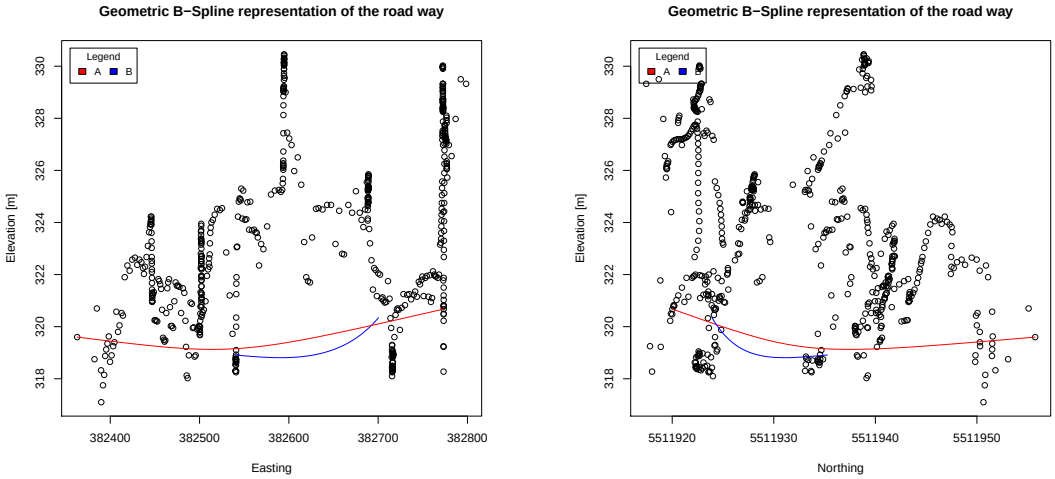

Figure 6.27: Open uniform (A) and uniform (B) knot vector B-Spline approximations compared against the elevation values at easting (left image) and northing coordinates (right image).

The differences in the open uniform and uniform knot vector B-Spline approximations become apparent in Fig. 6.27, with the open uniform knot vector estimates moving along the entire data-set. Whereas the uniform knot vector estimates only stretching half way across the data-set. The differences between the two B-Spline matrices can be found in Section 4.3. The length of the uniform knot vector is considerably short. It was unclear whether the program developed for the B-Spline approximation created the short length seen in the experiment or whether the nature of the matrix formation caused the uniform knot vector to be so short. Hence why the open uniform knot vector was chosen to determine the geometric profile of the road as it seemed not to have the same short comings as the uniform knot vector.

Figure 6.28: Comparison of the B-Spline open uniform knot vector estimates, shown in blue, to the Google elevation API estimates, seen in green, and the GPS elevation values, in red.

The Figure 6.28 highlights the B-Spline geometric profile of the road way, shown in blue, compared to the Google elevation values, in green. For the segment it can be seen that the B-Spline approximations have a smooth elevation profile. The control points used in the experiment were selected individually in a repeated process until

a smooth profile was determined. When comparing the B-Spline geometric profile against the Google elevation values, it can be seen that the geometric profile seems to be a very smoothed representation of the road–way. However, the elevation is several meters higher that the Google elevation estimates. However, selecting the control points allows for the selection of the best B-Spline approximation, this means that the profile may not be a true representation of the averages of the GPS elevation values.

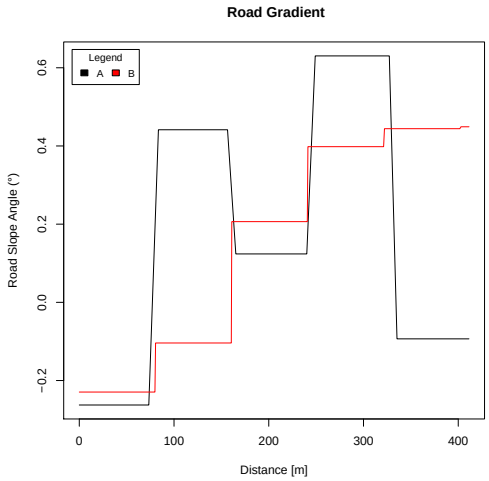

Figure 6.29: Road grade estimates of the B-Spline approximation of the road way (B) compared to the Google elevation API estimated road grade for the segment (A).

Fig. 6.29 represents the road grade estimates of the B-Spline approximations compared to the Google elevation API estimates. The profile of the B-Spline approximations has the advantage of being smoother and therefore less prone to the variation in road grade values seen in the Google elevation estimates. On the other hand, it is hard to determine whether road grade estimates are a fair representation as the test area was so small. On top of that, the process of determining specific control points creates a lot of manual re-work that prevents an automatic solution from being able to determine large scale road grade estimates.

The process of determine a geometric profile of the road–way is faulted with many time consuming processes that cause the overall approach to be inapplicable for this study. However, the process of cleansing data of errors and repetitions combined with a geometric profile does highlight the significance that the work does have in being able to produce accurate representation of the road way.

Chapter 7

Comparison of The Results

This Chapter outlines the benefits and limitations of the approaches replicated in this dissertation. The results obtained during the dissertation are explored and the best methods that the author thinks would be suited to ITS are identified. Concluding the two approaches that would be best suited to ITS.

Comparing the result of the different approaches to determining road grade, that was explored in this dissertation, using the criteria set out in Section 3.2, it becomes clear that only results that show accurate, scalable, free sourced estimates of road grade are applicable. In Chapter 6 the results are displayed in such a way that each of the Sections are evaluated individually on their basis to determine accurate road grade estimates. Therefore, the best methods from these evaluations are selected. Using the summary conclusions of each Section in Chapter 6 an overall evaluation can be determined on which of the replicated studies would be best suited to determining road grade estimations for ITS.

In Section 6.1 the use of GPS elevation values by themselves to determine road grade are dismissed due to the high error and unpredictability associated with the measurements. Using the measurements by themselves to estimate road grade would create estimates that were unreliable due to the errors associated with the GPS vertical measurements.

Similarly, in Section 6.2 measurements taken from the accelerometer were plagued by the acceleration of the vehicle and the placement of the On Board Unit (OBU) in the test vehicle. The accelerometer readings were heavily influenced by the acceleration of the vehicle, with period of high acceleration dictating the inclination angle of the accelerometer. However, period of lower acceleration the readings did mimic an over-estimated version of the road grade estimates for the region. However, the placement of the OBU and the bias of the accelerometer limited the accelerometers ability to measure accurate inclination values. Therefore, without investigating another way to improve the readings the use of the accelerometer is not applicable.

The results in Section 6.3 show the accuracy that can be determined from extracting elevation information from Digital Elevation Models (DEMs). Nonetheless, the studies replicated in this Section highlight the importance of determining better approximation of GPS points that are not located in the centre of the grid and the

use of a smoothing/filtering process to remove errors in the DEM. Subsection 6.3.1 shows the advantages of interpolating a better approximation of the elevation estimates, however the results are still affected by the inconsistencies and discrepancies in the DEM elevation profile. This has the adverse effect of causing the road grade estimates to be influenced by erroneous data points. On the other hand, the results in Subsection 6.3.2 do remove the erroneous data points in the elevation profile and provide a better approximation of the elevation values made with the smoothing/filtering process. Therefore, the results in Subsection 6.3.1, are not applicable for highly accurate road grade estimates, whereas the results in Subsection 6.3.2 are.

In Section 6.4 the use of repeated runs using the GPS device on board the test vehicle was used to determine road grade estimates. Subsection 6.4.1 shows the effect of utilising ten repeated runs of the elevation profiles, taken from the GPS device in the test vehicle, to determine road grade estimates for consecutive 80 m segments. Additionally, Subsection 6.4.2 looked to use a geometric representation of the road-way to determine road grade. As the approach in Subsection 6.4.2 was prone to a lot of manual rework, in selecting the right control points and segmenting the route, it was found that it would not be applicable for a large scale solution. On the other hand, the results in Subsection 6.4.1 suggest that with enough repeated runs a good approximation of road grade estimates can be determined.

Therefore, from the results obtain in the dissertation there are two applicable approaches that could be used to estimate large scale road grade profiles, according to the author. Namely the approaches shown in Subsections 6.3.2 and 6.4.1 are applicable. The results suggest that good estimations of road grade can be determine and the approaches can be applied to other ITS vehicles.

Chapter 8

Combined Approach

A combined approach is introduced which utilises several of the approaches to try to determine accurate road grade estimates. This Chapter highlights a combined approach of several of the replicated methods explored in Chapter 6, developed by the author, in order to improve the road grade estimations.

The two approaches seen in Subsections 6.3.2 and 6.4.1 do have limitation which could be addressed. The elevation estimates taken from the DEM could be enhanced by first determining a better approximation for the GPS points using the interpolation technique discussed in Subsection 6.3.1. Similarly the road grade estimates could be enhanced using repeated runs and estimating the road grade angle using linear regression. This would also have the advantage of improving the estimation of the true road way, with repeated runs, compared to the GPS trace which is may deviate slightly to the road way due to real life driving behaviour.

The elevation information used in the approach described in Subsections 6.3.2 filters elevation information extracted from the SRTM DEM. However, the method does not utilise an approach to estimate a better approximate of each extracted elevation point. Therefore, to improve the accuracy of the results the elevation information taken from the DEM could undergo the bilinear interpolation process seen in Subsection 6.3.1.

The process described in Subsection 6.4.1 does require the use of many repeated runs to acquire accurate estimates of road grade and for a large scale solution, like city wide road grade profiles, this may create the need for storage of many runs. In order to reduce this, combining the use of elevation information extracted from DEMs would mean that accurate road grade estimates could be made with fewer runs. Therefore, using the approach set out in Subsection 6.3.2 with several runs a number of accurate elevation profiles can be determined. The runs can then be combined to improve the accuracy using linear regression, every 80 m segments, similar to the approach shown in Subsection 6.4.1.

Using a combination of the three methods described above, would enhance the elevation estimates extracted by the DEM before they are filtered to remove discrepancies. The combined runs would then enhance the accuracy of the road grade estimate as well as mitigate any horizontal inaccuracies cause by random errors in

the GPS and real life driving behaviours. This can be seen in the study by (Boroujeni and Frey, 2014), where "GPS-based estimates of horizontal distance travelled are highly repeatable and thus not a significant source of error in road grade estimation". Whereas, not accounting for small errors in the horizontal positioning caused by GPS errors may cause the selection of elevation DEM values from a wrong grid, than the required one.

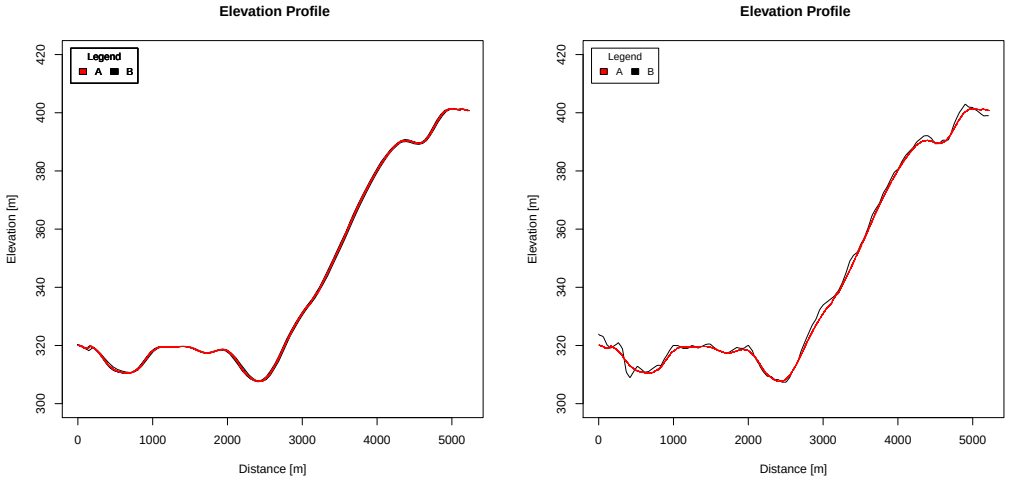

Figure 8.1: Left image – DEM extracted and smoothed/filtered elevation profiles (B) used in combination to determine linear regression of 80 m segments (A). Right image – linear regression, every 80 m, of combined DEM extracted and smoothed elevation profiles (A) compared to Google elevation API estimates (B).

To illustrate the use of multiple runs of extracted DEM elevation profiles, that undergo the smoothing process seen in Subsection 6.3.2, the Figure 8.1 is used. From the image on the left, it can be seen that the elevation profiles of the different runs correlate very strongly to each other and with hardly any differences in the profiles. However, the slight difference are thought to be caused by the fact that each run will have a slightly different estimate of distance due to real life driving cycles and behaviours which influence the distance between GPS points. However, the use of linear regression every 80 m can be seen by the red profile (A) and the line follows the elevation profiles of the runs very closely, almost perfectly. This indicates that an accurate estimate of the road grade should be determined. This assumption is also enforce in the image on the right, with the comparison of the linear regression profile (A) compared to the Google elevation API estimates (B). The linear regression profiles (A) correlates strongly with the Google elevation API estimates.

The added advantage of using multiple runs, similar to the method shown in Subsection 6.4.1, is that the road grade estimates improve with more repeated runs. This is primarily due to the fact that using an averaging method like the combining of the elevation datasets and applying linear regression allows for a better approximate of the road grade angle than using a single elevation value. Similarly, slight differences, caused by either GPS horizontal inaccuracies or real life driving behaviours, between runs can be corrected with an averaging effect.

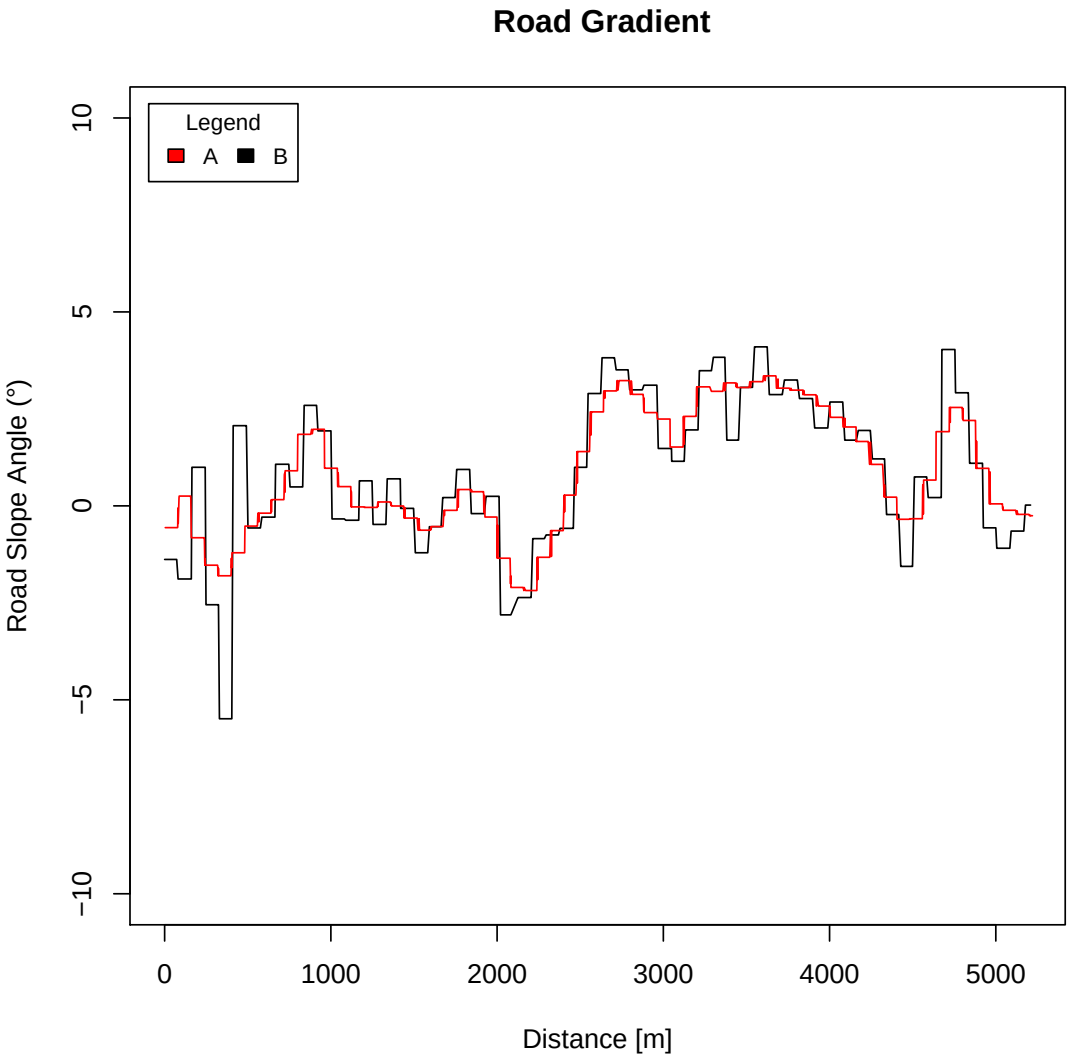

Figure 8.2: Road grade estimates of the combined approach (A) compared against Google elevation API road grade estimates (B).

The result of combining the different approaches as described above results in road grade estimates that more accurate than the individual approaches by themselves. Figure 8.2 illustrates the effects of road grade estimates determined by the combined approach (A) compared to the Google elevation API road grade estimates (B). The road grade profile of the combined approach have a high correlation with the Google elevation API estimates. However, there are slight differences in road grade estimates between the two. This is mainly due to the smoothing/filtering differences between the two examples. The Google elevation API smoothing/filtering process is not known but it can be seen that the process does not account for all of the inconsistencies found in the DEM, like areas where the road passes over a bridge or overpass. This would indicate that the combined approach has the advantage of not being affected by distinct inconsistencies in the elevation profile, however there might be slight discrepancies where the general elevation information was overestimated or underestimated due to the filtering process when compared to the Google elevation estimates.

Therefore, the results of the combined process show the significance of utilising the different aspects of the approaches discussed above to improve the road grade estimates. Mainly the advantage of improving DEM elevation estimates, before the filtration processes, due to the interpolation process. When interpolated elevation values are combined with the extensive filtering process the discrepancies in the elevation profile can be removed. Lastly, the estimates would be enhanced with multiple runs of the same segment, with an averaging effect using a linear regression approach to estimate road grade.

Chapter 9

Conclusion

The results collected in the experiments highlight approaches to determining road grade. The theoretical concept of determining large–scale data-sets of road grade profiles, using ITS–like advanced public buses, is then validated with the results of the experiments. From the replicated studies the best solutions from the experiments are presented and a further investigation is concluded to determine the effectiveness of a combined approach.

The theoretical approach put forward in this dissertation was to determine large–scale road grade profiles using Advanced Public Transport Systems (APTS) and in particular public buses. The results taken from the Tesco Bus Service, combined with the Bach box and the Openmatics cloud service, highlight the possibility for a large–scale collection of road grade profile in other cities. Public buses, connected with On-Board Units (OBUs) like the Bach box, offer a unique opportunity to measure large areas of cities. OBUs also offer the opportunity to capture a large amount of information from the vehicle or its sensors. As illustrated in the experiments the OBUs allow for the collection of the information to be stored on the device and then retrieved remotely for a post processing analysis of the road grade information. Conversely, a large advantage in using OBUs is the homogeneous nature of the collection of the data required for measuring road grade, making the process easily applicable to services similar to the Tesco Bus Service.

The studies replicated in this dissertation have several significant points: (A) the results validate the research done by the authors of the studies replicated, providing an independent evaluation; (B) the results collected in this dissertation interrogate the research done in previous studies, looking for improvements and quantifying the limitations of their approaches; and (C) the results provide extensive information into replication of the studies, making the replication of such studies easier for others.

Consequently, the method for determining road grade, chosen in this dissertation which looks at a combined approach of several studies, has a significant advantage over the individual approaches by themselves. Namely, the advantages would be seen in the improvements that could be achieved in using accurate DEM elevation information with repeated runs to reduce the confidence interval of accuracy of the road grade estimates. Another implication of all of the approaches for determining road grade, investigated in this dissertation, is the use of components in the OBU

or freely available information, like the DEMs. This is important when comparing against other databases which future studies might consider using. For instance, commercially available databases like the Google elevation API to determine large–scale road grade profiles offer an approach to determining large–scale road grade estimates.

The results of this research show that although the Google elevation API estimates are quite accurate, they do not seem to account for discrepancies, like the bridge and overpass. Therefore, future research which integrates the Google elevation estimates must account for this before determining road grade, allowing for improvements in the estimates.

Chapter 10

Future Work

Following the new understanding offered by this dissertation, one area of interest would be applying the combined approach developed by the author to a larger city-wide data-set.

The Dublin City Council Insight project (Council, 2013) provides a data-set recording of an entire twenty-four hour cycle of bus travel throughout Dublin city. At a preliminary look at the data, it is evident that a large amount of GPS data can be leveraged to produce a large–scale road grade map of the city. This can be observed in Fig. 10.1, where a single file of the entire data-set provided by the Insight project provides approximately one million GPS data-points.

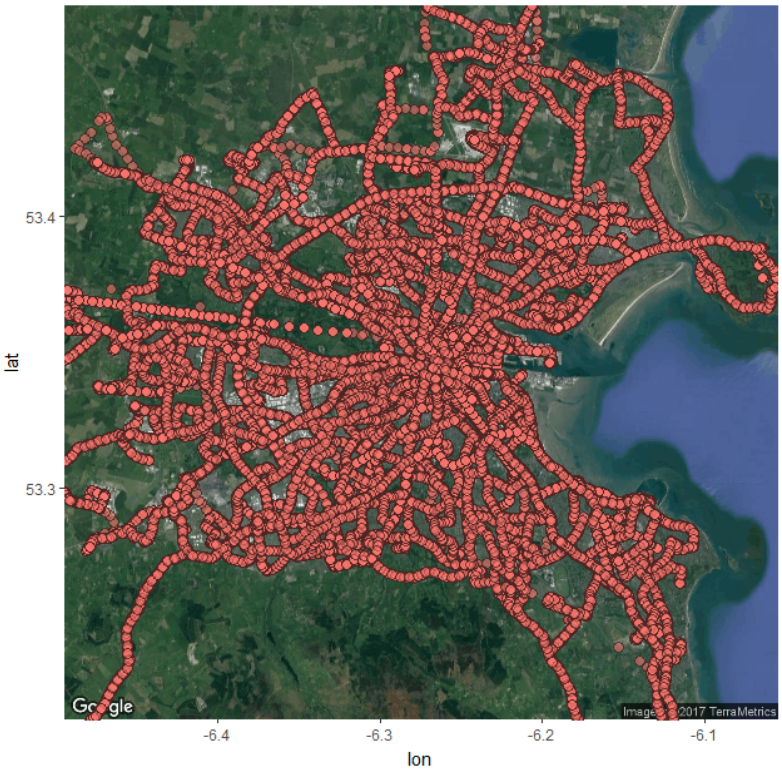

Figure 10.1: Google map of the Dublin, Ireland city boundary, overlaid with GPS data points taken from the Dublin Bus data-set. The data-set is an illustration of a small fraction of the entire data-set available from the Dublin Bus Insight Project.

The GPS traces provided by the Insight project only provide the longitude and latitude coordinates from each of the buses recorded. Correspondingly, the GPS data is only recorded every thirty seconds. These two facts cause the data-set to contrast significantly to that of the measurements obtained from the Tesco Bus Service.

Nevertheless, the data-set does seem promising for the combined approach developed in this dissertation. Where, elevation values could be extracted using the GPS longitude and latitude coordinates and this extra variable could be used to determine large-scale road grade estimates.

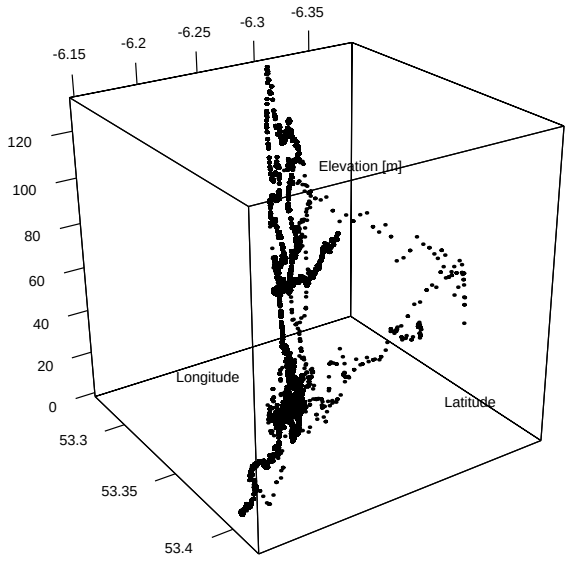

Figure 10.2: An illustration of the elevation profile obtain from querying the GPS locational information of the bus route 15 from one of the files provided from the Dublin Bus Insight project. GPS longitude and latitude coordinates are compared against elevation data extracted from a Postgres database containing the SRTM 1-arch tile for the regional area of Dublin.

The figure seen above, Fig. 10.2, illustrates the potential of being able to leverage the Insight data-set to extract elevation information from the SRTM 1-arch DEM. The image shows a 3D representation of the route taken by buses travelling on route 15, within Dublin. The clustering of the data-sets, represented by the darker regions, suggests that there are enough repeated runs to ascertain a good representation of the road-way and to determine accurate road grade. As figures 10.1 and 10.2 are only representative of a small proportion of the entire data-set, it is clear that there is a possibility to leverage a large-scale data-set of road grade for the city.

Bibliography

Z. AG. (2016) DRIVELINE CONSULTANCE FOR THE ZF BUS DIVISION. Accessed on the 10 January 2017. [Online]. Available: http://www.zf.com/brands/en_de/openmatics/news/driveline_consultancy_for_the_zf_bus_division/driveline_consultancy_for_the_zf_bus_division.html

U. E. P. Agency. (2016) Global Greenhouse Gases Emissions. Accessed on September 2016. [Online]. Available: http://www.epa.gov/ghgemissions/global-greenhouse-gas-emissions-data

L. L. Arnold and P. A. Zandbergen, "Positional accuracy of the wide area augmentation system in consumer-grade GPS units," *Computers & Geosciences*, vol. 37, no. 7, pp. 883–892, 2011.

. Asterweb.jpl.nasa.gov, "Asterweb.jpl.nasa.gov. (2016). ASTER Global Digital Elevation Map. ," 2016, accessed on September 2016. [Online]. Available: https://asterweb.jpl.nasa.gov/gdem.asp

M. Aubury and W. Luk, "Binomial filters," *Journal of VLSI signal processing systems for signal, image and video technology*, vol. 12, no. 1, pp. 35–50, 1996.

S. A. Aziz, B. L. Steward, L. Tang, and M. Karkee, "Multiple GPS measurements for digital elevation model," in *Computers in Agriculture and Natural Resources, 23-25 July 2006, Orlando Florida*. American Society of Agricultural and Biological Engineers, 2006, p. 329.

H. S. Bae, J. Ryu, and J. C. Gerdes, "Road grade and vehicle parameter estimation for longitudinal control using GPS," in *Proceedings of the IEEE Conference on Intelligent Transportation Systems*, 2001, pp. 25–29.

D. Ben-Arieh, S. Chang, and G. Zhang, "Geometric modeling of highways using GPS data and B-Spline approximation," in *IIE Annual Conference. Proceedings*. Institute of Industrial Engineers-Publisher, 2002, p. 1.

D. Ben-Arieh, S. Chang, M. Rys, and G. Zhang, "Geometric modeling of highways using global positioning system data and B-spline approximation," *Journal of Transportation Engineering*, vol. 130, no. 5, pp. 632–636, 2004.

U. o. C. S. C. Benjamin T. Bertka. (30th, May 2008) An Introduction to Bezier Curves, B-Splines, and Tensor Product Surfaces with History and Applications. Accessed on October 2016. [Online]. Available: http://fei.edu.br/~psergio/CG_arquivos/IntroSplines.pdf

Biomathematics and S. Scotland. (2016) Chapter 5 MATHEMATICAL MORPHOLOGY. Accessed on November 2016. [Online]. Available: http://www.bioss.ac.uk/people/chris/ch5.pdf

B. Y. Boroujeni and H. C. Frey, "Road grade quantification based on global positioning system data obtained from real-world vehicle fuel use and emissions measurements," *Atmospheric Environment*, vol. 85, pp. 179–186, 2014.

B. Y. Boroujeni, H. C. Frey, and G. S. Sandhu, "Road grade measurement using in-vehicle, stand-alone GPS with barometric altimeter," *Journal of Transportation Engineering*, vol. 139, no. 6, pp. 605–611, 2013.

C. Boucher and J.-C. Noyer, "Dual-GPS fusion for automatic enhancement of digital OSM roadmaps," in *2012 IEEE First AESS European Conference on Satellite Telecommunications (ESTEL)*. IEEE, 2012, pp. 1–6.

——, "Automatic estimation of road inclinations by fusing GPS readings with OSM and ASTER GDEM2 data," in *2014 International Conference on Connected Vehicles and Expo (ICCVE)*. IEEE, 2014, pp. 871–876.

M. Castro, L. Iglesias, R. Rodríguez-Solano, and J. A. Sánchez, "Geometric modelling of highways using global positioning system (GPS) data and spline approximation," *Transportation Research Part C: Emerging Technologies*, vol. 14, no. 4, pp. 233–243, 2006.

D. C. Council. (2013) Dublin Bus GPS sample data from Dublin City Council (Insight Project). Accessed on May 2017. [Online]. Available: https://data.dublinked.ie/dataset/dublin-bus-gps-sample-data-from-dublin-city-council-insight-project

L. Della Ragione and M. Giovanni, "The Influence of Road Gradient in an Integrated Approach of Real Driving Cycles and Emissions Factors Model," *Transportation Research Procedia*, vol. 14, pp. 3179–3188, 2016.

M. Doering and L. Wolf, "Opportunistic vehicular networking: Large-scale bus movement traces as base for network analysis," in *High Performance Computing & Simulation (HPCS), 2015 International Conference on*. IEEE, 2015, pp. 671–678.

A. Duran and M. Earleywine, "GPS data filtration method for drive cycle analysis applications," SAE Technical Paper, Tech. Rep., 2012.

L. Figueiredo, I. Jesus, J. T. Machado, J. Ferreira, and J. M. de Carvalho, "Towards the development of intelligent transportation systems," in *Intelligent transportation systems*, vol. 88, 2001, pp. 1206–1211.

H. C. Frey, K. Zhang, and N. M. Rouphail, "Fuel use and emissions comparisons for alternative routes, time of day, road grade, and vehicles based on in-use measurements," *Environmental Science & Technology*, vol. 42, no. 7, pp. 2483–2489, 2008.

G. Geography. (2016) DEM, DSM and DTM Differences - GIS Elevation Models. Accessed November, 2016. [Online]. Available: http://gisgeography.com/dem-dsm-dtm-differences/

N. Henriques and C. Bento, "Integration of GPS Traces and Digital Elevation Maps for Improving Bicycle Traffic Simulation Behavior," in *Transportation Research Board 92nd Annual Meeting, Transportation Research Board*, 2013.

Z. Hupák. (2016) ČSAD autobusy Plzeň a.S. - Tescobus. Accessed on the 10 January 2017. [Online]. Available: http://www.csadplzen.cz/?ob=tesco&ls1=menu_bez

H. Jansson, E. Kozica, P. Sahlholm, and K. H. Johansson, "Improved road grade estimation using sensor fusion," *Proceedings of the 12th Reglermöte in Stockholm, Sweden*, 2006.

jpl.nasa.gov , "Advanced Spaceborne Thermal Emission and Reflection Radiometer (ASTER) Global Digital Elevation Model," Website, 2016, accessed on October 2016. [Online]. Available: https://asterweb.jpl.nasa.gov/gdem.asp

L. Kang, S. Poslad, W. Wang, X. Li, Y. Zhang, and C. Wang, "A Public Transport Bus as a Flexible Mobile Smart Environment Sensing Platform for IoT," in *Intelligent Environments (IE), 2016 12th International Conference on.* IEEE, 2016, pp. 1–8.

E. Kaplan and C. Hegarty, *Understanding GPS: principles and applications.* Artech house, 2005.

W. Kester *et al.*, *Mixed-signal and DSP design techniques.* Newnes, 2003.

N. Kidambi, R. Harne, Y. Fujii, G. M. Pietron, and K. Wang, "Methods in vehicle mass and road grade estimation," *SAE International Journal of Passenger Cars-Mechanical Systems*, vol. 7, no. 2014-01-0111, pp. 981–991, 2014.

F. Kost, "Basic principles of vehicle dynamics," in *Fundamentals of Automotive and Engine Technology.* Springer, 2014, pp. 114–129.

M. Kubička, J. Klusáček, A. Sciarretta, A. Cela, H. Mounier, L. Thibault, and S.-I. Niculescu, "Performance of current eco-routing methods," in *Intelligent Vehicles Symposium 2016*, 2016.

M. G. P. S. G. Laboratory. (2016) GPS Accuracy. Accessed on October 2016. [Online]. Available: http://www.montana.edu/gps/slides/2GPSAccuracy.pdf

M. W. Levin, M. Duell, and S. T. Waller, "The effect of road elevation on network wide vehicle energy consumption and eco-routing," *Transportation Research Record: Journal of the Transportation Research Board*, 2014.

S. Mangan, J. Wang, and Q. Wu, "Measurement of the road gradient using an inclinometer mounted on a moving vehicle," in *Computer Aided Control System Design, 2002. Proceedings. 2002 IEEE International Symposium on.* IEEE, 2002, pp. 80–85.

T. Massel, E. Ding, and M. Arndt, "Investigation of different techniques for determining the road uphill gradient and the pitch angle of vehicles," in *American Control Conference, 2004. Proceedings of the 2004*, vol. 3. IEEE, 2004, pp. 2763–2768.

D. Meko. (2016) Filtering, GEOS 585A, Applied Time Series Analysis. Accessed on September 2016. [Online]. Available: http://www.ltrr.arizona.edu/~dmeko/geos585a.html#ctop

S. Mukherjee, P. Joshi, S. Mukherjee, A. Ghosh, R. Garg, and A. Mukhopadhyay, "Evaluation of vertical accuracy of open source Digital Elevation Model (DEM)," *International Journal of Applied Earth Observation and Geoinformation*, vol. 21, pp. 205–217, 2013.

M. Mukul, V. Srivastava, and M. Mukul, "Accuracy analysis of the 2014–2015 Global Shuttle Radar Topography mission (SRTM) 1 arc-sec C-Band height model using international Global Navigation Satellite System Service (IGS) network," *Journal of Earth System Science*, vol. 125, no. 5, pp. 909–917, 2016.

H. Müller and J.-C. Freytag, *Problems, methods, and challenges in comprehensive data cleansing*. Professoren des Inst. Für Informatik, 2005.

National Renewable Energy Laboratory , "Analysis Reveals Impact of Road Grade on Vehicle Energy Use," Website, 2014, accessed on November 2016. [Online]. Available: http://www.nrel.gov/docs/fy14osti/61678.pdf

L. Nepal. (2016) Reading SRTM data with Python. Accessed on October 2016. [Online]. Available: https://librenepal.com/article/reading-srtm-data-with-python/

J. Nett. (2016) Bilinear Interpolation. Accessed on October 2016. [Online]. Available: http://web.pdx.edu/~jduh/courses/geog493f09/Students/W6_Bilinear%20Interpolation.pdf

Z. Openmatics. (2016) ZF Onboard Unit Bach. Accessed on September 2016. [Online]. Available: http://www.zf.com/brands/en_de/openmatics/products_services_om/products/bach_benefits/bach-benefits.html

——. (2016) ZF Onboard Unit Mozart. Accessed on September 2016. [Online]. Available: http://www.zf.com/brands/media/openmatics/products_services/onboard_unit/Datasheet_Mozart1.pdf

K. Ord, "Charles Holt's report on exponentially weighted moving averages: an introduction and appreciation," *International Journal of Forecasting*, vol. 20, no. 1, pp. 1–3, 2004.

J. Parviainen, J. Hautamäki, J. Collin, and J. Takala, "Barometer-aided road grade estimation," in *Proceedings of the world congress of the international association of institutes of navigation. Stockholm, Sweden*, 2009.

J. J. R. Pasaye, J. A. B. Valencia, and F. J. Pérez, "Tilt measurement based on an Accelerometer, a Gyro and a Kalman Filter to control a self-balancing vehicle," in *Power, Electronics and Computing (ROPEC), 2013 IEEE International Autumn Meeting on*. IEEE, 2013, pp. 1–5.

M. Pedley, "Tilt sensing using a three-axis accelerometer," *Freescale Semiconductor Application Note*, pp. 2012–2013, 2013.

K. K. Qinglu Ma, "A Low-Cost GPS-Data-Enhanced Approach for Traffic Network Evaluations," 2016, accessed on September 2016. [Online]. Available: http://www.caee.utexas.edu/prof/kockelman/public_html/TRB17GPSforTrafficEvaluation.pdf

E. Rahm and H. H. Do, "Data cleaning: Problems and current approaches," *IEEE Data Eng. Bull.*, vol. 23, no. 4, pp. 3–13, 2000.

E. Ribar *et al.*, "Road slope introduction in vehicle route modelling," in *2016 Cybernetics & Informatics (K&I)*. IEEE, 2016, pp. 1–5.

P. Sahlholm and K. H. Johansson, "Road grade estimation for look-ahead vehicle control using multiple measurement runs," *Control Engineering Practice*, vol. 18, no. 11, pp. 1328–1341, 2010.

R. W. Schafer and L. R. Rabiner, "A digital signal processing approach to interpolation," *Proceedings of the IEEE*, vol. 61, no. 6, pp. 692–702, 1973.

Sherborne Sensors Whitepaper. (2014, January) A SPECIFICATION GUIDE TO INCLINOMETERS, ACCELEROMETERS AND LOAD CELLS. Accessed on October 2016. [Online]. Available: http://www.sherbornesensors.com/uploads/files/Files/A_Specification_Guide_to_Inclinometers_Accelerometers_and_Force_Transducers_FINAL.pdf

Sherbornesenors. A Specification Guide to Inclinometers Accelerometers and Force Transducers . Accessed on accessed November 2016. [Online]. Available: http://www.sherbornesensors.com/uploads/files/Files/A_Specification_Guide_to_Inclinometers_Accelerometers_and_Force_Transducers_FINAL.pdf

D. Starkey. (2016) Cox-deBoor Equations for B-Spline AUI Course. Accessed on October 2016. [Online]. Available: https://www.cs.montana.edu/paxton/classes/aui/dslectures/CoxdeBoor.pdf

U. G. Survey. (2016) SRTM 1 Arc description. Accessed on November 2016. [Online]. Available: https://lta.cr.usgs.gov/SRTM1Arc

——. (2016) SRTM 1 Arc Download Site. Accessed on September 2016. [Online]. Available: http://earthexplorer.usgs.gov/

——. (2016) SRTM Quick Guide. Accessed on September 2016. [Online]. Available: https://lpdaac.usgs.gov/sites/default/files/public/measures/docs/SRTM/Quick/Guide

O. Travesset-Baro, M. Rosas-Casals, and E. Jover, "Transport energy consumption in mountainous roads. A comparative case study for internal combustion engines and electric vehicles in Andorra," *Transportation Research Part D: Transport and Environment*, vol. 34, pp. 16–26, 2015.

U.S.Geological.Survey, "Shuttle Radar Topography Mission (SRTM) 1 Arc-Second Global ," 2016, accessed on September 2016. [Online]. Available: https://lta.cr.usgs.gov/SRTM1Arc

U. S. G. S. U.S.G.S. (2016) Digital Elevation Model (DEM). Accessed on November 2016. [Online]. Available: http://tahoe.usgs.gov/DEM.html

S. V. Vaseghi, *Advanced digital signal processing and noise reduction*. John Wiley & Sons, 2008.

C. Veness, "Calculate distance and bearing between two Latitude/Longitude points using Haversine formula in JavaScript," *Movable Type Scripts*, 2011, accessed on November 2016.

H. WANG, Z. SHI, and Z. REN, "GPS/IMU," *Journal of Computational Information Systems*, vol. 9, no. 18, pp. 7207–7214, 2013.

Y. Wang, X. Du, H. Yu, J. Huang, and Y. Li, "Impacts of road grade on fuel consumption of light vehicles by use of Google Earth DEM," in *Cyber-Enabled Distributed Computing and Knowledge Discovery (CyberC), 2015 International Conference on*. IEEE, 2015, pp. 360–363.

M. G. Wing and J. Frank, "Vertical measurement accuracy and reliability of mapping-grade GPS receivers," *Computers and electronics in agriculture*, vol. 78, no. 2, pp. 188–194, 2011.

M. G. Wing, A. Eklund, and L. D. Kellogg, "Consumer-grade global positioning system (GPS) accuracy and reliability," *Journal of forestry*, vol. 103, no. 4, pp. 169–173, 2005.

E. Wood, E. Burton, A. Duran, J. Gonder *et al.*, "Appending high resolution elevation data to GPS speed traces for vehicle energy modeling and simulation," *National Renew Energy Lab*, 2014.

E. Wood, E. Burton, A. Duran, and J. Gonder, "Contribution of road grade to the energy use of modern automobiles across large datasets of real-world drive cycles," SAE Technical Paper, Tech. Rep., 2014.

E. Wood, A. Duran, E. Burton, J. Gonder, and K. Kelly, "EPA GHG Certification of Medium-and Heavy-Duty Vehicles: Development of Road Grade Profiles Representative of US Controlled Access Highways," National Renewable Energy Laboratory (NREL), Golden, CO (United States), Tech. Rep., 2015.

B. Yazdani Boroujeni and H. C. Frey, "Road grade quantification based on global positioning system data obtained from real-world vehicle fuel use and emissions measurements," *Atmospheric Environment*, vol. 85, pp. 179–186, 2014.

K. Zhang and H. C. Frey, "Road grade estimation for on-road vehicle emissions modeling using light detection and ranging data," *Journal of the Air & Waste Management Association*, vol. 56, no. 6, pp. 777–788, 2006.

M. Zhou, H. Jin, and W. Wang, "A review of vehicle fuel consumption models to evaluate eco-driving and eco-routing," *Transportation Research Part D: Transport and Environment*, vol. 49, pp. 203–218, 2016.

Appendix

Evaluating Different Methods For Determining Road Grade Best Suited to ITS*

Jared Magrath[1] and Mike Brady[2]

***Abstract*—Real world fuel consumption and emission models are sensitive to road grade estimates. The developments of eco-routing and eco-driving solutions makes the development of large scale collections of road grade profiles of importance. Therefore, there is a need to collect accurate, large scale, road grade profiles. Existing intelligent transport systems (ITS) like modern public bus transportation systems provide an opportunity to collect large amounts of data for post processing development of road grade profiles. This paper explores different techniques for determining road grade estimates suited to ITS. Five studies were replicated in this work and evaluated in real world experiments against the Google Elevation API.**

***Index Terms*—Road Grade, ITS, On-Board Units, Advanced Public Transportation Buses.**

I. INTRODUCTION

Recent studies have investigated the effects of road grade on fuel consumption and determined the necessity of including them in fuel consumption models [1][2]. It is estimated that road grade accounts for approximately 1-3% of fuel consumption use in light duty vehicles [3].

There are new vehicle technologies which reduce energy consumption, however these are limited in their ability to provide large fuel saving opportunities [4]. Eco-routing has emerged as one of the strategies to reduce fuel consumption [5]. Eco-routing solutions allow for the prediction of the most fuel-economic routes and have become of interest to the transportation industry as they offer a way to dramatically reduce fuel consumption and emissions. Fuel consumption can be reduced as much as 12.5% when taking advantage of eco-routing solutions [5].

Road grade is often not included in fuel consumption models as can be seen in a comparison of various fuel consumption models in recent research carried out by Zhou et al. [4]. One of the key reasons as to why road grade is often not included in fuel consumption models lies in the difficulties in determining accurate estimates [2]. However, neglecting road grade in eco-routing leads to over- or under-estimation of fuel consumption. By creating a large dataset of road grade profiles, it may be possible to improve simulations and models of fuel consumption that could be implemented in eco-routing systems.

A study on measuring large scale road grade profiles and evaluating the effect of road grade on the energy use of light-duty vehicles was published by the National Renewable Energy Laboratory (NREL) [3]. However, there has been little development regarding large scale analysis of road grade effects on eco-routing performance according to the study done by Levin et al. [6]. Therefore, bridging the gap between the collection of large-scale datasets of road grade profiles and the incorporation of them into energy consumption models is of interest for developing eco-routing solutions.

There are different classifications of intelligent transportation systems (ITS). Advanced public transportation systems that utilise estimated arrival and announcement systems are a form of ITS [8]. There is potential for large-scale post-processing and analysis of data from modern public transportation systems like buses, as discussed in a paper produced by Doering et al. [9]. The collection of information from devices like the Bach box [10], an on-board unit (OBU) which is capable of collecting telematic information from vehicles, could be used to measure road grade for a large area when used in conjunction with a form of ITS. Other aspects of advanced public transportation bus systems of interest to this study are: their requirements for high position accuracy in real-time fleet management and the repeated traversal of routes, as they normally run on specified routes.

Fig. 1. OpenStreetMaps road network of the test area (Plzen, Czech Republic) with the route of the test vehicle, equipped with the Bach box, shown in red.

This paper evaluates different methods for determining road grade estimations from on-board units in advanced public bus transportation systems as a form of ITS and is divided into the following sections: Section II – experimental set-up; Section III – presentation of five studies replicated to evaluate road grade methods suited to ITS; and a determination of the method best suited for implementation for ITS is discussed in

*This work was supported by ZF Openmatics

[1]J. Magrath is a Masters of Engineering student at the University of Dublin, Trinity College Dublin. magrathj@tcd.ie

[2]M. Brady is a professor of Computer Science at the University of Dublin, Trinity College Dublin. brady@cs.tcd.ie

Section IV. For the remainder of this paper, ITS will refer to advanced public bus transportation systems.

II. Experimental Set-up

A. Equipment

On-Board Units (OBU) are small computers equipped with communication devices that are mounted inside vehicles which provide an opportunity to capture a large variety of information from vehicles. The Bach box, made by ZF Friedrichshafen AG, has the ability to capture precise positional information of vehicles and it has a number of other components associated with telematic operations that could be used to determine road grade [10].

However, the GPS component in the Bach box is susceptible to the same vertical inaccuracies as other consumer-grade GPS devices [13]. Therefore, in order to estimate road grade it is essential to improve the vertical accuracy of the GPS measurements or use other methods to substitute the elevation values for other measurements, as discussed below.

B. Different Methods of Estimating Road Grade

There are many different ways to measure road grade. Design drawings and surveying techniques have been used traditionally. However, these techniques are relatively time-costly, as they require a large amount of manual work, as discussed in the paper by Boroujeni et al. (2013). Therefore, automated approaches are of interest. Accelerometers and inclinometers can be used to determine inclination of a road from a vehicle while travelling [14]. Similarly, Digital Elevation Models (DEMs) created from satellites, and aircraft equipped with LiDAR devices, can be used to estimate road grade profiles when overlaid on a road network [15][16][17]. Different techniques using GPS devices can be used to determine road grade utilising repeated runs to mitigate errors over time [18][11].

The criteria which were used in this study to determine the method best suited to ITS were those methods that:

- do not require real-time analysis.
- are scalable to any city-wide ITS.
- use only freely available sources of information to aid the measurements.
- utilise only the components available on most OBUs.

C. Validating Results

The measurements of road grade come from information collected from a test vehicle using the Bach box OBU [10]. The measurements represent real-life driving behaviour in a public bus transportation system, operated by Tesco, taken from the same vehicle in the urban area of Plzen, Czech Republic.

To validate results, the measurements were compared to the Google Elevation API estimates, where elevation information was extracted using GPS longitude and latitude traces. In a study carried out by Zhou et al. (2016), the Google Elevation API was used to determine road grade for a large scale analysis [4]. The limitation of this approach is the large number of queries to the Google Elevation API. The Google Elevation API is subject to a query limitation when using the free service, and using the paid services available might prove expensive for large-scale deployment.

Estimates of road grade are provided in degrees and a sampling interval of 80 m is used. Typically, road grade is presented as a percentage of change in elevation over the horizontal distance. However, for purposes of comparison, the results are provided in degrees using the road slope angle derived from the angle of the change in elevation over horizontal distance. The 80 m sampling interval was selected to dampen the effect of high frequency components on the road grade profile [19]. Distance values were calculated using the Haversine formula, as seen in the study [19].

III. Studies Replicated

This Section examines five studies from different researchers in determining road grade and it presents a replication of those studies. Section III-A investigates the use of an accelerometer in a moving vehicle to determine road grade. Sections III-B and III-C consider alternative methods for determining road grade from DEM elevation values extracted using GPS longitude and latitude traces. In comparison, Sections III-D and III-E explore estimation of road grade from repeated runs of GPS longitude, latitude and elevation traces.

A. Measuring Inclination With An Accelerometer

In the study by Mangan et al. (2002), an inclinometer was used to estimate the inclination angle of a vehicle to determine the road grade [14]. The paper investigates methods to remove noise from an inclinometer caused by (i) vibrations of the vehicle and (ii) acceleration and deceleration caused by real life driving behaviours. High frequency noise created by vibrations of the vehicle was removed using a low pass filter. The paper discusses three different approaches to remove low frequency noise caused by the acceleration/deceleration in real life driving behaviours.

This present paper investigates the removal of high frequency noise using a low pass filter, and only investigates one of the three approaches to remove low frequency noise, namely the Mathematical Morphology approach, from the paper by Mangan et al. (2002). Since the Bach box does not include an inclinometer, a 3-axis accelerometer was used to measure the inclination of the vehicle. The pitch angle determined from the accelerometer in the test vehicle was used to estimate the road gradient.

1) Low pass filtering: The first step of replicating the study was to remove high frequency variations in the pitch angle estimates caused by vibrations of the vehicle, by applying a low pass filter. In the present study an exponential filter was applied.
2) High pass filtering: The second step was to use Mathematical Morphology (MM) to remove low frequency variations caused by the acceleration and deceleration of the vehicle.

The results in Fig. 2 show the accelerometer measured inclination (A) compared with the Google Elevation API estimated

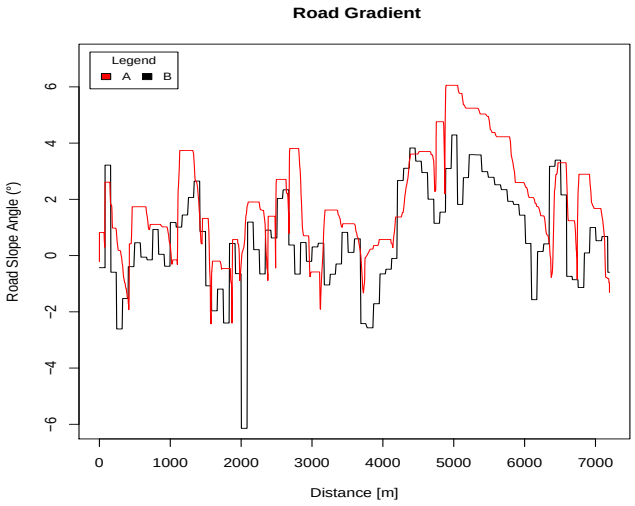

Fig. 2. Accelerometer estimated road grade (A) compared against Google Elevation API estimated road grade, at 80 m distances, (B).

road grade (B). The results of the accelerometer's readings, show correlation with Google Elevation API estimated road grade. However, it appears that the accelerometer values over-estimate the road grade values in general and there are slight discrepancies in some regions.

The findings indicate that the accelerometer was susceptible to bias and calibration errors. Similarly, the positioning of the Bach box, next to the driver's seat in the front of the vehicle, may have played a significant role in overestimating the road grade.

Digital Elevation Models

Digital Elevation Models (DEMs) are three-dimensional (3D) representations of a geographical area which include elevation information. Elevation values can be extracted from a DEM using GPS longitude and latitude points. There are several publicly available DEMs, such as the Advanced Space-borne Thermal Emission and Reflection Radiometer (ASTER) Global Digital Elevation Model (GDEM) and the Shuttle Radar Topography Mission (SRTM) DEM.

ASTER elevation information is provided in 1x1° tiles and covers 99% of the global land mass [20]. The ASTER GDEM is a one arc-second resolution DEM which means that a tile is made up of 3601 x 3601 pixels[1]. The height of the centre point of the pixel is taken as the height of the entire pixel. For this study, all of the DEM elevation estimates use the Shuttle Radar Topography Mission (SRTM) DEM. It was determined by experiment that the SRTM DEM elevation had less deviation than the ASTER GDEM elevation for the test area and provided better correlation with the Google Elevation API profile.

The SRTM DEM is a Digital Terrain Model (DTM) or a "bare earth" representation of the earth, and hence is void of vegetation and man-made structures. There is a need to account for discrepancies in the elevation profiles where lower values of the elevation were provided by the DEM.

[1]The 1x1° tiles over-lap neighbouring tiles by one pixel, hence there are 3601x3601 pixels instead of 3600 x 3600 pixels per tile, each with a resolution of approximately 30 x 30 m.

B. Bilinear Interpolation of Elevation profile from DEMs

A study by Henrique et al. explores the use of the ASTER GDEM to determine the slope of the elevation profile [21]. The elevation profile was extracted using GPS longitude and latitude traces of a cyclist from the ASTER GDEM, to be used for simulations in determining the effect of slopes on cyclists' performance.

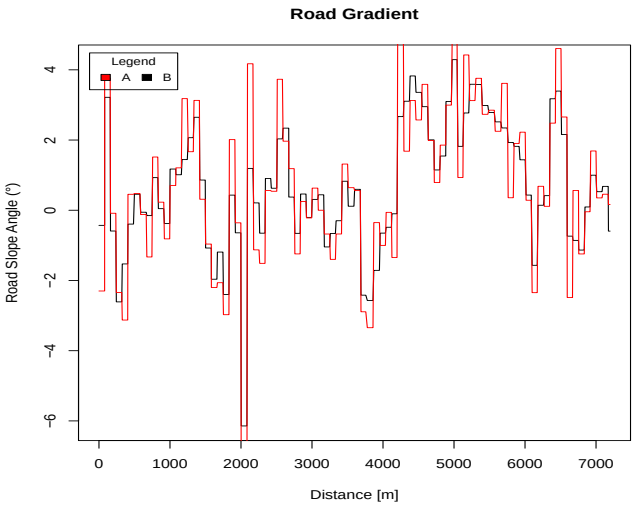

Fig. 3. Road grade derived from bilinear interpolation of SRTM DEM (A), using 80 m distances, compared to Google Elevation API road grade estimates (B), using 80 m distances.

Since the GPS longitude and latitude traces used in the study are regularly sampled and the relative speed of a cyclist means that there were multiple GPS points on a single DEM pixel, there was a need to smooth the elevation profile. Similarly, the elevation jump between pixels, combined with the inaccuracy of elevation values that are not at the centre of the pixel, means that there is a need to interpolate a better elevation profile before determining the slope of the road. The researchers infer a true estimate of the elevation for each GPS point on the DEM pixel using an extended version of bilinear interpolation.

Fig. 3 shows the estimates of the road grade deduced using elevation interpolated from the SRTM DEM. This method produces better estimates of the elevation values compared to using raw DEM values. However it does not dampen the inconsistencies and errors found in the DEM caused by the "bare earth" representation of the area. Fig. 3 shows good correlation with the Google Elevation API road grade estimates although fluctuations caused by the above mentioned inconsistencies and errors in the DEM are apparent.

By itself, this method produces sharp angles of estimated road grade with large variations. On the other hand, it does highlight the importance of estimating the true elevation of points that are not on the centre of the DEM pixel.

C. Smoothing/filtering of Elevation profile from DEMs

The technique employed in the NREL study by Wood et al. (2014), explores appending GPS speed traces, taken from vehicles, with elevation values extracted from the SRTM one-arc second DEM [16]. The researchers propose a method that examines smoothing/filtering the elevation profile from appended elevation, extracted from the SRTM DEM, to be used to determine road grade.

The aim of the smoothing/filtering technique is to improve the smoothness of the profile and to remove anomalous points caused by the SRTM DEM being a "bare earth" model. As stated in the study by Wood et al. (2014), the satellite reading measures elevation void of vegetation and man-made structures. Areas like overpasses and bridges are seen at the lowest point of their true elevation. This causes small troughs and peaks in the elevation profile which disrupts the continuity of the elevation profile.

The steps in the study are shown below:

1) Elevation versus distance: Compare raw SRTM elevation values against distance.
2) Down-sampling: Decimate the signal at 50 m intervals.
3) Filtering: Apply a Savitzky-Golay and Binomial combined filter to the sample signal to remove the troughs and peaks in the profile.
4) Removing outliers: Changes in elevation greater than 10 m are removed and backfilled using linear interpolation.
5) Filtering: Re-filter the signal to improve the smoothness of the profile.
6) Interpolation: Using the filtered elevation profile, interpolate the elevation data with the original distance values to get the elevation profile with the original dataset length.

The uniform sampling distance, used for down-sampling and the number of points of the filter were not specified in the study. Therefore, a nine point combined Savitzky-Golay and Binomial filter, and a uniform down-sampling distance of 50 m was chosen to replicate the study.

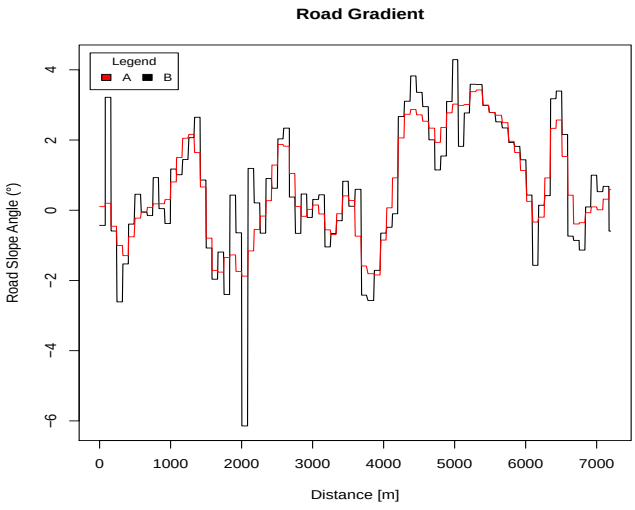

Fig. 4. Road grade derived from smooth/filter of SRTM DEM (A), using 80 m distances, compared to Google Elevation API road grade estimates (B), using 80 m distances.

Fig. 4 represents the road grade replicated using the smoothing/filtering process (A). The estimated road grade has a high likeness with the Google Elevation API estimated road grade (B). There are slight variations, but in general, it is a good fit and suggests that this method does produce highly accurate road grade estimates. However, it appears that the Google Elevation API estimates do not account for the discrepancies caused by the bare earth representations in some areas.

Therefore, this approach offers an automated, scalable way to estimate large datasets of road grade profiles as seen in a later study performed by the NREL [3].

D. Multiple Runs

In the paper by Boroujeni et al. (2013), multiple runs of GPS measurements, in the same direction of travel, of a given highway were performed to evaluate the ability of consumer grade GPS with Barometer Altimeters (GPS/BA) to determine road grade. The researchers took "approximately 100 one-way runs" and were able to deduce the need for a minimum of ten repeated runs to determine accurate road grade estimates, "depending on the desired precision of the average estimate of grade" [12].

Consumer grade GPS/BA devices have relatively poor vertical accuracy, as stated by the authors. However, the GPS/BA devices are less susceptible to signal loss than higher mapping grade differential GPS devices as seen in a later paper produced by the same authors, Boroujeni et al. (2014). The conclusion of the study is that, with enough repeated runs, it is possible to achieve a high precision of road grade.

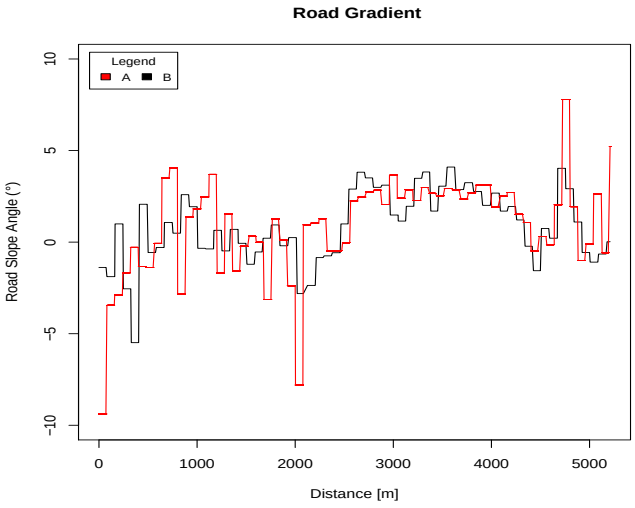

Fig. 5. Road grade derived from 10 repeated runs, using linear regression to estimate road grade (A), in 80 m segments, compared to Google Elevation API road grade estimates (B), using 80 m distances.

The experimental procedure in replicating the study used ten repeated runs and a shorter segment of the test route was chosen. The steps followed in the replication of the study are stated below:

1) Segment and determine the direction of travel: Segment the route into a shorter area of the entire test vehicle's route and determine the direction of travel.

2) Estimate total accumulated distance: Combine the runs into a large dataset with the overall distance decided by the averaging of the total accumulated distances for ten runs (a similar method was performed in the later paper by Boroujeni et al. [11]).
3) Linear regression of segments: Segment the total distance of the combined dataset into 80 m segments and apply linear regression to each of the segments.
4) Slope of the regression line: Determine the slope coefficient of the linear regression line for each of the segments to estimate the road grade for that segment.

The researchers provide a method that quantifies the number of repeated runs needed to achieve a specific precision. Fig. 4 shows the road grade estimated from the elevation profiles of all of the repeated runs that were combined, for every 80 m segment of the test area. The results of the repeated runs experiment (A) were compared to the Google Elevation API (B) estimated road grade.

The results show a relatively good match, with only ten repeated runs, with the Google Elevation API road grade estimates. However, there are slight discrepancies between the road grade estimates, with the repeated runs approach producing high variations of road grade estimates compared to the Google Elevation API estimates. Nonetheless, it is thought that, with enough repeated runs, the accuracy of the road grade estimates from the repeated runs would increase and the variation of the road grade would decrease. Therefore, this method does provide a scalable approach to ITS.

E. Geometric modelling of the roadway using B-Spline Approximations

Another approach to be considered is to investigate the possibility of using geometric models of roadways from a collection of GPS readings, as seen in the paper by Ben-Arieh et al. (2002), to estimate road grade [22].

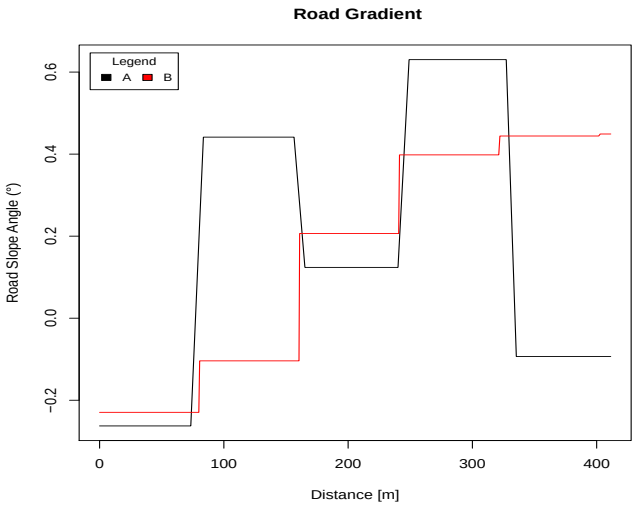

Fig. 6. Road grade derived from B-Spline approximation of 3 repeated runs (B), in 80 m distances, compared to Google Elevation API road grade estimates (A), using 80 m distances.

The paper investigates 3D-geometric modelling of the Kansas highway network (U.S.A.). The researchers use GPS data collected over several seasons from a test van for a period of five years. The method uses B-Spline approximations of GPS elevation, longitude, and latitude points to estimate segments of the highway into a geometric model.

The steps followed in the replication of the study were:

1) Converting GPS coordinates to a UTM projection: GPS latitudinal and longitudinal coordinates were converted into a Cartesian coordinate system. The original study used the Lambert projection system, however the Universal Transverse Mercator (UTM) projection system was chosen for this study.
2) Sorting the data based on the direction of travel: For this study, a segment of the test area was chosen that represented one way repeated runs of the test vehicle, in a very short straight segment of the entire route of the test vehicle.
3) Cleansing the data: This method involved a several step process to remove outliers from the combined data.
4) Applying a B-Spline approximation, using four GPS points (each point consists of a longitude, latitude and elevation estimate) as the control points of the Spline.
5) Estimating the road grade: This step extends the study done by Ben-Arieh et al. (2002), using the geometric profile of the road to estimate road grade. Road grade was estimated for 80 m distances and compared to the Google Elevation API estimated road grade for that segment.

Fig. 6 shows the results obtained from the Geometric modelling of the highway. It is difficult to estimate the correlation with the Google Elevation API road grade estimates as the total length of the chosen segment is relatively small compared to the previously studies replicated in Section III. Therefore, slight variations are exaggerated in comparison to larger segments seen in the previous replicated studies. The use of the B-Spline to approximate the geometry of the highway has the advantage of producing a smoother profile with fewer variations than seen in the Google Elevation API road grade estimates. In determining road grade estimates, results that produce fewer variations in the estimates between consecutive points are desirable as road ways are usually built to avoid large variations in road grade.

On the other hand, the method employed in the study requires the use of small segments and requires the user to select the control points for the Spline. When applying this to a large scale collection of road grade, this method is not appropriate due to the manual rework and time it takes to derive road grade estimates.

IV. CONCLUSIONS

The results indicate that two of the methods to determine road grade would be best suited to ITS: the methods shown in Sections III-C and III-D could be used to collect large–scale road grade profiles using advanced public transportations systems. Their post–processing abilities makes them suited for large scale analysis and estimation of road grade profiles using ITS for eco-routing purposes. The two approaches also meet

all the requirements set out in the defined criteria of this paper: they do not require real-time analysis; they are scalable to any city-wide ITS; they use only freely available sources of information to aid the measurements; and they utilise only the components available on most OBUs. The results highlight the range of approaches to determine road grade which may be applied to ITS when using OBUs. This paper provides an independent evaluation of existing methods for determining road grade.

REFERENCES

[1] Della Ragione, L. and Giovanni, M., 2016. The Influence of Road Gradient in an Integrated Approach of Real Driving Cycles and Emissions Factors Model. Transportation Research Procedia, 14, pp.3179-3188..

[2] Wang, Y., Du, X., Yu, H., Huang, J. and Li, Y., 2015. Impacts of road grade on fuel consumption of light vehicles by use of Google Earth DEM. In Cyber-Enabled Distributed Computing and Knowledge Discovery (CyberC), 2015 International Conference on pp. 360-363. IEEE.

[3] Wood, E., Burton, E., Duran, A. and Gonder, J., 2014. Contribution of road grade to the energy use of modern automobiles across large datasets of real-world drive cycles (No. 2014-01-1789). SAE Technical Paper.

[4] Zhou, M., Jin, H. and Wang, W., 2016. A review of vehicle fuel consumption models to evaluate eco-driving and eco-routing. Transportation Research Part D: Transport and Environment, 49, pp.203-218.

[5] Kubika, M., Klusek, J., Sciarretta, A., Cela, A., Mounier, H., Thibault, L. and Niculescu, S.I., 2016, June. Performance of current eco-routing methods. In Intelligent Vehicles Symposium (IV), 2016 IEEE pp. 472-477. IEEE.

[6] Levin, M.W., Duell, M. and Waller, S.T., 2014. The effect of road elevation on network wide vehicle energy consumption and eco-routing. Transportation Research Record: Journal of the Transportation Research Board.

[7] Travesset-Baro, O., Rosas-Casals, M. and Jover, E., 2015. Transport energy consumption in mountainous roads. A comparative case study for internal combustion engines and electric vehicles in Andorra. Transportation Research Part D: Transport and Environment, 34, pp.16-26.

[8] Figueiredo, L., Jesus, I., Machado, J.T., Ferreira, J. and de Carvalho, J.M., 2001. Towards the development of intelligent transportation systems. In Intelligent transportation systems, Vol. 88, pp. 1206-1211.

[9] Doering, M. and Wolf, L., 2015. Opportunistic vehicular networking: Large-scale bus movement traces as base for network analysis. In High Performance Computing & Simulation (HPCS), 2015 International Conference on, pp. 671-678. IEEE.

[10] OPENMATICS, On-board Unit Bach Developed for high performance in your vehicles. [online] Available at: https://www.zf.com/brands/en_de/openmatics/products_services_om/products/bach_benefits/bach-benefits.html [Accessed: Sept. 2016].

[11] Boroujeni, B.Y. and Frey, H.C., 2014. Road grade quantification based on global positioning system data obtained from real-world vehicle fuel use and emissions measurements. Atmospheric Environment, 85, pp.179-186.

[12] Boroujeni, B.Y., Frey, H.C. and Sandhu, G.S., 2013. Road grade measurement using in-vehicle, stand-alone GPS with barometric altimeter. Journal of Transportation Engineering, 139(6), pp.605-611.

[13] Wing, M.G., Eklund, A. and Kellogg, L.D., 2005. Consumer-grade global positioning system (GPS) accuracy and reliability. Journal of forestry, 103(4), pp.169-173.

[14] Mangan, S., Wang, J. and Wu, Q.H., 2002. Measurement of the road gradient using an inclinometer mounted on a moving vehicle. In Computer Aided Control System Design, 2002. Proceedings. 2002 IEEE International Symposium on, pp. 80-85. IEEE.

[15] Boucher, C. and Noyer, J.C., 2014. Automatic estimation of road inclinations by fusing GPS readings with OSM and ASTER GDEM2 data. In 2014 International Conference on Connected Vehicles and Expo (ICCVE), pp. 871-876. IEEE.

[16] Wood, E., Burton, E., Duran, A. and Gonder, J., 2014. Appending high resolution elevation data to GPS speed traces for vehicle energy modeling and simulation. National Renew Energy Lab.

[17] Zhang, K. and Frey, H.C., 2006. Road grade estimation for on-road vehicle emissions modeling using light detection and ranging data. Journal of the Air & Waste Management Association, 56(6), pp.777-788.

[18] Bae, H.S., Ryu, J. and Gerdes, J.C., 2001. Road grade and vehicle parameter estimation for longitudinal control using GPS. In Proceedings of the IEEE Conference on Intelligent Transportation Systems, pp. 25-29.

[19] Ribar, E. and Murn, J., 2016. Road slope introduction in vehicle route modelling. In Cybernetics & Informatics (K&I), 2016, pp. 1-5. IEEE.

[20] Asterweb.jpl.nasa.gov, 2016. ASTER Global Digital Elevation Map Announcement. ASTER Global Digital Elevation Map. [online] Available at: https://asterweb.jpl.nasa.gov/gdem.asp [Accessed Sep. 2016].

[21] Henriques, N. and Bento, C., 2013. Integration of GPS Traces and Digital Elevation Maps for Improving Bicycle Traffic Simulation Behavior. In Transportation Research Board 92nd Annual Meeting, Transportation Research Board.

[22] Ben-Arieh, D., Chang, S. and Zhang, G., 2002. Geometric modeling of highways using GPS data and B-Spline approximation. In IIE Annual Conference. Proceedings, p. 1. Institute of Industrial Engineers-Publisher.